



A study of the vascular effect of photodynamic therapy with oxygen variation on chorioallantoic membrane model

Master Thesis in Medical Physics

by
Luis Lauro Aizpuru Vargas

Elaborated in the

Institute of Physics

Submitted to the

Faculty of Physics

of the

Pontificia Universidad Católica de Chile

December 2022

Student ID. 21103046

© 2022, Luis Lauro Aizpuru Vargas

Se autoriza la reproducción total o parcial, con fines académicos, por cualquier medio o procedimiento, incluyendo la cita bibliográfica que acredita al trabajo y a su autor.

Academic Supervisors

Main Supervisor: Assistant Professor, Hilde Harb Buzzá, PhD
Pontificia Universidad Católica de Chile

Co-Supervisor: Associate Professor, Ignacio Espinoza Bornscheuer, PhD
Pontificia Universidad Católica de Chile

Corrector: Associate Professor, Denis Fuentealba Patiño, PhD
Pontificia Universidad Católica de Chile

Declaration of Authorship

I, Luis Lauro Aizpuru Vargas, hereby declare that this thesis titled, “*A study of the vascular effect of photodynamic therapy with oxygen variation on chorioallantoic membrane model*” was formulated by myself and the work presented in it is my own. I confirm that:

- This work was done while in candidature for a Masters degree at the Pontificia Universidad Católica de Chile.
- Where I have consulted the published work of others, this is always clearly attributed.
- Where I have quoted from the work of others, the source is always given. With the exception of such quotations, this thesis is entirely my own work.
- I have acknowledged all main sources of help.

Signed: _____

Date: _____

Acknowledgements

First, I want to thank the professors and staff at the Pontificia Universidad Católica de Chile for their excellence and constant support. Their expertise and uplifting spirit was greatly appreciated. I am really happy and grateful for the opportunity of having being part of this program.

Second, I would like to thank Agrícola Chorombo S.A. and its manager Rafael Covarrubias for donating all of the fertilized eggs for this experiment.

Third, I would like to thank Prof. Hilde Harb Buzzá for her guidance throughout my thesis period. Her understanding, mentorship and patience shows her level of commitment towards her job.

Fourth, I want to express my gratitude towards the Chilean (and fellow foreign) friends I made throughout my time here. I hope that the relationships we have built will last for a long time. I want to especially thank Karol, Catalina and Ignacio for their support in the experimental phases of this thesis.

Fifth, I would like to thank my mother, father and brother for their financial and moral support starting from the admission process up until the defense of this thesis.

Sixth and last, I want to dedicate this piece of work to my unborn children. I haven't met you yet, but I love you already. You are the motivation behind all of my actions.

"Own only what you can always carry with you: know languages, know countries, know people. Let your memory be your travel bag."

— Aleksandr Solzhenitsyn

Abstract

Chicken chorioallantoic membrane (CAM) assays have been proven to be very effective models to study the impact of chemical and biological agents on its vascular network. The study of pharmaceutical drugs, xenografts and photosensitizers on these assays are current areas of research. In particular, the use of photodynamic therapy (PDT) has been shown to induce a significant decrease in both the diameter and number of blood vessel ramifications of the CAM. Given that molecular oxygen is so important for the effectiveness of this therapy, it opens the possibility of testing bio-compatible photosynthetic microalgae capable of locally producing oxygen. Even though there is ample evidence of the use of bio-compatible microalgae in scaffolds for wound recovery, there is little to no research done on the combination of microalgae and PDT in CAM assays. In this thesis work, we present a study that explores how microalgae, PDT and the combination of these two change the vascularization of the CAM. Throughout this experiment, the photosensitizer that was used was methylene blue whilst the microalgae that was used was *Chlamydomonas reinhardtii*. In order to perform the quantitative measurements, an image analysis software allowed us to count the number of bifurcation points. Firstly, four groups were defined to study how the PDT at different days of embryonic development (EDD) might change blood vessel ramifications. These groups were defined as control, only light, only methylene blue and the PDT groups. It was found that after 24 hours, for EDD8, the ramifications for the PDT case dropped by 40% whilst for EDD10 they dropped by 60% with light at 630 nm with 30 mW/cm^2 for 5 minutes. Second, it was explored how illuminated microalgae might possibly increase the vascular networks with the same light parameters. It was found that after 24 hours for EDD8 the network grew by 30% and for EDD10 it grew by 20%. Moreover, the combination of a photosensitizer and microalgae was studied to analyze if it might change the effectiveness of the PDT. It was found after 24 hours that for all the explored permutations for both EDD8 and EDD10 all the eggs were dead, showcasing the effect of an oxygen-enriched PDT. Given that the effect was way to strong, the methylene blue solution was diluted by a factor of x10 (0.03 mg of MB/mL) to see if this resulted in a measurable effect on the eggs for the combination case. Indeed, it was found that the decrease from the baseline ramification levels was 30% for the PDT and 60% for the oxygen enhanced PDT. The novel element of this work was that it was one of the first to explore the possibility of creating an oxygen-rich PDT in a CAM assay. This showed that it is possible to combine microalgae and a photosensitizer in a way that enhances the effectiveness of the PDT. This might translate into the possibility of employing this technique in an in-vivo trial with mice or other mammals to guarantee its safety. In conclusion, we found that illuminated photosynthetic microalgae raises the effectiveness of PDT in the vascular network of CAM assays.

Keywords:

chorioallantoic membrane, methylene blue, photodynamic therapy, *Chlamydomonas reinhardtii*

Contents

1 Overview and Background	13
1.1 Biophotonics	13
1.2 Photodynamic Therapy (PDT)	15
1.2.1 PDT Overview	15
1.2.2 PDT Parameters	18
1.2.3 PDT Applications	19
1.3 Oxygen Concentrations and Microalgae	22
1.3.1 Microalgae and Oxygen Tension	22
1.3.2 Pre-Clinical and Clinical Applications	24
1.4 Biomedical Research with Animals	26
1.5 Chorioallantoic Membrane (CAM)	28
1.6 Motivation	32
1.6.1 Primary Objective	32
1.6.2 Secondary Objective	32
1.6.3 Tertiary Objective	32
2 Methodology	33
2.1 Light Source	33
2.2 Characterization of PS and Microalgae	34
2.2.1 Absorbance Spectra and Photobleaching of PS	34
2.2.2 Absorbance Spectra and Photobleaching of Microalgae	35
2.2.3 Absorbance Spectra and Photobleaching of Combination	35
2.3 In-vivo Experimental Setup	36
2.3.1 CAM Model	36
2.3.2 Microalgae and PS in CAM	37
2.3.3 Acquisition and Analysis of Images	38
2.3.4 LINCE Device	39
2.4 Experimental Outline	40
2.4.1 Only Light	40
2.4.2 PDT Groups	41
2.4.3 Microalgae Groups	42
2.4.4 Oxygen-Rich PDT Groups	42
3 Results and Discussion	43
3.1 Characterization of Parameters	43
3.1.1 Biotable Irradiance	43
3.1.2 PS Photobleaching Interaction	44
3.1.3 Microalgae Photobleaching Interaction	49
3.1.4 PS + Microalgae Combination Characterization	51
3.2 Vascularization of the CAM	54

3.2.1	Only Light	54
3.2.2	Methylene Blue and PDT Groups	56
3.2.3	Microalgae and Light	63
3.2.4	Microalgae, Methylene Blue and Light: High Concentration	66
3.2.5	Microalgae, Methylene Blue and Light: Sub-Dose	71
4	Limitations of our work	74
5	Summary and Conclusions	75
6	Appendix	77
6.1	Methylene Blue Calculations	77
6.2	Microalgae Calculations	78
6.3	Approval Document from Ethics Committee	79
6.4	Approval Documents from Lab Safety Committee	80
6.5	Chicken Development Stages	83
7	Notes	84
8	Bibliography	85

List of Figures

1	Biophotonic Clinical Protocols	13
2	Different Light Qualities	14
3	Different Light Sources	15
4	PDT Jablonski Diagram	16
5	Approved PS Worldwide	18
6	S.Brasiliensis Fungus DLI Times	19
7	In-Vitro Death Cell Counting	20
8	PDT Clinical Progression	21
9	Consequences of Hypoxia	23
10	Engrafted Scaffolds Mice	24
11	Skin Wound Microalgae	25
12	Biocompatible Microalgae	26
13	Chicken Embryo Development	27
14	Anatomical Depiction Chicken Embryo	28
15	Extra-embryonic Structures	29
16	CAM Cultivation Methods	30
17	CAM Imaging Methods	31
18	Biotable Device	33
19	Egg incubator	37
20	Bio-safety cabinet	38
21	ImageJ Analysis	39
22	Experimental setup	40
23	Biotable Instrumental Setup	44
24	Experimental MB Spectral Profile	45
25	Literature MB Spectral Profile	46
26	MB Decaying Process	47
27	Photobleaching Effect of MB Low Concentration	47
28	Photobleaching Effect of MB High Concentration	48
29	Photobleaching Effect of MB Both Concentrations	48
30	Microalgae Spectral Profile	49
31	Microalgae Degradation Effect High Concentration	50
32	Microalgae Degradation Effect Low Concentration	50
33	Microalgae Degradation Effect Both Concentrations	51
34	Combination Spectral Profile	51
35	Combination Degradation Effect	52
36	Degradation Effect of All Cases	52
37	Spectra Different Cases	53
38	Spectra Theoretical and Experimental	53
39	Group "OL1" EDD12 Only Light	55
40	Group "OL2" EDD12 Only Light	55
41	Group "OL3" EDD12 Only Light	55

42	Control Group	56
43	Group 1 (EDD8): Methylene Blue + Light	57
44	Group 2 (EDD8): Only Light	57
45	Group 3 (EDD8): Only Methylene Blue	58
46	Group 4 (EDD8): Control	58
47	Group 5 (EDD10): Methylene Blue + Light	59
48	Group 6 (EDD10): Only Light	60
49	Group 7 (EDD10): Only Methylene Blue	60
50	Group 8 (EDD10): Control	61
51	Bar charts EDD8 MB Groups	61
52	Bar charts EDD10 MB Groups	62
53	Group 9 (EDD8): Algae + Light	63
54	Group 11 (EDD8): Only Algae	64
55	Group 13 (EDD10): Algae + Light	64
56	Group 15 (EDD10): Only Algae	65
57	Bar charts EDD8 Microalgae Groups	65
58	Bar charts EDD10 Microalgae Groups	66
59	Group 17 (EDD8): Combination a) Algae + Light → PS → DLI → + Light	67
60	Group 18 (EDD8): Combination b) Algae + PS → DLI → + Light	67
61	Group 19 (EDD8): Combination c) PS → DLI → Algae + Light	68
62	Group 20 (EDD10): Combination a) Algae + Light → PS → DLI → + Light	68
63	Group 21 (EDD10): Combination b) Algae + PS → DLI → + Light	69
64	Group 22 (EDD10): Combination c) PS → DLI → Algae + Light	69
65	Bar charts EDD8 Combination Groups	70
66	Bar charts EDD10 Combination Groups	70
67	Group 23 (EDD10): Methylene Blue + Light Low Concentration	71
68	Group 24 (EDD10): Combination b) Low Concentration	72
69	Bar charts EDD10 Diluted Combination Groups	72
70	Approval Document for Animal Use	79
71	Approval Document for Lab Safety Pt.1	80
72	Approval Document for Lab Safety Pt.2	81
73	Approval Document for Lab Safety Pt.3	82
74	Chicken embryo development EDD4 - EDD7	83

List of Tables

1	Only Light Parameters	41
2	PDT Parameters	41
3	Microalgae Parameters	42
4	Biotable irradiances configuration	43

Introduction

In general terms, biophotonics research is focused on the study of how visible light affects and interacts with biological systems. The field of biophotonics has been gaining a lot of attention over the past couple of decades. The vast scope of possible applications attracts scientists from a diverse set of backgrounds such as quantum electronics, biology, laser physics and medicine, amongst others. Biophotonic science, studies the mechanism of light-tissue interactions and light induced biological effects. Phenomena such as photobiomodulation (PBM) therapy aims at alleviating pain and inflammation by modulating the response from the immune system in order to promote healing and tissue regeneration through the use of lasers in the visible range of the EM spectrum [Arany, 2016]. There also exists a particular application of biophotonics called photodynamic therapy (PDT).

The use of PDT has been growing as a viable alternative to treat and cure tumors and other diseases compared to the more complex gold standard treatments, such as surgery or radiotherapy (RT). Its main objective is to treat and manage malignant and non-malignant diseases through the toxic reactions that occur when light, oxygen and a photosensitizer (PS) interact. When this happens, the produced toxic singlet oxygen locally damages the malignant tumor or the site of the microbial infection. Given the economic constraints an expensive RT treatment entails for clinics across developing and least developed countries, PDT emerges as a cheap and accessible candidate to treat the millions of cases of malignant and non-malignant diseases on those countries.

The presence of irradiated photosynthetic microalgae in biological systems increases the local quantities of molecular oxygen and this invariably has a physiological effect on the organism. The new development of oxygen releasing bio-materials has the potential of modifying and/or controlling critical metabolic processes. In fact, oxygen is so important that: “[...] *Oxygen tension controls cellular behaviour via metabolic programming, which in turn controls tissue regeneration, stem cell differentiation, drug metabolism, and numerous pathologies*” [Willemen et.al, 2021]. For this reason, the investigation of the effect that locally produced oxygen has on an organism is very valuable for the understanding of the subsequent biological effects. The microalgae that must be used in this scenario must be both bio-compatible to prevent an acute response from the immune system and also be highly sensitive to light from the visible part of the spectrum. Within the context of PDT, molecular oxygen levels are critical if one is trying to produce singlet oxygen to fight a tumor or an infection. The depletion of molecular oxygen levels either in a tumor or at the location where the PDT is performed is thus not desired and constant replenishment of oxygen from photosynthetic microalgae stands out as a possibility with clinical potential.

The chicken chorioallantoic membrane (CAM) is a good biological model that allows for the experimentation of a diverse set of phenomena such as the study of angiogenesis. Given the CAM’s resemblance to human tissues, it would be possible to deduce a similar response in a

clinical setting. The motivation for using fertile eggs lies in the fact that the CAM within it is highly vascularized and resembles human organs. The embryo development day (EDD) range that will be used throughout this study will never surpass the 14th day mark and thus entails no animal pain [Ribatti, 2016]. This model is therefore a good alternative to animal tests and allows for real time measurements of the vascularization network development.

In this thesis project there will be three main aspects that will be experimentally studied: 1) PS and microalgae characterization, 2) vascularization of CAM and 3) CAM & PDT. For the first set of measurements, our main interest is to understand how the photo-degradation of both the PS and the microalgae occur when exposed to controlled conditions of LED light. This will allow us to determine which time ranges of light exposure are better for our particular objectives of improving vascularization or for exacerbating the efficiency of PDT. For the second aspect, the goal is to determine which days of irradiation of the microalgae applied topically over the CAM promotes angiogenesis. Finally, for the third aspect the objective is to see if (and how) the combination of different amounts of microalgae with PDT might lead to greater damage in the CAM. For the last two experimental goals the vascularization growth will be quantitatively assessed through the analysis of photographs of the CAM. The potential use of the data recollected in this pre-clinical study ultimately has the goal of enriching the available literature of the field and thus has a potential of impacting the lives of people, especially for those living in countries and communities whose medical infrastructure cannot support complex and expensive medical procedures. The simplicity and accessibility of the materials both for capillary development through photosynthetic microalgae and local cellular death through PDT makes this line of research a compelling topic.

It is for these reasons, that working on pre-clinical studies on chicken embryos to determine the optimal temporal combinations and quantities of irradiated photosynthetic microalgae (oxygen), PS and light provide valuable information that in the future might lead to more efficient and effective treatments for human beings. In particular, what is interesting and a main point of exploration in this thesis is the effect that microalgae might have in the PDT process. Also, it is not known if the temporal dependence of oxygen exposure during the therapy might lead to a better or worst result regarding local cellular death from PDT. It is for this reason, that the exploration of novel combinations of PDT and microalgae is of great scientific and clinical interest.

1 Overview and Background

1.1 Biophotonics

The field of biophotonics has been emerging as a multidisciplinary endeavour that combines quantum electronics, lasers, fiber optics, electro-optics and applies it to the fields of biology and medicine. The applications vary from the theoretical and pre-clinical laboratory experiments to the applied clinical settings with real human patients. More and more, these kinds of technologies have been gaining ground in biomedical research and public health due to their minimally invasive nature, cost effectiveness, monitoring and treatment of different ailments. The non-ionizing radiation that a visible light emitting diode produces is very efficient in achieving high spatial resolution in the micron, submicron and even nanometric range.

The interdisciplinary nature of this kind of research has attracted scientists from distinct areas of expertise. Amongst these, there are four main areas: 1) bioimaging, 2) biosensing, 3) biophotonic science and 4) biophotonic technology [Ilev et.al, 2014]. For our particular case, we are mainly focused on the third area: biophotonic science, which studies the mechanisms of light-tissue interactions and light induced biophotonics effects. There has been a lot of research done regarding this topic, amongst it in the fields of dermatology, ophthalmology, oncology and dentistry.

The effects of light on the organism are quite diverse and can have multiple positive effects on the human body depending on its location, intensity and dose. In Figure 1, we present a chart showing the diverse applications, suggested different irradiances and acting mechanisms of biophotonics. Each of these constitute an active area of research and only demonstrates the eclectic nature of biophotonic usage in the lab and in the clinic.

Wound Healing Application	Therapeutic Protocols Suggested *	Primary Biological Rationale	Primary Causal Mechanisms (Putative / Established)	Other Effects (Bystander)
Surgical	High Irradiance, Extremely short pulses	Debridement	Extreme heating	Yes
Antimicrobial #	Low-Medium Irradiance, Continuous wave	Disinfection	High heat and ROS-mediated cell death	Yes
Analgesia	Medium-Low Irradiance, Short pulses	Peripheral and Central responses	Modulates neuroperception and conduction Low Heat / ROS - TRPV1?	Likely
Anti-Inflammatory / Immunomodulation	Medium-Low Irradiance, Effects of pulsing unclear	Improve resolution, Reduce detrimental damage	Low ROS-NFκB, others	Likely
Promote Healing	Low Irradiance, Continuous wave	Enhance reparative processes	Low ROS-TGF-β1, others	Yes

Figure 1: Enumeration of distinct clinical protocols and their purposes along with the efficacy and rationality for the use of different biophotonic methods [Arany, 2016]

In the case of skin ailments, two low-dose biophotonics treatments are usually utilized: photobiomodulation (PBM) and PDT. PBM therapy can be used to alleviate pain, modulate the

inflammatory or immune responses, and promote wound healing and tissue regeneration while PDT focuses on eliminating infections such as bacteria, fungi, and virus as well as various types of tumors [Chen et.al, 2006 in Rahman et.al, 2017]. For instance, PBM is used as a technique to provide adjunctive supportive care in oncotherapy such as radiotherapy, chemotherapy (and their combination). This is done to diminish the secondary effects of these therapies such as oral mucositis due to the secondary effects changing the integrity of the mucous membrane, oral microbiota and salivary composition [Medeiros-Filho et.al 2004 in Rahman et.al, 2017]. Given this, it is important to explore alternatives that promote healing and restoration to better the life quality of the patients.

Other examples where PBM can be used are in pathologies ranging from skin diseases to autoimmune disorders and viruses which only exemplify the wide range of uses that this technique could have in a clinical environment. On the other hand, we have PDT that has been used in endodontics with the unique quality of eliminating (or reducing at a great extent) microbial infections within the root canal. For both PBM and PDT the quality of the laser diode is very important as to guarantee the effectiveness of the treatment. In Figures 2 and 3 different lasers are shown as to elucidate the fact that it is of upmost importance to guarantee the quality of the light sources used in any experimental setup. It is best to use a light source with a known homogeneous profile and intensity. In order to achieve these homogeneous qualities certain filters are needed. There is a whole field of study involving photonics and electronics that tries to optimize these parameters.

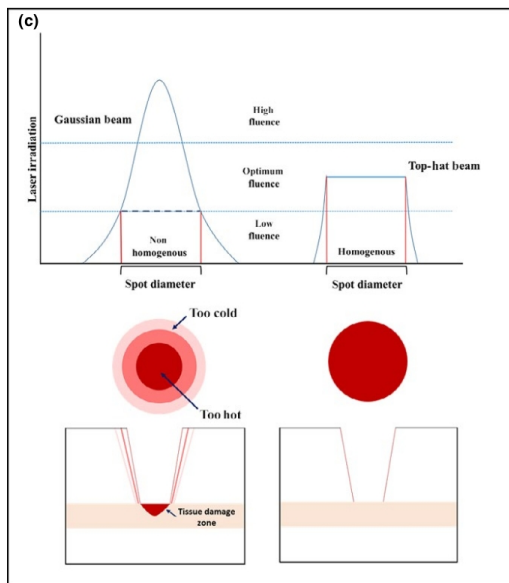


Figure 2: Different light qualities [Rahman et.al, 2017]

For both antimicrobial PDT (aPDT) and oral cancer treatments diode lasers nearing the red color (650 nm) are used given the higher sensitivity of the PS to this wavelength of light to

produce singlet oxygen [Rahman et.al, 2017]. In figure 3, what is shown is the properties of different light sources. For therapies such as aPDT, monochromatic and quasi-chromatic sources are used given the affinity of certain PS to a narrow range of wavelength values.

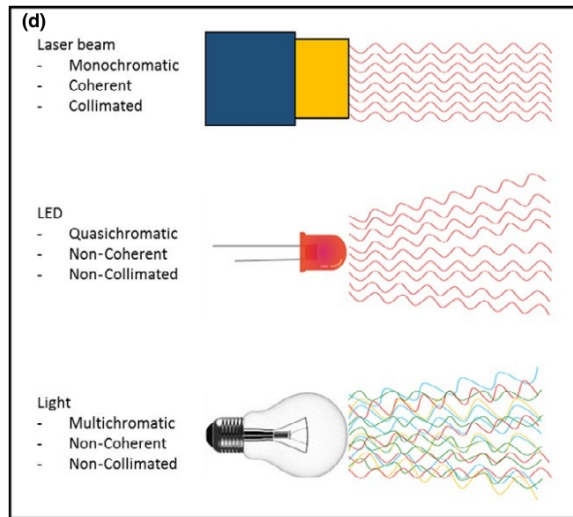


Figure 3: Different sources of light are shown as to exemplify the range of possibilities that exist for the health care practitioner to achieve any specific health outcome [Rahman et.al,2017].

1.2 Photodynamic Therapy (PDT)

1.2.1 PDT Overview

PDT is emerging as a complementary way to treat and manage malignant and non-malignant diseases. PDT combines the “*[...] photophysical and photochemical process to bring about a biological effect*” [Chilakamarthi & Giribabu, 2017]. In PDT, three elements come together to bring about cellular death locally: oxygen, a photosensitizer and visible light of a specific wavelength. Each of them individually is not toxic but, in combination, they interact in a toxic manner to kill cancer cells or microorganisms [Chilakamarthi & Giribabu, 2017].

The accepted mechanism of action of PDT consists of a PS molecule that is illuminated by light of the appropriate wavelength, absorbs the energy and then a toxic reaction takes place. More specifically, when the photon interacts with the PS the energy state of the molecule's electrons change. First, an electron goes into an excited state and from here one out of three things might happen. First, it might go through a radiative process and become fluorescent. Second, it might go through a non-radiative decay process called internal conversion that entails the emission of the excited electron through an EM interaction with the orbital electrons of the molecule. Third, there might be an ISC or intersystem crossing where a transition between two electronic states with different spin multiplicity occurs. If this last process takes place three things might occur. The first two processes entail going back to the non-excited state either

through a radiative process or an ISC. If neither of these two things happen the molecule sits in a meta-stable state that allows it to interact with the molecular oxygen in the environment. The first type of reaction produces reactive oxygen species (ROS) through via the transfer of electrons that produce great damage in the surrounding cells that it induces necrosis. The other possibility happens via the transfer of energy, turning a molecule of oxygen into singlet oxygen which is also very toxic but it instead induces apoptosis or autophagy. The chemical classification of these types of reactions that occur from the PS are referred to as type I and type II, respectively as can be appreciated in Figure 4. [Maiya, 2000].

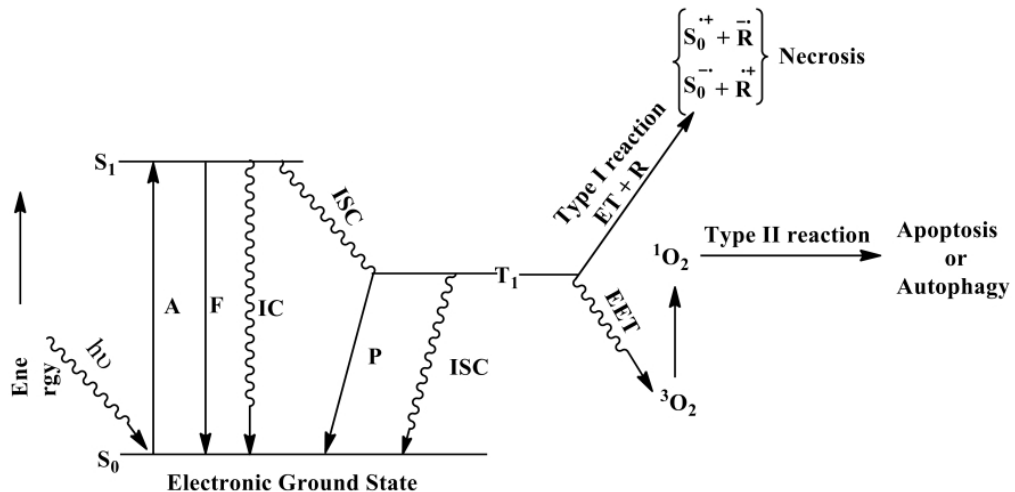


Figure 4: The modified Jablonski energy level diagram shows how PDT works utilizing the three primordial elements: Oxygen, PS, and light. It also shows the different types of reactions and its corresponding biological effect [Chilakamarthi & Giribabu, 2017]

One great advantage of PDT is its capacity to only target very local and specific regions and avoid negative effects to healthy tissues. For instance, the PS can be tagged with distinct peptides or antibodies that target the molecule differentially to tumors [Chilakamarthi & Giribabu, 2017]. Given the efficiency of type II reactions to induce cellular damage, these are highly preferred. For this reason it is of vital importance to maintain a high enough oxygenation level to maximize the efficacy of PDT. The design of novel and biocompatible oxygen-producing materials in-situ at the tumor site is thus highly desired [Qi et.al, 2021].

Especially, over the last decade there has been quite a significant advancement of PDT research via the use of nanotechnology. The combination of PS with nanomaterials can improve the efficacy of the therapy. The PS naturally accumulates in higher concentrations in cancer cells and microorganism compared to regular healthy cells. In relation to a tumor, this is due to the tendency of PS to combine with low density lipoproteins (LDL). The role of LDL in cell division is very important and rapidly dividing cancer cells show an increased uptake of LDL

[Cruz et.al, 2013]. On the other hand, nanotechnology can help with the targeting of the PS to the area of the disease through the use of capsules and other nano-receptors that guide the PS.

Furthermore, it is known that PDT affects the vasculature of a tumor and thus stimulates an immune system reaction through the activation of coagulation and accumulation of inflammatory cells [Huang et.al, 2008]. The development of the PS has also been an active field of research by the chemistry community. There are a couple of important characteristics that an ideal PS must have [Kwiatkowski et.al, 2018]:

- High degree of chemical purity.
- Stability at room temperature.
- Photosensitivity only in the presence of specific wavelength.
- Absorption range between 400 nm and 800 nm to prevent photosensitivity from other light sources.
- Easy solubility in the tissues of the body.
- Inexpensive, simple synthesis and easy availability.

Thus, the choice of PS is critical to the successful treatment using PDT for any disease. Understanding the mechanism of cellular death in PDT is of great importance in order to make the therapy more efficient. The mechanisms of damage are thus induced by different pathways depending on many things such as the type of PS and protocol used, dosage and localization of PS, genotype of cells subjected to PDT and oxygen level. The PS localized in the mitochondria is more likely to manifest apoptosis, while those localize in plasma membrane and lysosomes cause necrosis [Chilakamarthi & Giribabu, 2017].

There is not only evidence of the effectiveness of PDT in complex in-vivo biological systems but there also exist a whole background of research concerning in-vitro trial and PDT. The biological effect of PDT on the surrounding cells depends heavily on things such as PS concentrations, light fluency (J/cm^2) and the time interval between the PS administration and the irradiation of the area [Vasconcelos-Moraes et.al, 2021]. Understanding the effect of these parameters in a controlled environment is paramount before trying to translate it into a clinical context.

Human melanoma cells (B16F10) were used to investigate how using a particular PS (aluminum-phthalocyanine) could lead to the production of damage-associated molecules such as HMGB1, which are in turn a trademark of immunogenic cell death. It was found that for higher concentrations of aluminum-phthalocyanine these molecules were produced and interacted with the cells even after the end of the PDT session. It was found that this PDT caused cell apoptosis, increased reactive species and provoke cell arrest at the G0/G1 phase, something particularly good when dealing with cancer cells [Tu et.al, 2016].

1.2.2 PDT Parameters

There are three main parameters that can be adjusted depending of the desired results of the treatment in question. They can be broadly classified as:

- PS Concentration
- Light Dose
- Drug Light Interval (DLI)

In general, the higher the concentration of PS, the higher the probability that an incoming photon will interact with a single PS molecule which in turn will produce a ROS or a singlet oxygen molecule. Equally, an increase in the fluence of the emitting LED or laser will linearly increase the dose. It is important to highlight that the biological medium through which the liquid PS diffuses is highly consequential when planning a treatment. For instance, if one is trying to alleviate a microbial infection it is paramount to know if the bacteria is either gram-positive or gram-negative. The lower diversity of molecular structures within the wall for gram-positive bacterium make them more ideal for perfusion of an outside agent. It is here where the DLI parameter comes into play. This parameter is defined as the time that it takes between the application of the PS and the irradiation from the light source. This time is constrained on the one side by the diffusivity of the PS into the tissue and on the other side by the homogenization of the PS throughout the organism. It is because of this that there exist in-vitro research that looks into the optimization of this parameter. There exists a great variety of options for medical professionals to use a diverse set of PS to treat a specific disease, each of them with a particular effectiveness, indication and excitation wavelength as can be appreciated in the table right below (Figure 5).

Table 1.2: List of approved photosensitizers as of 2017 [20]

Photosensitizer	Excitation Wavelength	Approval	Indication
Porfimer Sodium/Photofrin®	630 nm	Worldwide, withdrawn in EU for commercial reasons	High-grade dysplasia in Barrets Esophagus. Obstructive esophageal or lung cancer
5-ALA/Ameluz®/Levulan®	635 nm	Worldwide	Mild to moderate actinic keratosis
Metvix®/Metvixia®	570-670 nm	Worldwide	Non-hyperkeratotic actinic keratosis and basal cell carcinoma
Temoporfin/mTHPC/Foscan®	652 nm	Europe	Advanced Head and neck cancer
Talaporfin/NPe6/Laserphyrin®	664 nm	Japan	Early centrally located lung cancer
Verteporfin/Visudyne®	690 nm	Worldwide	Age-related macular degeneration
Synthetic Hypericin/SGX301	570-650 nm	Orphan status in EU	Cutaneous lymphoma T-cell
Redaporfin®/LUZ11	749 nm	Orphan status in EU	Biliary tract cancer

Figure 5: Approved PS in different regions of the world for use in a clinical context [Van Straten et.al 2017 in McFadden, 2020]

In a recent study, researchers were trying to figure out if a *Sporothrix* fungi was sensible to a particular PS. While investigating the concentrations and light dose (fluence) needed to exterminate the fungi colonies in the multiwell plate it was necessary to determine the specific DLI optimal for those particular conditions. It was found that the best time to wait between the application of the PS and the irradiation of the plate was around 20 minutes. This is important because the single oxygen lifetime is quite short and the cytotoxic damage only happens close to where it actually generated [Tiburcio et.al, 2022]. The different DLI times for which the researchers waited when studying the effect of PDT in this specific fungi can be appreciated in Figure 6.

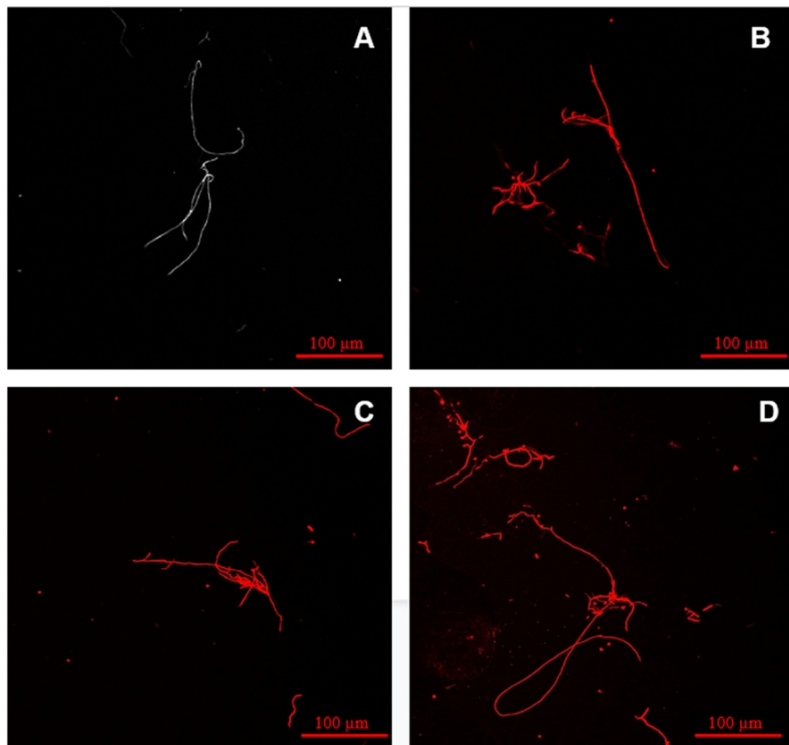


Figure 6: *S. brasiliensis* fungus in its mycelial (filamentous) form for the absence of PS A) and for different incubation times B) 10 mins, C) 20 min and D) 60 mins [Tiburcio et.al, 2022].

1.2.3 PDT Applications

The rise of antimicrobial photodynamic therapy (aPDT) has been developed as an alternative approach of killing bacteria, mainly due to the growing resistance to antibiotics and antisepsitics using the principles of the traditional PDT. In a recent review on antimicrobial resistance sponsored by the UK Department of Health it reported that: “*the number of deaths attributable to global antibiotic resistance will increase to 10 million per year until 2050 compared to the current 700,000 annual deaths*” [Renwick et.al 2016 in Cieplik et.al, 2018]. This big number of deaths need urgent solutions, and aPDT remains a valuable option to attend this growing

problem. Most of the research that has been done has been in-vitro studies but there are hopes for translation into clinical practice. For instance, more complex biofilms models that simulate the biofilms found in-vivo in oral cavities, skins surfaces, wounds or catheters are being explored. All of these different pathways and mechanisms have the ultimate goal of bettering the quality of life of patients. It is common for open wounds on the skin due to diverse causes, to have a hard time achieving cicatrization. Is in these scenarios that PDT might result useful. The benefits of treating an ulcer infected with bacteria using aPDT is that: 1) its bactericidal effect might lead to faster healing and 2) the multiple use of PDT on the area does not lead to drug-resistant strains. An in-vitro cell quantification study showed that different concentrations of PS alone were able to induce cellular death as can be seen in Figure 7. This might be of help when considering the parameters of a aPDT.

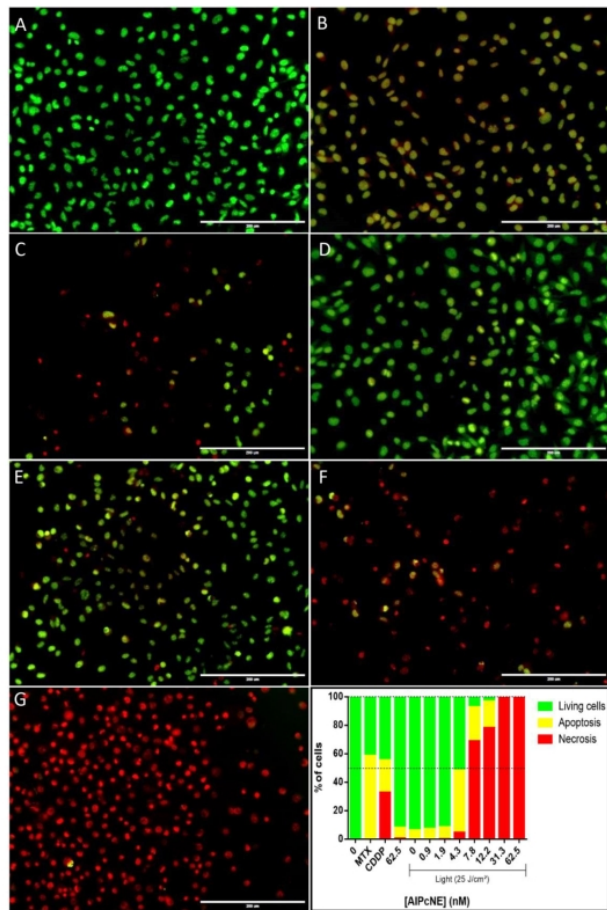


Figure 7: In-vitro death cell quantification for different PS and for different concentrations of particular PS (aluminum-phthalocyanine). The take-away is that the higher the PS concentration the higher the cellular death rate. The pictures A through G represent growing amounts of the PS [Vasconcelos-Moraes et.al, 2021]

Specifically, it has been reported in a scientific paper of a 72 year old female patient with a chronic recalcitrant venous ulceration in the right lower leg. The ulcerated area was almost 20 square centimeters and was resistant to diverse topical antiseptics. The skin ulceration improved considerably after PDT with red light of 630 nm. After the treatment, the bacterial culture was negative and no adverse sequels were observed [Clayton & Harrison, 2007]. The importance of oxygenation for both the PDT and the cicatrization process is very relevant for the optimal completion of the treatment. As it can be appreciated in Figure 8, the progression of a PDT treatment for two distinct clinical cases shows a clear positive progression as days go by. These are the kind of results that demonstrate the viability and efficacy of PDT treatment for these types of infected open wounds.



Figure 8: In the upper half the wounds of a first patient was evaluated before, after 3 days and after 6 days of PDT. In the lower half the wounds of a second patient were evaluated before and after 3 days of PDT. A betterment of outcome can be observed after PDT [Xia et.al, 2015]

Due to the high prevalence of predisposing factors such as sedentary lifestyle, nutritional disorders and higher survival rates in general, the prevalence of chronic wounds has increased. In the case of diabetic patients ulcers are a side effect that approximately 15 percent of patients present at one point or another throughout their disease [University of Michigan Health, 2022]. For instance: “*Venous leg ulcers, arterial ulcers, diabetic foot ulcers, pressures sores and non-healing surgical wounds represent an important burden on the healthcare system, requiring frequent hospitalizations and expensive treatments.*” [Sen et.al, 2009 in Mihai et.al, 2014]. What happens is that when the skin barrier is impaired by one of the previous causes, tiny microorganisms rapidly colonize the surface of the wound and then if the conditions are favorable they multiply, which in turn might lead to acute or chronic infections to the patient [Scales & Hunningale, 2013]. In a study it was found that the most frequent species of bacteria isolated from chronic ulcers in patients were *S.aureus* and *P.aeruginosa* [Mihai et.al, 2014]. The setback that might occur in these kinds of situations is the an antibiotic might not be effective to a resistant strain of bacteria. For this reason, a combination of PDT that kills the bacteria through the

use of a toxic singlet oxygen and of a photosynthetic microalgae that stimulates the wound repair mechanism through the production of oxygen in-situ might be greatly beneficial for the proper healing and cicatrization of a deep wound.

All of the above highlights the importance of having the correct PS, a well adjusted set of light parameters and an adequate presence of oxygen for an effective treatment.

1.3 Oxygen Concentrations and Microalgae

1.3.1 Microalgae and Oxygen Tension

The effect of oxygen within PDT plays an important role in the development of clinical treatment plans. Due to the direct role oxygen plays in PDT it is known that when molecular oxygen is deficient, the overall efficiency of the therapy is significantly reduced. To counter this situation, it is possible to use some microorganisms that can continuously produce molecular oxygen under visible light illumination. Algae are photosynthetic organisms that grow in a range of aquatic habitats, including lakes, ponds, rivers, oceans, and even wastewater. They can also tolerate a wide range of temperatures, salinities, and pH values; different light intensities; and conditions in reservoirs or deserts and can grow alone or in symbiosis with other organisms [Barsanti et.al, 2008 in Khan et.al., 2018]. Furthermore, regarding their size, macroalgae are multicellular, large and visible to the naked eye. Meanwhile microalgae are microscopic single cells that could be either prokaryotic or eukaryotic, similar to cyanobacteria or green algae, respectively [Khan et.al, 2018]. Microalgae are rich in carbon compounds which can be used in biofuel, health supplements, pharmaceuticals, cosmetics, etc... [Aziz, Obbard; 2011]. They also have applications in wastewater treatment, carbon dioxide mitigation and can be used to produce bioproducts such as polysaccharides, lipids, pigments, proteins, vitamins, bioactive compounds and even antioxidants [Brennan & Owwned, 2010]. These microorganisms have a wide range of uses in our manufacturing endeavors and scientific research. One particular application is the increase in the local quantities of molecular oxygen through the use of illuminated photosynthetic microalgae.

When using a special gel containing the photosynthetic microorganisms and sodium alginate it was found that for in-vivo trials the hypoxic microenvironment at the tumor site can be reversed and thus the effect of PDT was enhanced [Wang et.al., 2021]. Photosynthetic microalgae used for in-situ oxygen generation have been found to not only be effective for improving the sensitivity to PDT of tumor cells but also as an imaging agent. As far as the light parameters are concerned, it has been found that under red light (660 nm light emitting diode) algae show higher photosynthetic activity compared to natural white light. Exposure to red light caused the algae to produce a high amount of molecular oxygen within the hour as compared to white light [Qiao et. al., 2020]. In this same study, it was demonstrated that Red Blood Cell Membrane (RBCM) engineered algae can be effectively delivered to tumors via intratumoral or intravenous injection. This procedure elevates the available oxygen loading to sensitize cancer cells to both conventional RT and PDT in xenograft tumor models. Furthermore, in an in-vivo

study of photosynthetic bacteria in mice with cancer cell inoculation, it was found that these microorganisms enhanced immune response through the induced infiltration of T lymphocytes [Zheng et. al, 2021]. This indirect immune response represents a promising new possibility in cancer therapy that may lead to hybrid therapeutic strategies. In Figure 9, the biological consequences of hypoxia in an organism are shown with the intent of conveying the idea that biological feedback loops emerge when low concentrations of oxygen exist.

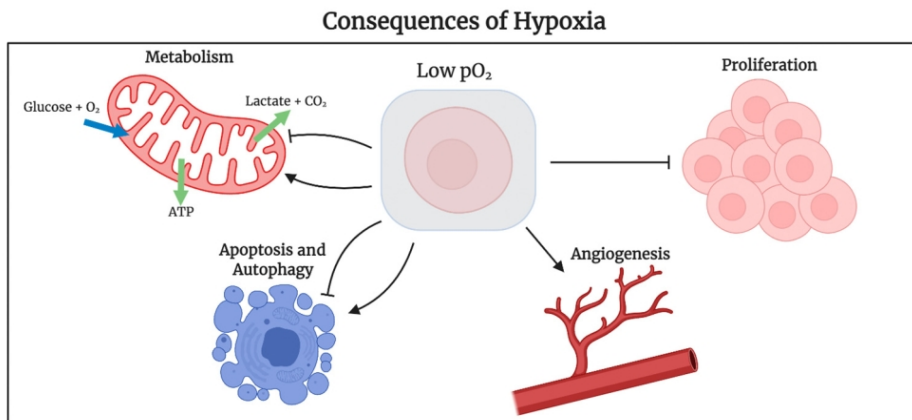


Figure 9: Schema of the biological consequences of inducing local hypoxia in an organism [Willemen et.al, 2021].

Furthermore, it has been studied that photosynthetic microalgae could be potentially used in organ transplants. In preliminary studies, the same species of microalgae as used in the previous example (*Chlamydomonas reinhardtii*) was utilized to explore the feasibility of ex-vivo organ preservation. Given that hypoxia is one of the main challenges for preserving an organ in-situ, oxygen sources are of great use. From the organ extraction from a donor all throughout surgical attachment to the needing patient, new oxygen producing techniques are being explored. In this case, this microalgae were incorporated in a standard preservation solution. In terms of its viability, the photosynthetic solution proved not harmful and provided sufficient oxygen in rats and pork kidneys transplants [Veloso-Giménez et.al, 2021]

The dependence of the biological response of cells to other therapies, such as ionizing radiation, has been studied for many decades. In the context of RT, the cell surviving fraction curves as a function of oxygen have been measured for mammalian cells. The parameter referred to as the Oxygen Enhancement Ratio (OER) measures the augmentation of radiation damage under the presence of oxygen. The oxygen-fixation hypothesis proposes that the damage induced by high energy photons in the DNA produces radicals. These DNA radicals are able to react with oxygen from the local environment resulting in permanent DNA damage and strand breaks. This process initiates a complex biological process leading to cellular death. [Joiner & van der Kogel, 2009]. For instance, the difference between the survival curves of oxic and hypoxic conditions is larger for treatments that utilize irradiation. It has been experimentally shown that

biological tissues are more sensitive to oxygen presence (or lack thereof) when radiotherapy treatments utilize photons [Wenzl & Wilkens, 2011].

In summary, oxygen concentrations play a critical role in the survival and death of cells when exposed to ionizing radiation. Particularly, the use of photosynthetic microalgae might play an important role in providing the necessary oxygen for both RT and PDT to work more effectively. In addition to therapies, the presence of oxygen can help in the normal processes of the body such as in cicatrization and vascularization.

1.3.2 Pre-Clinical and Clinical Applications

There has been ample research on the application of photosynthetic microalge in in-vitro studies as well as in animal studies that have been performed in order to determine if it is possible to reduce hypoxia without generating a negative immunological response. A study was performed to determine if the algae based scaffolds are biocompatible enough to help mice cure deep skin wounds [Schenck et.al, 2015]. It was found that the amount of partial oxygen concentrations were about 50 times higher than with using pressurized gas. It was found that the scaffolds with *Chlamydomonas reinhardtii* did not generate a negative immune response. In this study, it was possible to determine that microalgae do not cause a negative immune response. [Schenck et.al, 2015]. All of this paints a promising picture for the use of these techniques in a clinical context. In Figure 10 what is shown is that in animal trials the inclusion of a photosynthetic microalgae in scaffolds does in fact increase the amount of blood vessels in the area of injury.

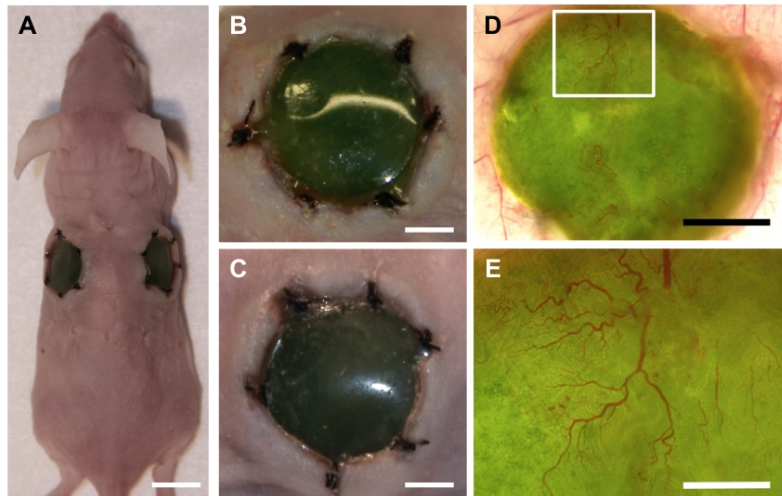


Figure 10: Engrafted scaffolds in a mice for bilateral skin wounds. Each of the sub-images show a close up of the scaffolds. For instance B and C are a close up of A, while D and E are a close up of B. It can be appreciated that the D and E sub-images shows a great deal of vascularization. [Schenck et.al, 2015]

In an in-vitro study, mice brains were dissected and the cortical assays were immersed in a TAP (Tris-acetate-phosphate) media with a culture of *Chlamydomonas reinhardtii*. The TAP media contains a wide range of chemical compounds but the main ones are: Ammonium Chloride, Tris-base, Potassium Phosphate, Magnesium Sulfate and Disodium Salt. It was found that photosynthetic active culture of this microalgae can indeed produce enough amounts of oxygen to meet the elevated metabolic demands of a slice of cerebrocortical tissue without the any short or medium term toxic effect. The conclusion of this study was that an oxygen producing microalgae could potentially be used to rescue avascularised brain tissue in humans after a brain injury [Voss et.al, 2021].

The use of microalgae plays a critical role in biological experimental studies. The uses and applications of photosynthetic algae are quite diverse. In a recent clinical study, researchers put this idea to test in a human beings. In this particular case, eight patients with full thickness skins wounds were implanted with photosynthetic scaffolds for dermal regeneration. The specific microalgae used corresponded to *Chlamydomonas reinhardtii* and it was found that after 90 days full tissue regeneration was achieved, making this the first attempt to treat patients with photosynthetic cells [Obaid et.al, 2021]. In Figure 11, it can be clearly observed that the wound healing evolution through the use of topically applied microalgae produces a positive clinical outcome for a deep skin wound of a real patient.

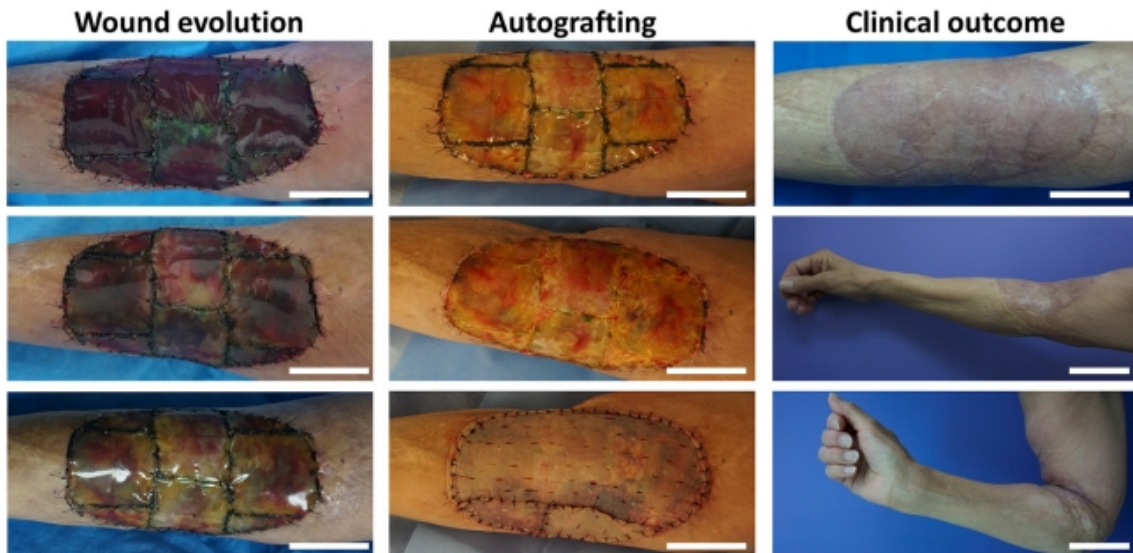


Figure 11: Recovery from a deep skin wound evolution from the moment when the microalgae implants where applied, to autografting a few weeks later and finally the recovered wound after 90 days [Obaid et.al, 2021]

The pervasive presence of skin injuries and other similar chronic wounds in a subsection of the population has led to a growing interest in the biomedical community to try to experiment with alternatives that lead to a better cicatrization and elimination of bacteria. It is well known that

when such damage to the skin occurs, macrophages play a central role in all stages of wound healing [Delavary et.al, 2011]. Furthermore, it is known that when healing of wounds occur, the density of new capillaries is up to 10 times denser than in normal non-healing tissue [DiPietro, 2016]. For this reason the availability of oxygen plays a critical metabolic role. Without it, the cells involved in the wound cannot optimally be repaired and that might lead to bacterial or other type of complications due to a longer exposure to the environment. Fortunately, new research has allowed the possibility of using photosynthetic microalgae topically applied over the wound to generate oxygen in an in-vivo fashion. Preliminary studies have shown that microalgae applied directly to the wound in a gel can be up to a 100 times much more efficient than topical gaseous oxygen for curing skin wounds in diabetic mice [Chen et.al, 2020]. These types of discoveries paint a very promising picture for future clinical trials and applications that could help people suffering from skin diseases or from ulcers.

It can be said that photosynthetic microalgae might be used in a collaborative manner alongside RT and PDT. In a recent study, it was found that genetically engineered microalgae can help with the oxygenation of an hypoxic tumor therefore making the radiotherapy session more effective given what we know of the oxygen effect for MeV photon treatments. After this happens, the chlorophyll is released and it itself acts as a PS that then my be activated by red laser light to start a PDT session, this is very clearly illustrated in Figure 12 [Qiao et.al, 2020]. The importance of this study rests in the fact that indeed it has been proven that it was viable to combine RT and PDT in the same session.

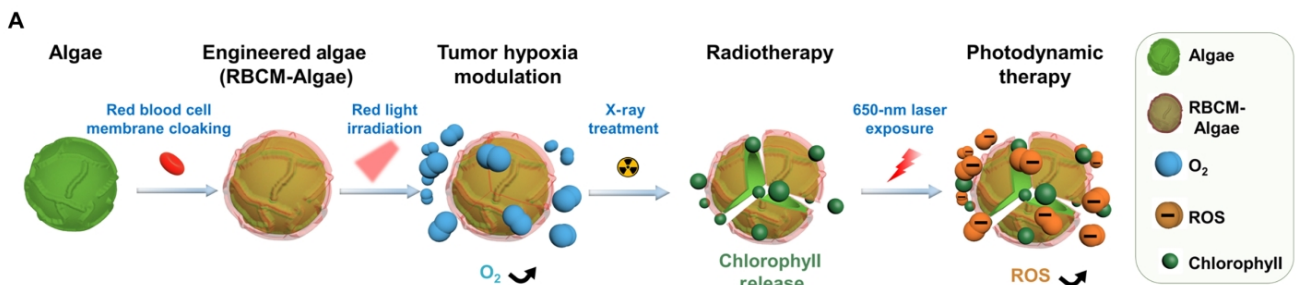


Figure 12: Depiction of the step by step bio-engineering process of a bio-compatible microalga that is used to decrease hypoxia in a tumor for a RT treatment followed by a PDT session [Qiao et.al, 2020].

1.4 Biomedical Research with Animals

Since antiquity in ancient Greece, physicians have dissected vertebrate animal species for anatomical studies in order to get an insight into the human body [von Staden, 1989]. Important ancient historical figures such as Aristotle, Docles, Praxagoras (4th century B.C.E) performed exploratory surgery on live animals [Maehle & Tröhler, 1987]. For the ancient Greek society, the use of live animals experiments did not raise relevant moral questions. It was during the Dawn of the Enlightenment period in Europe during the 17th and 18th Centuries that this type of experimentation became more common once again. Other contemporary philosophers

such as Spinoza (1632-1677) said about animals that even though they could feel we should: “*use them as we please, treating them in a way which best suits us; for their nature is not like ours*” [Spinoza, 2006 (reprint) in Franco, 2013].

It was in Great Britain during the 19th century that the first animal protection society was formed to ban animal experiments under the leadership of Frances Power Cobbe (1822 - 1904) [Franco, 2013]. After this, a middle ground that ethically respected the well being of animals and at the same time promoted the progress of biological research was promoted by many scientists including Charles Darwin (1809-1882). In the 21st century the ethical institutional framework that we consider as paramount and indispensable in our laboratory settings is in fact a vestige of a long tradition of a philosophical dialectic.

For example, the use of animals for testing of cosmetic products has been prohibited in the United Kingdom, but it is generally accepted that animals can be used for medical research if the reasons are justified [Morton, 1999]. For over 60 years the principles of the three R's: Refinement, Reduction and Replacement have been the main ethical framework applied for conducting animal research. The design of this principle: “*Has been used as a policy tool to ameliorate the suffering animals and to reduce the use of animals in research [...]*” [Crespi-Abril & Rubilar, 2021]. For this particular reason, it is important to take animal suffering very seriously. For instance, embryos from *Gallus Gallus Domesticus*, commonly known as a farm chicken, are a commonly used as biological assays. For chicken embryos, when they don't surpass a certain developmental stage they don't experience pain or suffering [Case Western Reserve University, 2008]. In such guideline it is explicitly said that chick embryos younger than EDD15 are assumed to be unable to experience pain. In Figure 13, the daily changes in weight and form of a developing chick embryo are shown.

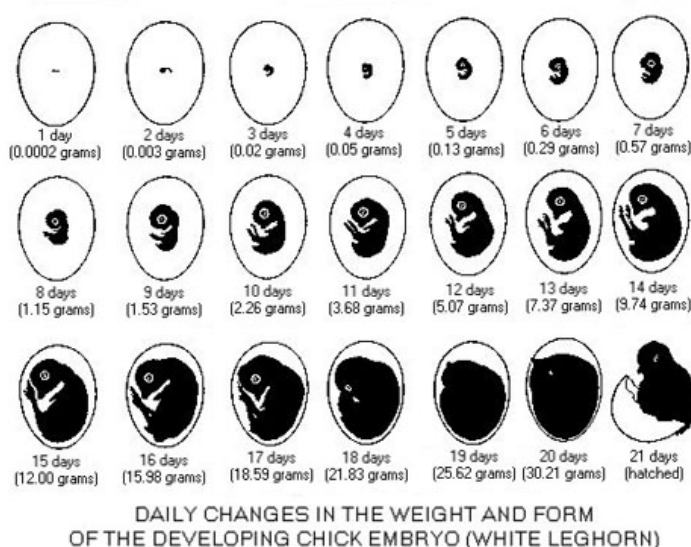


Figure 13: Daily changes in development of chick embryo [Mississippi State University, 2022]

1.5 Chorioallantoic Membrane (CAM)

Due to the ethical constraints that animal experiments entail, a very attractive alternative has been the realization of experiments in chorioallantoic membrane (CAM) assays of chicken eggs. The CAM is a highly vascularized, non-innervated extra-embryonic membrane that can be effectively used for experiments such as the engraftment of tumor cells [Kunz et al., 2019]. In recent years, the advancement of medical and bio-engineering research has been expanding at an ever growing pace. In particular, the role that vascularization networks have in the areas of transplant biology, cancer research and drug development [Nowak-Sliwinska et.al, 2014].

In mammals, the allantois extends extra embryonically from the ventral wall of the endodermal hind-gut. The CAM develops similarly in the egg, although in birds it fuses with the chorion to form the chorioallantoic membrane. At first, the CAM is avascular but very quickly it acquires a hierachic complexity of arteries and veins. Also, it worth mentioning that the growth of the CAM starts at EDD3, is completed by day EDD10 and it is fully differentiated by day EDD13 [Nowak-Sliwinska et.al, 2014]. The CAM has the functionality of a respiratory organ as the interchange of gases of the chicken embryo occurs within it. It also has a fully developed lymphatic system which holds a lot of similarities to lymphatics in mammals. [Papoutsi et.al, 2001]. One of the most important advantages of using CAM as a biological models is that it develops in a very short time from an avascular membrane into a structure with complex vascular networks that cover most of the entire inner surface of the shell. In Figures 14 an anatomical depiction and location of the CAM within the egg is shown.

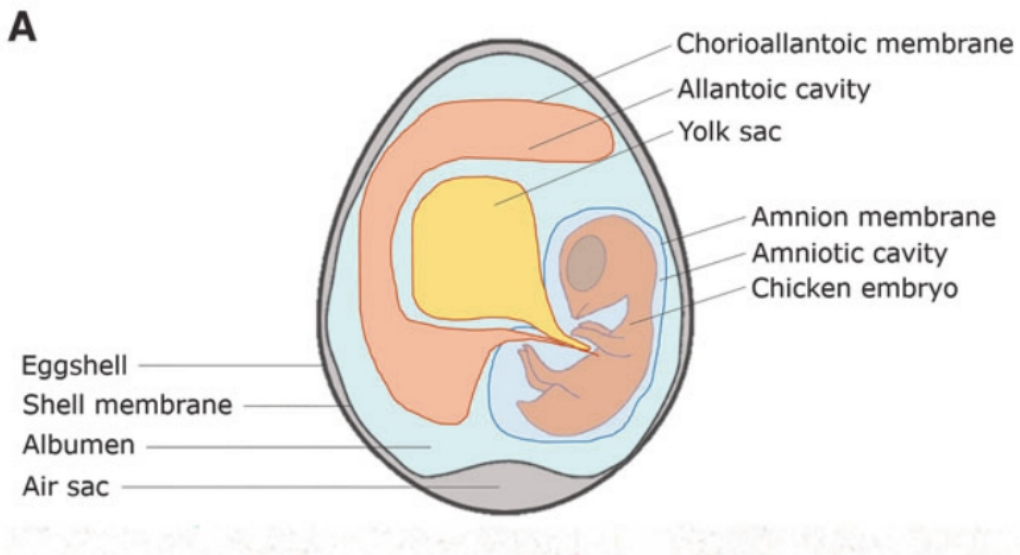


Figure 14: Anatomical depiction of a developing *Gallus gallus domesticus* embryo inside an egg [Merckx et.al, 2020].

In Figure 15, what can be seen is the growth of the CAM according to its developmental stage. It can be clearly appreciated that the growth and vascularization grows considerably in just over a week of development which in turn is a great advantage for any experimentalist wishing to study this phenomena.

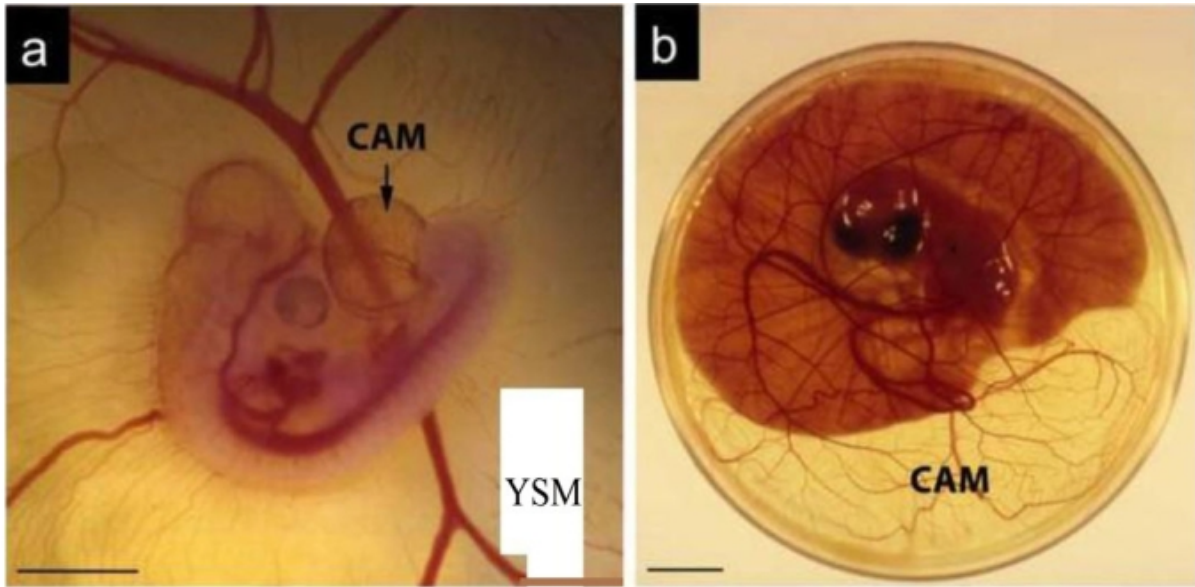


Figure 15: Extra-embryonic structures of chicken embryo. Image a) shows embryo at 4 days post-fertilization with the CAM and the YSM (Yolk Sac Membrane). Image b) shows a stage 12 days after fertilization where the CAM volume has grown considerably [Nowak-Sliwinska et.al, 2014]

Amongst the disadvantages, there are certain reagents that are not fully compatible with avian species such as antibodies, cytokines and primers. Also, there exist technical difficulties with grafting due to vasculature growth. [Nowak-Sliwinska et.al, 2014]. There are ways to develop this model, which involve the presence or not of the eggshell. In-ovo cultivation significantly improves the survival of the embryos compared to ex-ovo methods. This is mainly due to the rupture of the yolk membrane during or after the culture. In in-ovo cultivation, the fertilized eggs are transferred to the incubator with a rotating mechanism for three days. In the case of ex-ovo cultivation it is quite important to be careful of the humidity conditions. It is known that poor humidity conditions in this type of cultivation induce considerable cell division and keratinization of the upper CAM epithelial layer. This makes it difficult to deliver soluble molecules to the underlying vascular system [Nowak-Sliwinska et.al, 2014]. It is for this reason, that for this experiment the cultivation method will be in in-ovo, as to prevent this type of problems, especially because we are dealing with topically applied solutions. The difference in cultivation methods can be visually appreciated in Figure 16, where the presence or not of the egg shell determines the methodology of the experiment.

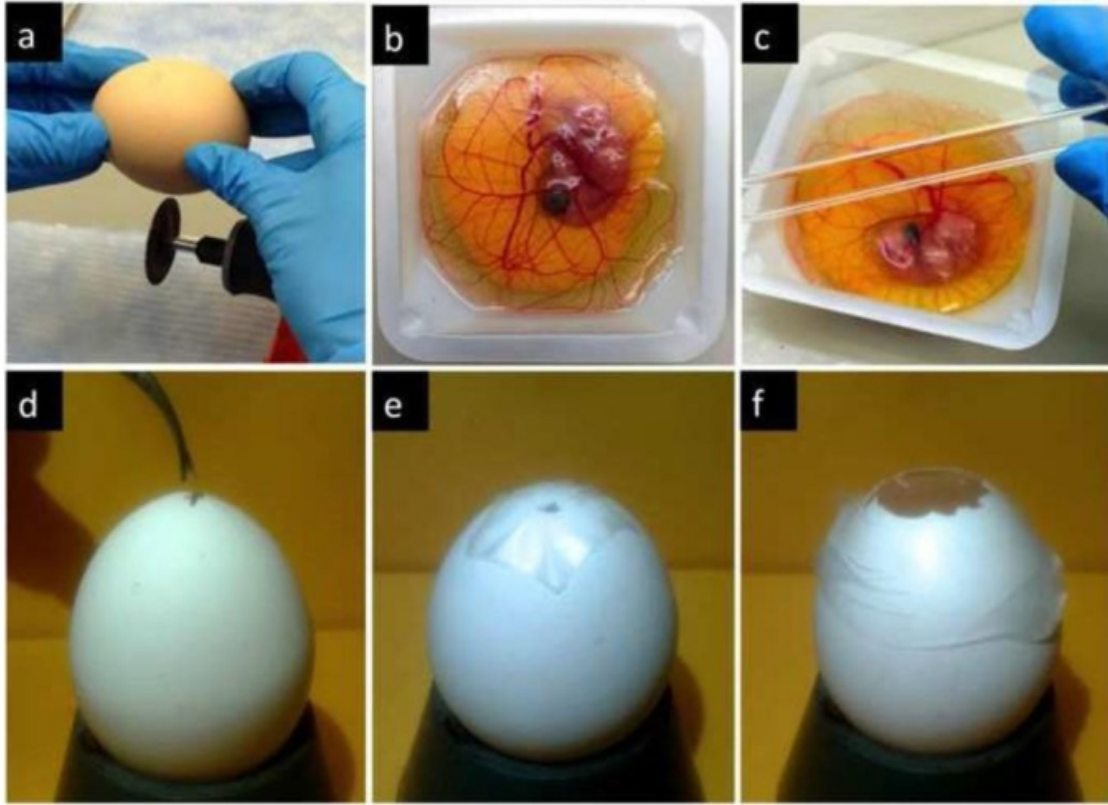


Figure 16: Cultivation methods for the chicken CAM. In the upper half they perform an ex-ovo protocol. In the lower half the perform an in-ovo protocol such as the one that we will do in our own experimental trials [Nowak-Sliwinska et.al, 2014]

A particular use of CAM models has been to study tumor growth and metastasis. It has been observed that tumor cells placed on the CAM follow all the steps of tumor progression: growth, angiogenesis, invasion, extravasation, and metastasis. Drug delivery has also been another important area of research involving the chicken CAM due to its condition as an intermediate step between in-vitro and in-vivo pre-clinical methodologies [Vargas et.al, 2007]. As an example, growth factors such as the distinct variants of VEGF known to induce angiogenic activity have been researched in great detail in the CAM [Steffens et.al, 2004]. Anti-angiogenic drugs have also been studied using the CAM. These kinds of drugs are useful when attached to a receptor that localizes itself in tumor sites to therefore damage the cancerous tissue's vasculature. Nanoparticle delivery technology has been shown to arrest tumor angiogenesis as well as renal cell carcinoma growth [Yalcin et.al, 2009]. This technique is directly related to the application of PDT and its consequences in local cellular death.

Moreover, the great diversity of imaging options makes it an ideal model to study the vasculature. Some of the modalities include: microscopy, MRI and PET. Also, due to the transparency of the superficial layers any visible wavelength can potentially be used for fluorescence imag-

ing. In Figure 17, different imaging techniques used to visualize the chicken CAM vasculature development are presented.

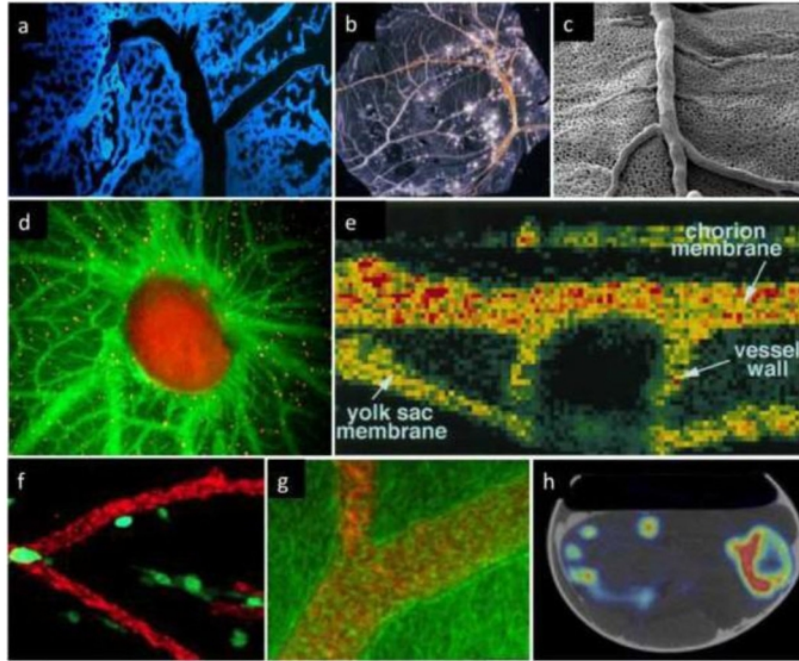


Figure 17: Selected imaging techniques used to visualize the chicken CAM vasculature. Technique such as a) confocal microscopy, b) light microscopy, c) scanning electron micrscopy, d) fluoresence microscopy e) Doppler tomography, f) fluorescent tagged LCA, g) Laser Scanning microscopy and h) PET and CT images

Finally, the specific effect that oxygen has on angiogenesis is of vital interest as it has direct translational implications to a clinical context. It has been found that when a chicken embryo is directly faced with hypoxic stress in a moderated and controlled manner angiogenesis in tissue naturally begins. Concretely, a reduction of 17% in oxygen concentrations had an effect on the circulatory system that led to an increase in blood oxygen carrying capacity [Druyan et al., 2018]. In a clinical context, the process of wound repair is heavily influenced by the body's angiogenesis abilities. For instance, in healing wounds, new capillaries grow into a network that is up to 10 times denser than in normal non-healing tissue. The creation of new capillaries is regulated by growth factors such as VEGF. These growth factors are positively produced as a response to controlled hypoxic conditions [DiPietro, 2016] and can influence certain therapeutic responses.

Based on all the aforementioned background, it is possible to study the effects of PDT and the changes of vascularization using the CAM.

1.6 Motivation

The motivation of this thesis is to understand how oxygen variations affect the vasculature of a chicken CAM and how these changes in oxygen could in turn affect the efficiency of PDT treatments.

1.6.1 Primary Objective

The first objective of this work was to analyze in solution the ability of light to interact with photosensitizer compounds, in this case methylene blue and microalgae individually and in combination. Analysis of the absorption spectrum and its degradation were made to understand the individual interaction and to know if their mixture affected the photobleaching rate.

1.6.2 Secondary Objective

The second objective of this study was to analyze the influence of microalgae and light parameters in the angiogenic process of the CAM model. For this, multiples steps were performed using the corresponding number of eggs for the control and experimental groups. The working hypothesis is that indeed the presence of microalgae promotes the creation of new blood vessels through the creation of molecular oxygen in the CAM. In order to determine this, the resulting images of the capillary network were analyzed using a specialized imaging software in order to quantitatively measure them.

1.6.3 Tertiary Objective

The third objective was to determine the optimal combination of PS, light and algae to ascertain the highest local cellular death from photodynamic therapy. The main idea was to find which temporal combination of parameters leads to the best result of local cellular damage by PDT. The working hypothesis is that there is a specific combination of parameters of algae, PS and light that leads to higher local damage.

2 Methodology

2.1 Light Source

Different light sources were used in this study. For the liquid solution experiments, a device with 24 LEDs, with emissions centered at 3 different wavelengths (450, 530 and 630 nm) was used, emitting light homogeneously. This device was developed to be used with 24 well plates, where each well receives the equivalent of approximately 50 mW/cm². This prototype present current controllers and heat dissipation modules and was developed by the Technological Support Laboratory (LAT) of São Carlos Institute of Physics, University of São Paulo, Brazil. For the CAM experiments, a device LINCE (MMOptics, Brazil) was used, which is composed of an array of LED, emitting at (630±10) nm, arranged in a circle at the tip of the probe, and a piece of light collimator to focus the produced beam. The irradiance was set up for 50 mW/cm² and the distance between the probe and the sample was 1.7±0.1 cm to delivery 30 mW/cm² on the CAM surface.



(a) *Biotable* Blue Configuration.



(b) *Biotable* Green Configuration.



(c) *Biotable* Red Configuration

Figure 18: Three color settings for the *Biotable* device

In order to determine the irradiance of the *Biotable* and the LINCE light sources a power meter (Model DM100D) from ThorLabs was utilized to determine such values (See Results section). This step was critical to ensure the irradiance values reported by the manufacturer.

2.2 Characterization of PS and Microalgae

Before starting with the biological experimental part of the thesis with the CAM model it is of upmost importance to characterize the properties of the PS and microalgae just by themselves. For this reason, different measurements were performed with a spectrometer in order to determine how they degrade as a function of light fluence. In this study, three different characterizations were performed: 1) spectra and photobleaching effect of PS, 2) spectra and photobleaching effect of microalgae and 3) spectra and photobleaching effect of combination of PS and microalgae.

2.2.1 Absorbance Spectra and Photobleaching of PS

The first part of this characterization consisted on the measurement of the absorbance spectra of methylene blue (MB) using the *Biotable* device. The first thing that was done to achieve this goal was to prepare the MB stock solution. Based on previous empirical measurements performed by the research group of Prof. Fuentealaba it was found that 0.3 mg of MB/mL of water was a good starting point. The process was the following: the required amount of MB was measured in a well-calibrated digital balance and was transferred to a 10 mL glass jar. After that, with a 1000 μ L pipette 5 mL of water was added to the jar. With a sonicator the jar was mixed for about 60 seconds to effectively disintegrate any leftover lumps of the MB powder. After doing this we proceeded to perform a set of trials to find the optimum dilution as to achieve a spectra within the bounds of 0 and 1 AU (Absorbance Units). It was found that for the selected original stock concentration a dilution by a factor of x100 was ideal. After finishing this trials, the rest of the measurements were performed.

The procedure for doing the measurements was the following: 1) the diluted MB solution was placed in the wells (1 mL per well) of the *Biotable* and irradiated for a given number of minutes, 2) the solution was then placed in a UV-cuvette and 3) the cuvette was placed in a spectrometer (Analitica Weisser 8453 from Hewlett Packard) and analyzed with the HP 845x UV-Visible System software. From there, the spectra were obtained (See Figure 24). To reduce the uncertainty of the data points two sets of measurements were done.

The second part of the characterization consisted on the study of the photobleaching effect of MB. This step was very closely intertwined with the measurement of the absorbance spectra. Specifically, what was done was first to determine the characteristic peak of the spectra. In this case it was found that for 664 nm there was a distinct peak. For each greater light exposure time the peak noticeably decayed. Given this fact, it was possible to create a new parameter space where the normalized AU was plotted as a function of fluence. With this new curves it was possible to quantitatively determine how strong was the decay of MB. Another aspect that

is worth mentioning is that for the initial measurements of the spectra the concentration at which the irradiation happened was too low. To solve this, what was done was to introduce an extra step in which the irradiated solution by the *Biotable* had higher concentration. In this particular case, a dilution of x40 was done to the MB stock solution, then it was irradiated and then another dilution of x2.5 was done when mixing it with water in the cuvette. This step allowed for more differentiated photodegradation curves (See Figure 27). After all of this was done, it was possible to fully characterize the behaviour of MB due to its interaction with light. In the next subsection we will discuss how this same characterization procedure was performed on the microalgae.

2.2.2 Absorbance Spectra and Photobleaching of Microalgae

Continuing with the description of the methodology, the next experimental step that was done was to measure the absorbance spectra and the photobleaching of the microalgae by itself. The procedure was very similar to the one described above but, of course, there were some important differences. Firstly, the preparation of the microalgae was not done in our lab but was donated to us by Prof.Tomas Egaña's research group of the IIBM. The microalgae that was tested was *Chlamydomonas reinhardtii* which effectively converts visible light into molecular oxygen. Based on measurements using the optical density of the solution it was determined that the concentration/mL was 10^6 microalgae. Based on this initial stock concentration it was found that a dilution of x5 was needed to obtain absorbance values between 0 and 1.

The procedure for doing the measurements was very similar to the one done before for MB. In this case it followed that: 1) the diluted microalgae was placed in the wells (1 mL per well) of the *Biotable* and irradiated for a given number of minutes, 2) the solution was placed in an UV-cuvette and 3) the cuvette was placed in the spectrometer. As with the MB case, two sets of measurements were performed.

For the characterization of the photobleaching effect of the microalgae it was less of a straightforward process. This was primarily due to the fact there was not a single characteristic peak in the spectra (See Figure 30). Nonetheless, it was decided that 695 nm was the appropriate peak to select and base the decaying curves. Following the example of MB, a high and low concentration solutions were prepared to see if there were differences in the relative values of decay. For this, what was done was first to prepare a solution diluted by a factor of x5 from the stock and proceeded to the irradiation and subsequent measurement with the spectrometer. Likewise, a higher concentration solution diluted by a factor of x2.5 at the moment of irradiation was used. For all of the dilutions in this section TAP was utilized instead of water as to replicate the conditions in which the microalgae ideally live thrive upon.

2.2.3 Absorbance Spectra and Photobleaching of Combination

The third and final part of the methodology regarding the characterization deals with the combination of the PS and microalgae in the same solution. This step consisted of using the known

dilution factors to properly add the corresponding amounts of each of them before irradiating them. The medium used as a diluting agent for the combination of PS and microalgae was always TAP. As with the previous two steps, the procedure for performing the measurements consisted on the same three steps. The dilution factor for the MB solution at the moment of irradiation was x40 while for the microalgae solution was x2.5. Nonetheless, it seemed that the MB had a stronger impact on the combination and thus the peak of this new spectrum was located at 664 nm but with other signature curves in the middle and lower wavelength values. This effect can be appreciated in Figure 34.

2.3 In-vivo Experimental Setup

2.3.1 CAM Model

The CAM model is already well described in the literature [Nowak-Sliwinska et.al, 2014]. Given that we were dealing with chicken embryos ethical questions naturally arise. For this it was necessary to clear out some requisites by the ethics committee of the university. After providing all the necessary evidence that the experiment would not entail animal suffering we were given an approval document with I.D. 220107006 that in fact certified us to experiment on chicken embryos. The chicken eggs were obtained by donation from local producers Avícola Chorombo S.A. with its distribution headquarters located in Pirque, Chile. On the first embryo development day (EDD), the eggs were cleaned with alcohol 70% before being placed in the incubator at 37 °C. During EDD1 and EDD2, the eggs were in constant slow rotation motion– half period each 30 min. On EDD3, a small hole in the shell was made to remove 3-4 mL of albumin with a syringe and the rotation will be interrupted. A window of 2 cm^2 was opened and sealed with adhesive tape until the day of experiment. All experiments were performed before the EDD14, which means that no animal pain was involved in this project due to the lack of innervated networks in the CAM [Ribatti, 2016]. A digital egg incubator with capacity of 50 eggs was utilized to provide with them with the right temperature and humidity conditions throughout the incubation period and a slow sideways rotation for the first three days. The image of such device is shown below in Figure 19.



Figure 19: Electronic egg incubator

2.3.2 Microalgae and PS in CAM

The CAM model by itself ideally develops a robust vascular network capable of supplying the growing embryo with the oxygen it requires to develop. In this thesis work the idea was to test if foreign agents such as microalgae and/or MB can affect this growth. To test this idea different groups were chosen as to explore some of the possible combinations. For all the cases 200 μL of the respective solution was added over all the surface area of the CAM. Only in the case of the combination of MB and microalgae 100 μL of each solution was poured topically over the CAM. Another aspect to contemplate is the time between the application of the solution over the CAM and the delivery of light on it. For the case of the microalgae the Drug-Light Interval (DLI) was of 0 minutes while for the PS it was of 20 minutes.

Given that we are dealing with a biological agent, it is important to take the precautions to avoid contamination of our samples. For this reason, a bio-safety cabinet was used at all times when doing the manipulation of both the eggs and the microalgae. The way this bio-safety cabinet works is by circulating laminar layers of air that prevent the contamination from airborne particles in the environment. Once the machine is turned on, one must wait a couple of minutes to ensure the stability of the air flow. Also, the sliding window is always at a height

such that only the hands are able to get inside the cabinet. As a manner of hygiene and control a UV light is turned on for 30 minutes to guarantee the cleanliness of the inside of the cabinet.



Figure 20: Bio-safety cabinet

2.3.3 Acquisition and Analysis of Images

A USB Digital Microscope® (AVANTGARDE, China) was used and all images were captured before, immediately after each illumination and at 0.5 hours, 1.5 hours, 7 hours and 24 hours later. The camera was positioned over the eggs for a better visualization of blood vessels on the CAM. All components were positioned inside the laminar flow chamber to avoid contamination. All images were analyzed with the software ImageJ to quantify the vascular effect caused by the oxygenation and/or PDT. The number of ramifications in the pictures was the parameter which was used to measure the growth in vascularization. An example of such measurement can be seen in the screenshot depicted in Figure 21.

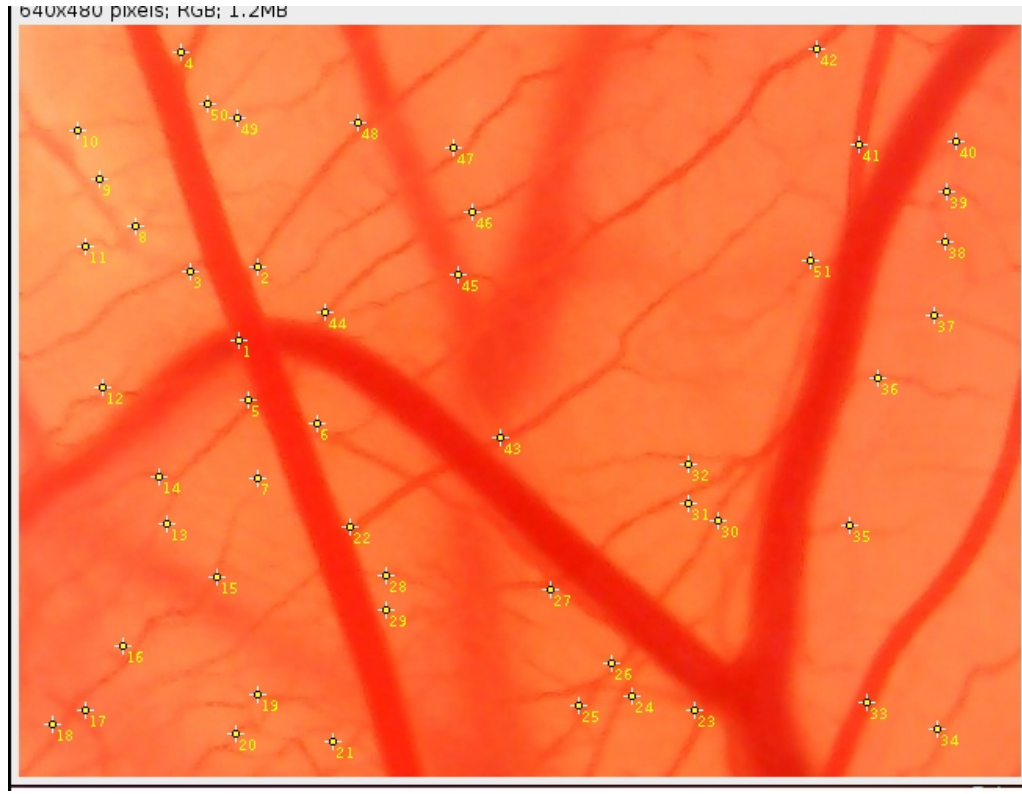


Figure 21: Analysis of the ramifications of a CAM using the ImageJ software.

2.3.4 LINCE Device

In order to deliver the irradiance of 30 mW/cm^2 the LINCE device was used. As described above, the device emits at 630 nm and has an interactive screen where it is possible to adjust certain settings. To guarantee the proper delivery of the light one of the movable arms was attached to a support system that allowed it to be located just above the eggs. Once the alignment between the arm and the egg was ensured the setting was set to an illumination time of 5 minutes. Whilst emitting the light the adhesive tape was removed so the photons could enter through the egg's window directly. The experimental setup inside the bio-safety cabinet was such that it allowed for all the devices and samples to be in a clean environment to avoid contamination. Exactly this can be seen in Figure 22.

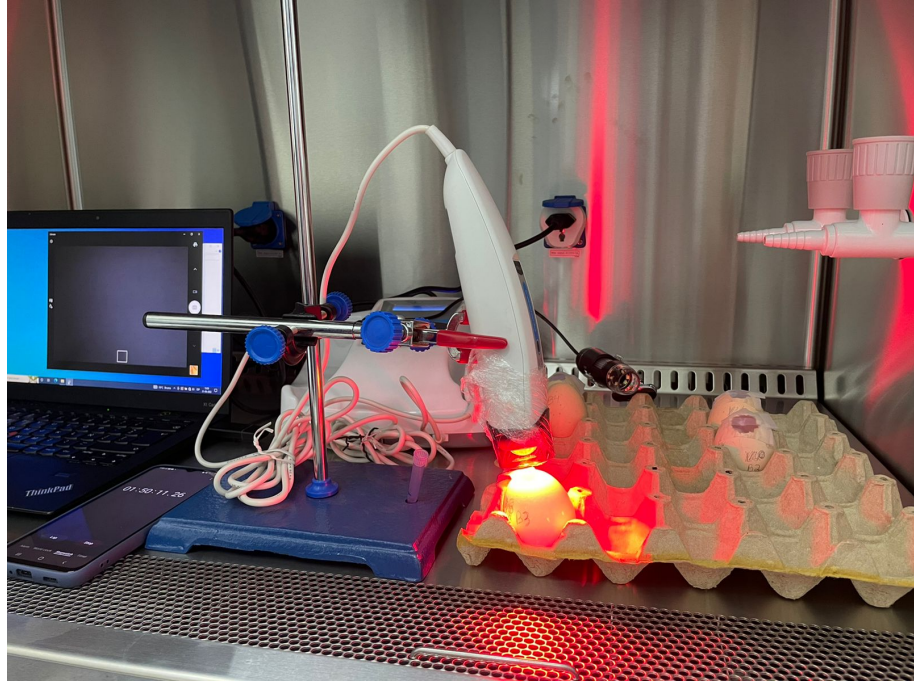


Figure 22: Experimental setup inside the bio-safety cabinet with the computer, the illumination device and an egg.

2.4 Experimental Outline

The methodology of this study consists of four independent but causally related parts. Each of these parts contain 4 groups of at least 3 fertile chicken eggs seeking to explore the effect of MB, microalgae and its combination at different days of development. Control groups were included as to determine the effect of each of the components (Light, MB and microalgae). The groups were designed to determine the best parameters in relation to:

- 1) Only Light
- 2) PDT Groups
- 3) Microalgae Groups
- 4) Oxygen-Rich PDT Groups

2.4.1 Only Light

For the first part we irradiated chicken eggs of EDD12 with one wavelength (red at 630 nm) and three different light irradiances: 30 mW/cm^2 for 5 minutes, 30 mW/cm^2 for 10 minutes and 10 mW/cm^2 for 30 minutes with these being equivalent to 9 J/cm^2 , 18 J/cm^2 and 18 J/cm^2 , respectively. The objective was to confirm the findings of the literature in which light delivery alone at these doses did not heavily affect the vascularization network. For all the cases of

illumination the device used was the *LINCE* device. The parameters are summarized in Table 1 below.

Plan of illumination	Time	Group
30 mW/cm^2	(5 mins)	Group OL1
30 mW/cm^2	(10 mins)	Group OL2
10 mW/cm^2	(30 mins)	Group OL3
Control		Group C

Table 1: Table showing the parameters for the case of only irradiating the CAM.

All experimental trials were performed only with light resulting in 4 groups with 5 eggs each. The total for this first part therefore utilizes 20 eggs.

2.4.2 PDT Groups

MB was applied topically into the CAM to study the changes in the vascularization network via PDT. Different combinations were tried out, to have a better understanding of the processes happening within the CAM. These combinations were the following: PDT, only light, only MB and a control group. They were tested at different days of development to determine the difference the stage of embryonic maturity has on the effectiveness of the therapy. For the case of MB alone, this was done to guarantee that the used concentration of 0.3 mg of MB/mL did not had an effect by itself. For all of the groups the same light dose (30 mW/cm^2 for 5 minutes) was used. The summary of this is shown in Table 2.

Item	Group	Days
Control	Group 4	EDD8
Only MB	Group 3	EDD8
Only Light	Group 2	EDD8
MB + Light	Group 1	EDD8
Control	Group 8	EDD10
Only MB	Group 7	EDD10
Only Light	Group 6	EDD10
MB + Light	Group 5	EDD10

Table 2: Table showing the parameters for the case of applying the PDT to the CAM.

As part of the standardized procedure for all the groups dealing with PDT the DLI was always set to 20 minutes. All the manual handling of the eggs going from the topical application of the MB, the irradiation and the taking of pictures was done in the bio-safety cabinet. This meant that for that time the eggs were exposed to room temperature of about 27 degrees Celsius which is about 10 degrees less than its incubation temperature. For this reason, only a subsection

of the eggs were used at the same time to avoid thermal stress. After the experimentation was completed they were returned to the egg incubator. The experimental trials that were performed resulted in a total of 8 groups of 5 eggs each, totalling in 40 eggs.

2.4.3 Microalgae Groups

Algae was applied topically into the CAM as it was done with the MB of the previous part. Similarly, different combinations were tried out. In this case, the new groups were the microalgae + light and only microalgae groups for days EDD8 and EDD10. This resulted in 4 groups of 5 eggs each making the total number of eggs for this section 20.

Item	Time	Group	Days
Algae + Light	(5 mins)	Group 9	EDD8
Only Algae	(5 mins)	Group 11	EDD8
Algae + Light	(5 mins)	Group 13	EDD10
Only Algae	(5 mins)	Group 15	EDD10

Table 3: Table showing the parameters for the case of applying the microalge to the CAM.

All experimental trials were performed with algae and light resulting in 8 groups with 5 eggs each. The total for this first part therefore utilizes 40 eggs.

2.4.4 Oxygen-Rich PDT Groups

Now, with the best light and algae parameters, an oxygen-rich photodynamic therapy tests was performed. The methodology for this step was no different than the previous ones. The eggs were placed inside the cabinet and the MB and microalgae were topically applied over the cam. The total volume was always 200 μL . The DLI time when applying the PS was always 20 minutes whilst the delivery of light after the application of the microalgae was immediately after. The MB and microalgae concentration and the light doses were the same as the ones established for individual therapies.

To determine the combination of algae oxygenation and PDT effects, the order of application was studied. The permutations tested were:

- a) Algae + Light \rightarrow PS \rightarrow DLI \rightarrow + Light
- b) Algae + PS \rightarrow DLI \rightarrow + Light
- c) PS \rightarrow DLI \rightarrow Algae + Light

The experimental trial performed for this part will result in 3 different groups for two different development days to analyze if this parameter would interfere in the vascular effect of CAM.

3 Results and Discussion

3.1 Characterization of Parameters

In this section the characterization of the PS and the microalgae will be presented. This procedure is of utmost importance because when dealing with complex biological systems the implications of introducing a new variable might entail having second order effects or unknown feedback processes. For this reason, we must know exactly how these variables behave independently under different circumstances. For this part of the thesis four variables were characterized:

- 1) Biotable Irradiance
- 2) PS Photobleaching
- 3) Microalgae Photobleaching
- 4) PS + Microalgae combination

3.1.1 Biotable Irradiance

A very important part of the characterization of the experimental setup is the understanding of the parameters of the LED irradiation instrument. The custom-made *Biotable* instrument courtesy of the University of São Paulo (São Carlos, Brazil) provides us with an almost homogeneous emission of visible light for three distinct wavelengths: Red (630 nm), Green (516 nm) and Blue (450 nm) and four different irradiances configurations. The measurement of the peak emission wavelengths was performed with the atomic absorption spectrometer OceanOptics USB2000 using the software Oceanview 1.6.7 Lite. The power meter (Model DM100D) and the photodiode power sensor (Model 5121c) were both from ThorLabs (New Jersey, USA). Table 4 corresponds to the measured power in mW for the different configurations. All the calculations presented correspond to the color red (630 nm) of the instrument.

Intensities	Trial 1	Trial 2	Trial 3	Trial 4	Trial 5	Average (mW)	Error (mW)
1st	33.7	36.1	34.0	28.1	34.9	33.4	1.4
2nd	34.5	27.8	26.8	30.6	26.1	29.2	1.5
3rd	24.3	24.2	26.3	19.8	24.7	23.9	1.1
4th	10.4	10.8	16.5	10.1	11.6	11.9	1.2

Table 4: Biotable irradiances configuration

In this thesis, the only two relevant quantities correspond to the 1st and 2nd intensity levels of the red light configuration. These quantities can be converted to irradiance if the diameter of the photodiode power sensor is considered. The circular powermeter diameter is 9.5 mm, which in turn corresponds to a surface area of 0.71 cm^2 . This in turn gives us the irradiance for the first configuration level:

$$I = \frac{33.4 \text{ mW}}{0.71 \text{ cm}^2} = 47.0 \frac{\text{mW}}{\text{cm}^2} \quad (1)$$

And the irradiance for the second configuration level:

$$I = \frac{29.2 \text{ mW}}{0.71 \text{ cm}^2} = 41.1 \frac{\text{mW}}{\text{cm}^2} \quad (2)$$

For the calculation of the photodegradation curves both for the PS and the microalgae (and their combination) it was required to have the value of the fluence, which is the multiplication of the time by the irradiance values. It is worth mentioning that for the measurement of the photodegradation of the PS and microlagae the multi-well grid was used (Figure 23) when performing the irradiation. The great advantage of this is that the irradiation was very homogeneous across wells and the quantity of liquid for each of them was measured with a micro accuracy pipette.



Figure 23: Biotable instrumental setup

3.1.2 PS Photobleaching Interaction

Different light irradiances were used to see how the degradation of the exposed MB changed as a function of the fluence [J/cm^2]. A 3 mL of solution was irradiated with red light (630 nm) of two different intensities in a multiwell plate. The irradiated 3 mL solution with a concentration of 0.3 mg/mL of MB with a dilution factor of x100 was then extracted from the multiwell plate

with a pipette and placed on a quartz cuvette. This cuvette was then placed in a spectrometer (Analitica Weisser 8453 from Hewlett Packard) and analyzed with the HP 845x UV-Visible System software. In Figure 24, an example of the spectral profile of MB for different times after illumination is shown at the initial MB concentration of 0.3 mg/mL. It can be clearly be appreciated that for a selected prominent spectral peak there is a clear degradation in the value of the absorbance units, which in turn can be used to plot the photobleaching curves as a function of fluence.

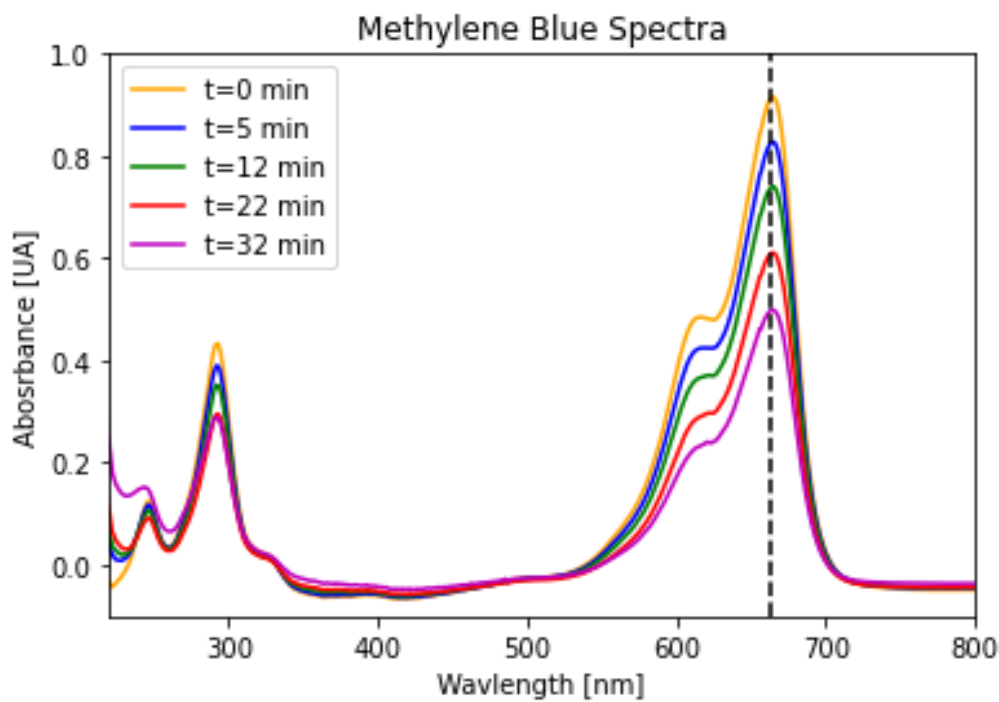


Figure 24: Example of a spectral profile of MB for the visible light range with a characteristic peak located at 664 nm after different illumination times of 47 mW/cm²

Moreover, in Figure 25 it can be appreciated that the spectral profile we obtained was very similar to the one obtained in the literature, confirming that MB was freshly prepared and corresponded to the same molecule.

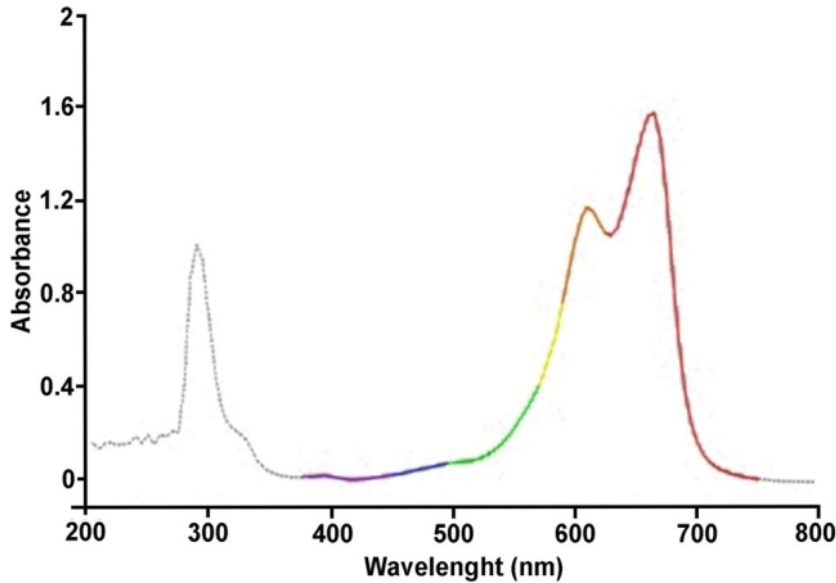


Figure 25: Absorbance spectrum of Methylene Blue [Gianelli & Bani, 2018]

For the first trial, red light of two different intensity levels (47.0 mW/cm^2 and 41.1 mW/cm^2) was used to measure the photobleaching effect of MB. It was found after the analysis that the concentrations used in this trial were low and thus did not produce the desired outcome of producing two distinct exponential curves.

To change that, we kept the concentration of 0.3 mg/mL of MB but instead of irradiating the solution continuously to then perform the measurement in the spectrometer we included an intermediate step where a weaker dilution was to take place. Once that was done, the procedure was the following: 1) the stock solution with the aforementioned concentration was prepared, 2) the solution was irradiated for the corresponding time and 3) the irradiated solution was diluted and used a UV cuvette to perform the measurement in the spectrometer.

There is evidence that MB follows a two step decaying process as shown in Figure 26 [Nassar et.al, 2019]. What is shown in this figure is that MB decays through an internal system conversion to an excited state. If there is molecular oxygen present it adducts with oxygen and then a second decay occurs. It is for this reason, that two decaying constants arise from this process. The fitting of the data points took into consideration and this resulted in a specific set of a , b , c and d values as per equation three. In this specific equation, b and d represent the exponential decay of the function while a and c represent multiplication factors of the exponential :

$$f(x) = a * e^{-(bx)} + c * e^{-(dx)} \quad (3)$$

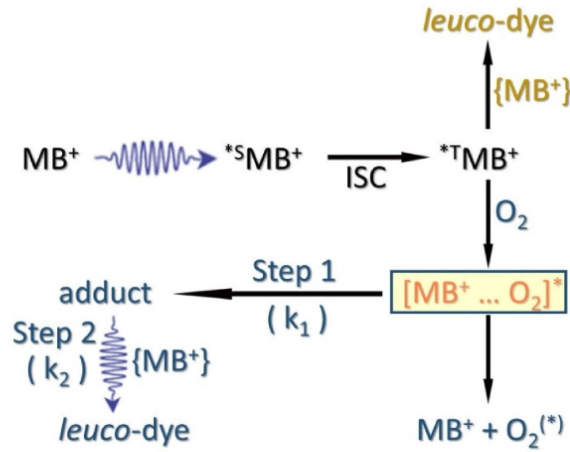


Figure 26: Two step decaying process for MB [Nassar et.al, 2019]

The reason this was done was basically because the incoming light could have a higher probability of interacting with the MB molecules and thus create a more defined photobleaching curve [Meroli, 2022]. The process of measuring the sample with the spectrometer and diluting was repeated for each time step. For a more detailed calculation of the MB dilution process proceed to the Appendix. In Figures 27 the photodegradation for the two highest irradiance values of 47.0 mW/cm² (33.4 mW) and 41.1 mW/cm² (29.2 mW) is shown both as a function of time (Figure 27-a) and of fluence (Figure 27-b).

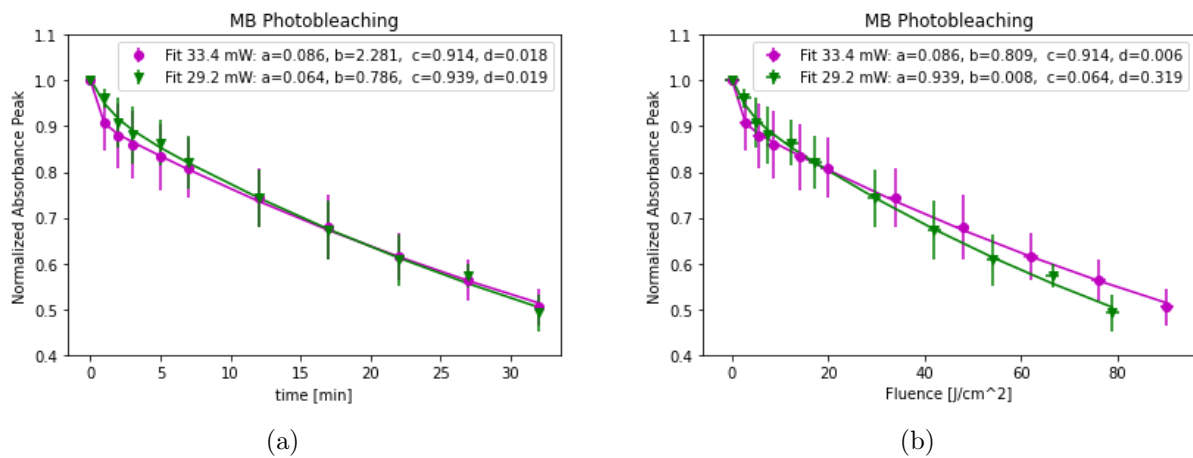


Figure 27: Photobleaching Effect of Methylene Blue at a high dilution (x100 of 0.3 mg MB/mL) as a function of a) time and 2) fluence.

In Figure 28 the photobleaching effect of the PS as a function of the fluence for the high concentration with different medium is shown. The reason TAP and water were used was to see if there was a significant difference in the degradation effect to the presence of salts in the TAP and also because for the combination case if MB + microalgae TAP would be used as a medium. It was found that there were no statistical differences between water and TAP.

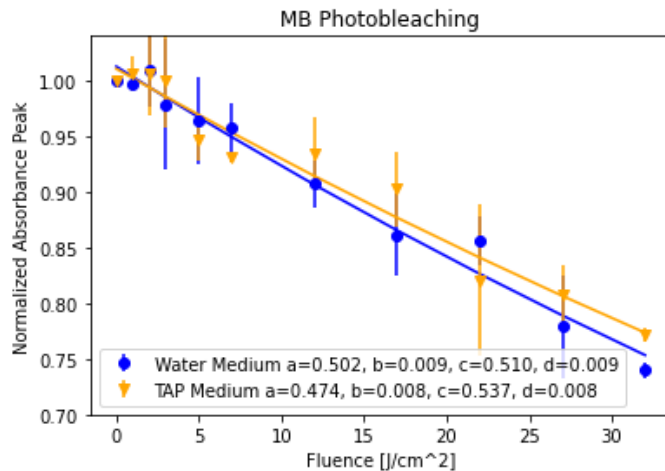


Figure 28: Photobleaching Effect of Methylene Blue at a low dilution (x40 of 0.3 mg MB/mL) for two different mediums (TAP and water) as a function of fluence

In Figure 29, the direct comparison of the degradation curves for both high and low concentrations as a function of the fluence are shown as to elucidate the effect the initial concentration of MB molecules have on the relative decay due to exposure of light.

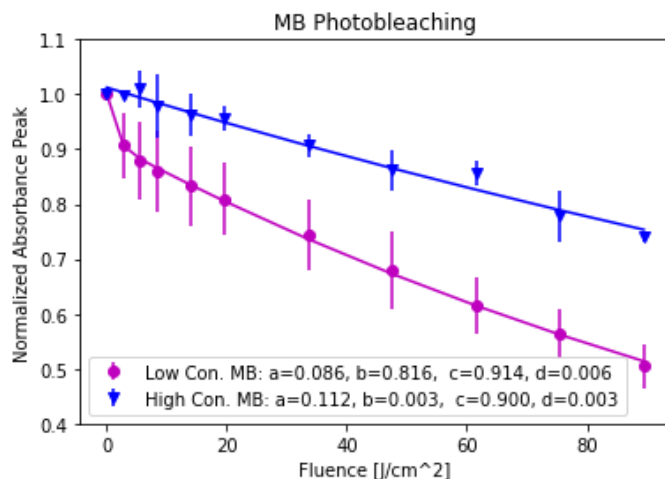


Figure 29: Photobleaching Effect of Methylene Blue at a high and low dilutions (x100 and x40) as a function of fluence

With the best concentration of MB to see the photobleaching effect, the same analysis for algae and light interaction was performed.

3.1.3 Microalgae Photobleaching Interaction

It is important to characterize the microalgae used throughout the experiment. As with the case of the PS, a spectra of the microalgae was performed. In Figure 30, it can be appreciated that there are several characteristic bands and the spectra resembles a flattened out curve. Nonetheless, the peak that was chosen was located at 695 nm which corresponds to the nearest peak of MB and the wavelength used for illumination.

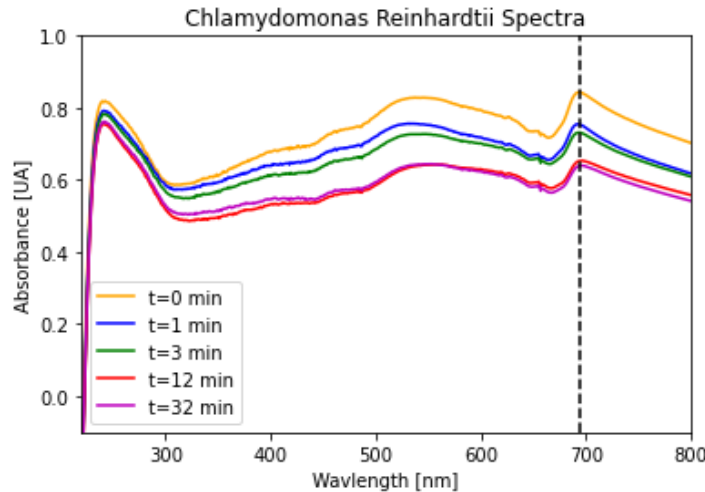


Figure 30: Spectral profile of the microalgae solution (*Chlamydomonas reinhardtii*) for the visible light range with a characteristic peak located at 695 nm

As with the previous section, the degradation curves for the microalgae solution were performed using the same procedure as with the PS. For each time step the sample was irradiated with the *Biotable* device and then the sample was put into a UV-cuvette to have its spectrum measured with the spectrometer. Following the same logic as with the previous part of the MB the measurements of high and low concentrations an intermediate step was made to study the high concentration case. The selected characteristic absorbance peak was used as a marker from which the relative decay of the values was measured. In Figure 31, the degradation effect for the high dilution appears to show a plateau in the higher fluence range. This result is the opposite than the case of the lower concentration of PS in which the relative decays was more pronounced than its higher concentration counterpart. These differences can be appreciated separately in Figure 31 and 32 and together in Figure 33.

In particular, what can be appreciated in Figure 31 is the slow decay at higher fluence values. The working hypothesis is that there is some type of clustering between the microalgae and the ions of the TAP that prevent further degradation regardless of the inciding light.

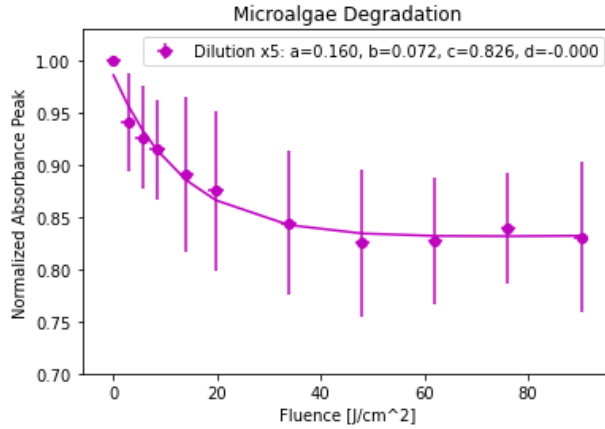


Figure 31: Degradation effect of the microalgae solution (*Chlamydomonas reinhardtii*) with a dilution of x5 at the moment of irradiation as a function of fluence

On the other hand, in Figure 32 it can be appreciated that for the lower dilution the relative decay was steeper.

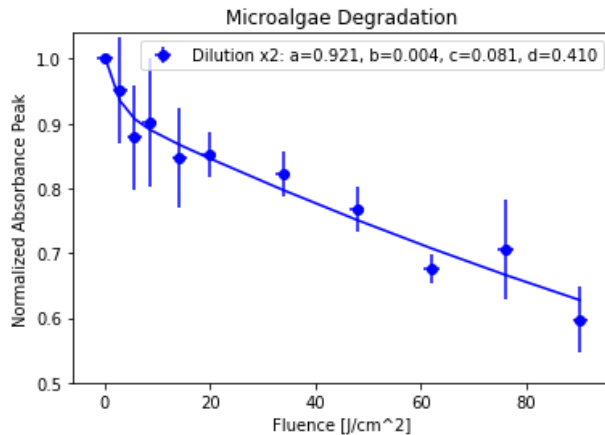


Figure 32: Degradation effect of the microalgae solution (*Chlamydomonas reinhardtii*) with a dilution of x2 at the moment of irradiation as a function of fluence

Finally, and as a conclusion for this subsection the two different curves are shown simultaneously. The medium used for both cases was TAP and the only thing that changed between them was the concentration at the moment of irradiation.

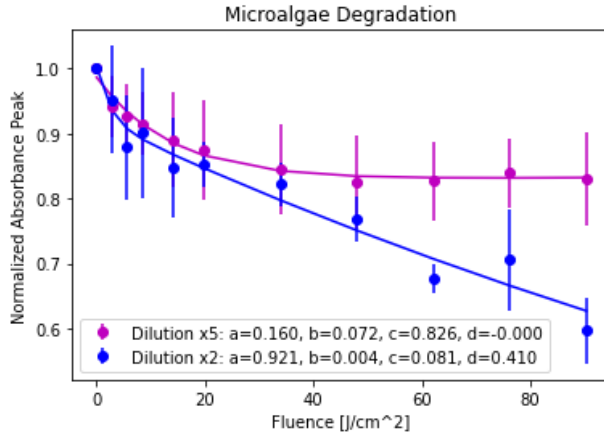


Figure 33: Degradation effect of the microalgae solution (*Chlamydomonas reinhardtii*) with a dilution of x2 and x5 at the moment of irradiation as a function of fluence

The understand of the light interaction with individual compounds (MB and alga) enables to perform the same the analysis of the combination of them.

3.1.4 PS + Microalgae Combination Characterization

Finally, the last part of this characterization process was to evaluate how the combination of the microalgae and the PS interact with incoming LED light. Here it is important to study the spectra of the solutions to see if there are any formation of potential molecular aggregates [Hooper, 2022]. Figure 34 clearly shows that there is a peak at 664 nm as well as significant valley for shorter wavelengths.

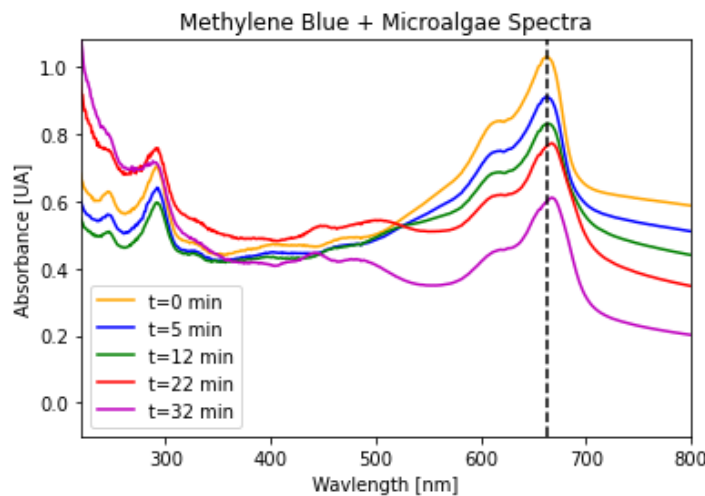


Figure 34: Spectral profile of the microalgae (*Chlamydomonas reinhardtii*) + MB solution for the visible light range with a characteristic peak located at 664 nm

The degradation curve for the combination of PS and microalgae follows a similar trend as both of them separately. The fitting curve is as well a double exponential and the range for the measured relative absorbance values range between 0.6 and 1.0. In figure 35, this curve with its data points and error bars is shown.

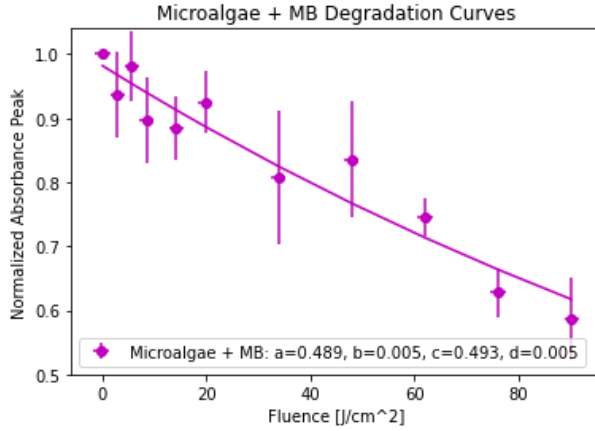


Figure 35: Degradation effect of the microalgae (*Chlamydomonas reinhardtii*) + MB solution with a dilution of x40 for the MB and x2 for the microalgae at the moment of irradiation as a function of fluence.

Likewise, and as a manner of a summary the degradation curves for all the three combinations are shown in Figure 36. The interesting thing about this result is that the presence of microalgae in the PS solution creates a stronger relative decay as compared to the PS by itself. This seems to indicate us that the created extra molecular oxygen is causing a higher photobleaching. Thus, making this combination a feasible possibility to increase vascular damage in a CAM model.

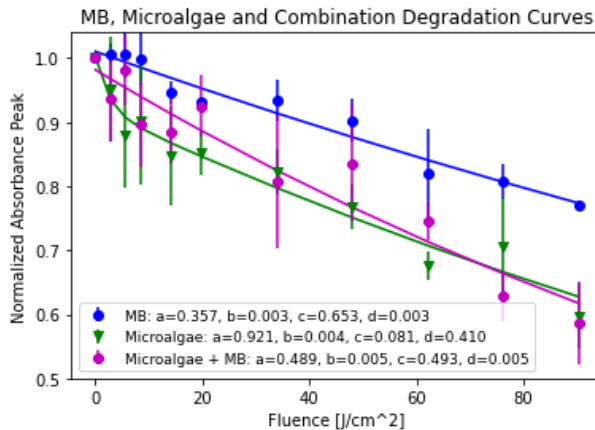


Figure 36: Degradation effect of the microalgae (*Chlamydomonas reinhardtii*) + MB, MB and Microalgae solutions all together as a function of fluence.

Finally, in Figure 37 the spectra at time zero for the different cases (MB, microalgae) is presented. The interesting fact about this figure is that the characteristic peak for the combination are different amongst each other indicating a maximum sensitivity at different wavelengths.

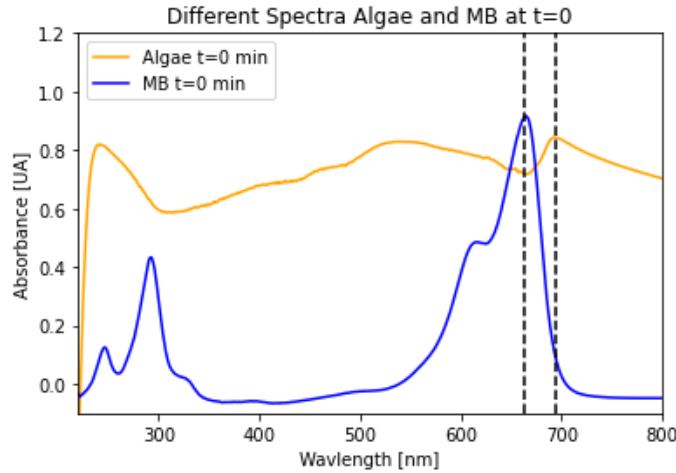


Figure 37: Spectra at $t=0$ for the two different independent cases

On the other hand, the experimental and theoretical spectra at time zero for the combination of microalgae + MB are shown in Figure 38. For the experimental case, the two solutions were simply combined and put into a spectrometer while for the theoretical curve the individual spectra were added with each of them with a weighting factor of one half. This resulted in a very similar shape between the two curves, which can indicate that the combination did not form any other molecular species.

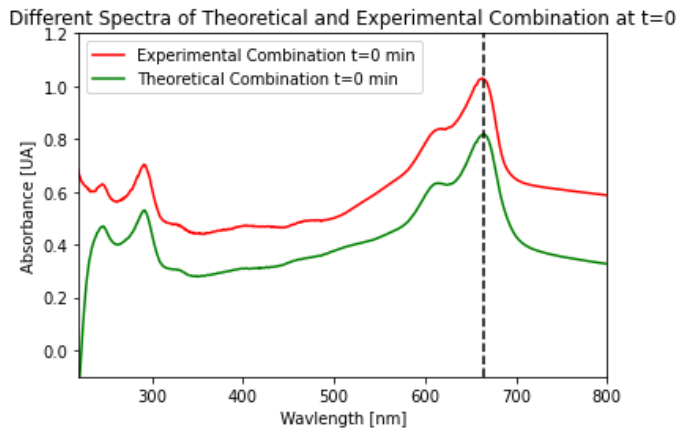


Figure 38: Spectra at $t=0$ for the theoretical and experimental combinations cases

In terms of the available scientific literature, there is optical characterization of MB [Chilakamarthi & Giribabu, 2017] but not so much in relation to the microalgae used in this experiment.

There are few studies about the photobleaching characterization. The vast majority describe the interaction of algae with light to identify oxygen production and not to observe the absorbance spectra before and after illumination [Hemschemeier, 2013] It is for this reasons that this thesis work appears to be the first one that not only characterizes *Chlamydomonas reinhardtii* but also utilizes it in CAM models and, for this, this initial part was very important to understand the interaction with light. In the next section the use of this chemical and biological components will be tested on CAM to see their effect on the vascularization networks.

3.2 Vascularization of the CAM

For the following section, a visual depiction of the changes in the vascularization of the CAM model under different circumstances are shown. The goal of this whole section is to understand the effect the light, MB, microalgae and their combinations have on the vascular network of the chorioallantoic membrane in chicken eggs. This will consist of four subsections each of them focusing on a different experimental parameters.

- 1) Only Light
- 2) Methylene Blue
- 3) Algae
- 4) Oxygen-Rich PDT

3.2.1 Only Light

We defined the groups “OL1” for 5 minutes of irradiance 30 mW/cm^2 , “OL2” for 10 minutes of 30 mW/cm^2 , “OL3” for 30 minutes of 10 mW/cm^2 and “C” for the control for EDD12. There is ample evidence in the literature that light by itself does not produce a significant change in the vasculature of a chicken embryo only qualitative analysis was performed [Miller et.al, 2004]. In Figure 39, the time evolution of the vascular network for 5 minutes of irradiance 30 mW/cm^2 at EDD12 and it can be appreciated there is no significant change in the network. In Figure 40 the same is shown but instead, an illumination of 10 minutes with an irradiance 30 mW/cm^2 was performed. In Figure 41, the same is shown but instead of an irradiance of 30 mW/cm^2 , 10 mW/cm^2 were used in this case. Finally, in Figure 42 what can be appreciated is the control group where no illumination was applied. The images of the CAM are shown below in Figures 39-42:

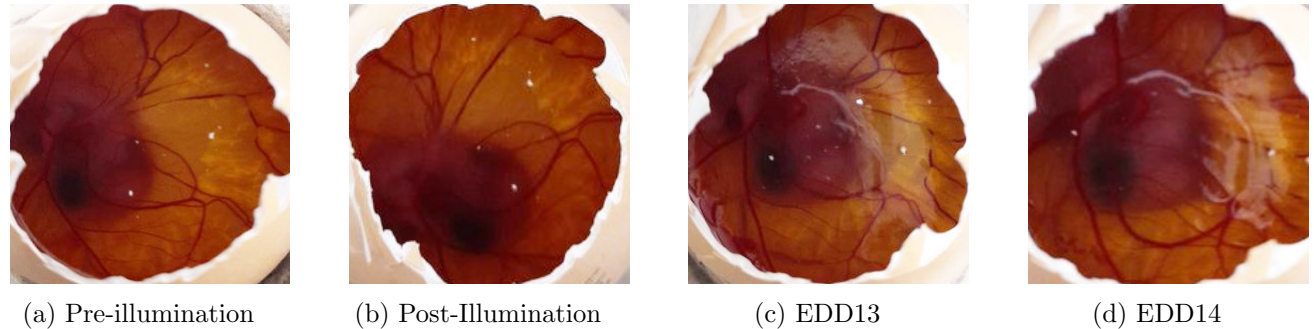


Figure 39: Group "OL1" EDD12 Only Light: 30 mW/cm² for 5 minutes

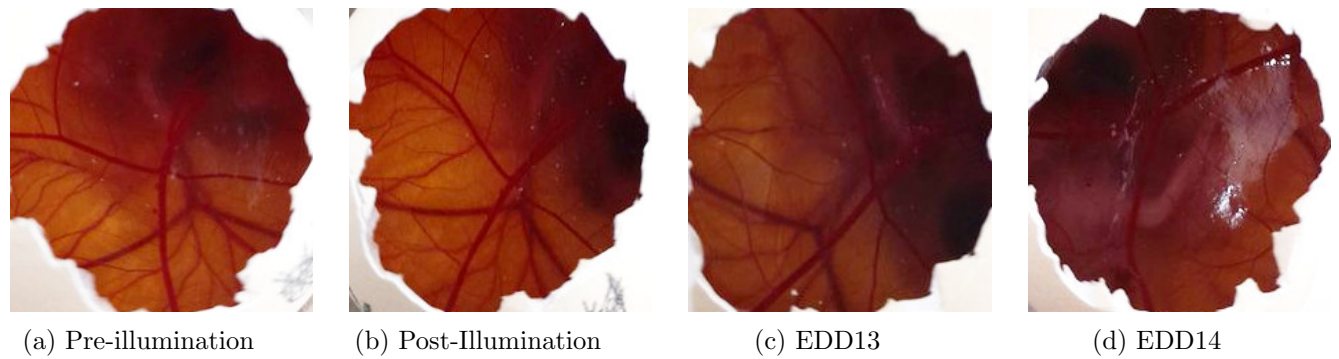


Figure 40: Group "OL2" EDD12 Only Light: 30 mW/cm² for 10 minutes

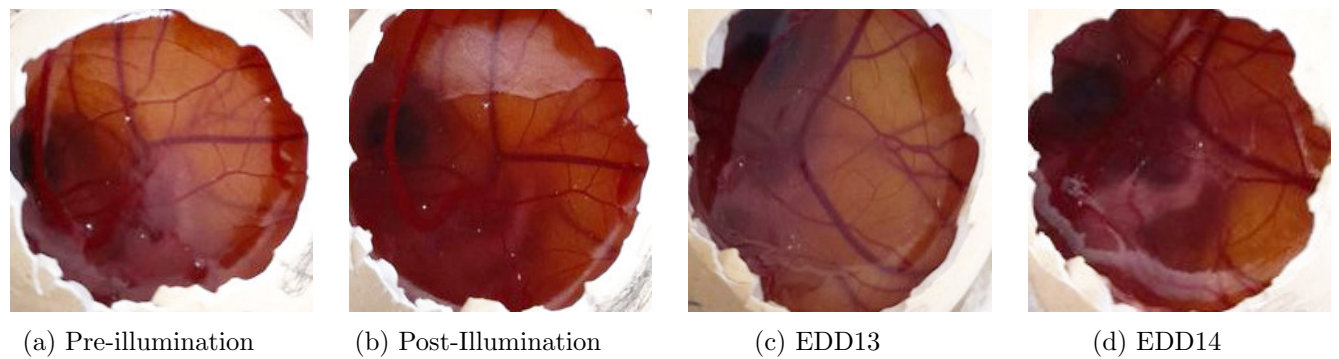


Figure 41: Group "OL3" EDD12 Only Light: 30 minutes of 10 mW/cm²

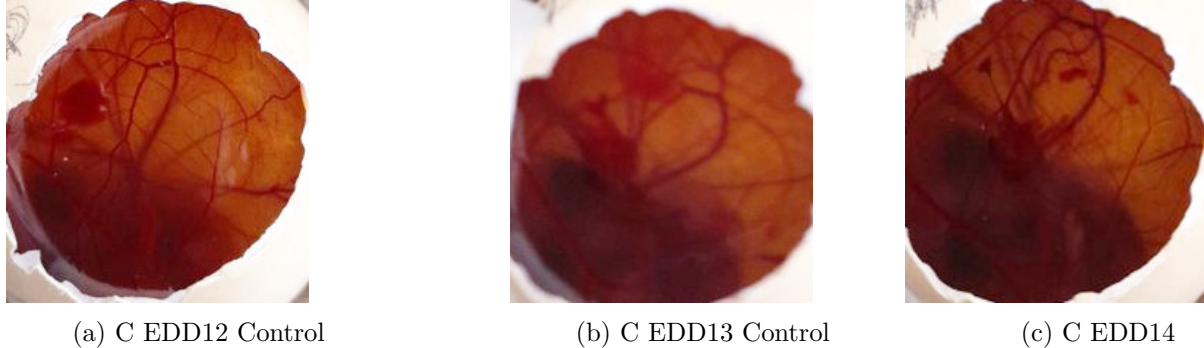


Figure 42: Group "C" without Light

These groups were selected to guarantee the effect of light with the chosen parameters. Since only light did not cause great changes in the vascular network, any change observed with the addition of PS and/or algae can be attributed to the interaction with them. From this analysis, as both irradiances did not present vascular changes, the highest irradiance (30 mW/cm^2) was used for the other experiments.

3.2.2 Methylene Blue and PDT Groups

For this subsection we defined four groups for two different days of development (EDD8 and EDD10). In the first case for EDD8 group 1 was defined as MB + light, group 2 as only light, group 3 as only MB, and group 4 as the control group. On the other hand for EDD10 group 5 was defined as MB + light, group 6 for light only, group 7 as only MB and group 8 as the control group, as described in Table 2 in the Methodology.

In Figure 43, what can be appreciated is the time evolution for the PDT group (MB + Light) of the topical application of MB over a CAM assay at EDD8. The reason that the post-illumination image is blue is because the MB is still in the CAM and has not been absorbed by the blood vessels. In contrast, after 7 hours it can be appreciated that the background changed colors and became less blue. After 24 hours, the overall strength of the blood vessels is visibly reduced. It can also be observed that the secondary blood vessels are collapsed. In Figure 44, what is presented is the time evolution vascular network when only light is applied. As expected, there is no considerable change in the number of ramifications nor on the diameter of the blood vessels given that only light is not toxic. In Figure 45, only MB was applied topically to the egg at EDD8, and what can be seen is that the background became momentarily blue but after one day of exposure the blood vessel ramifications did not decrease significantly. Finally, in Figure 46 the control group is shown with no changes vascular network and that can be used as a comparison to the PDT group. These different combinations can be appreciated clearly in Figures 43-46.

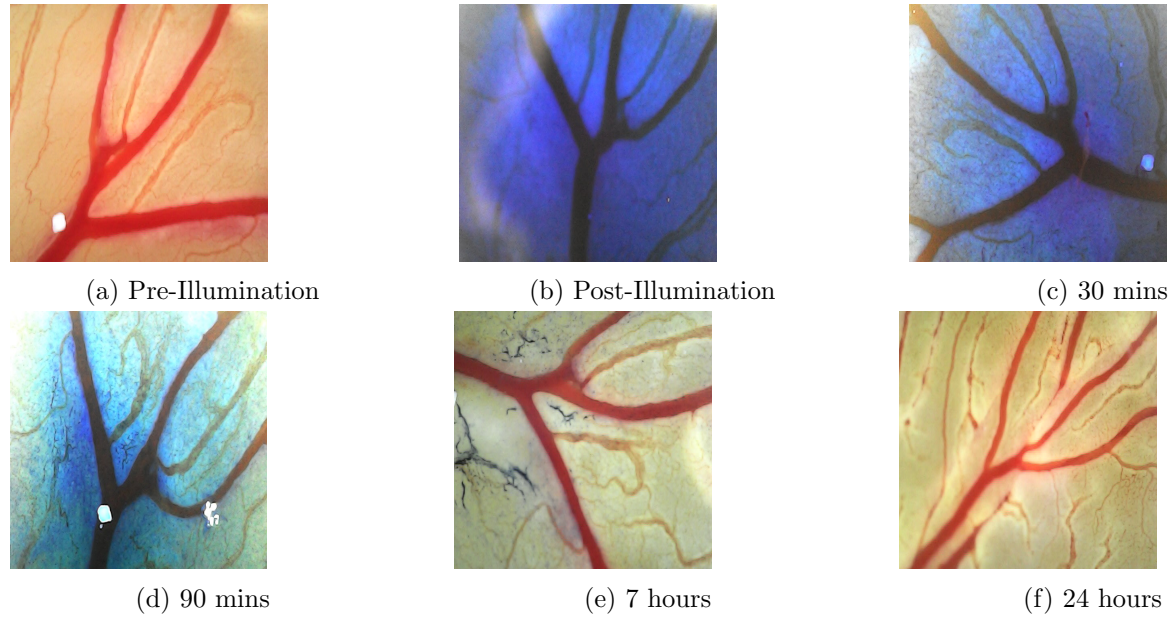


Figure 43: Group 1 (EDD8): Methylene Blue + Light

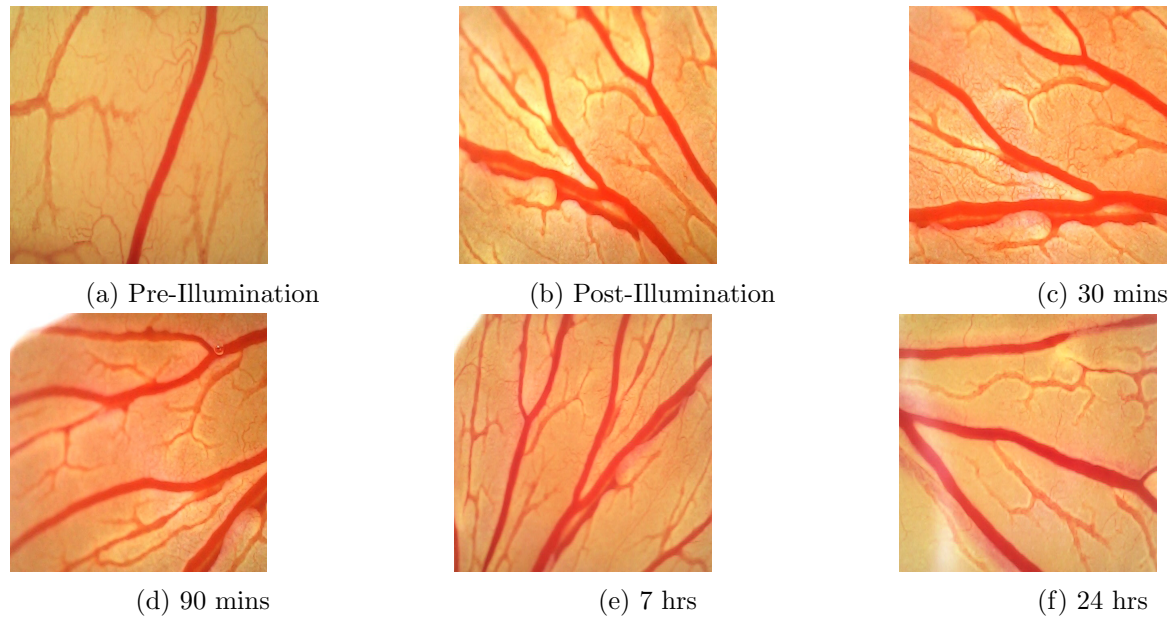


Figure 44: Group 2 (EDD8): Only Light

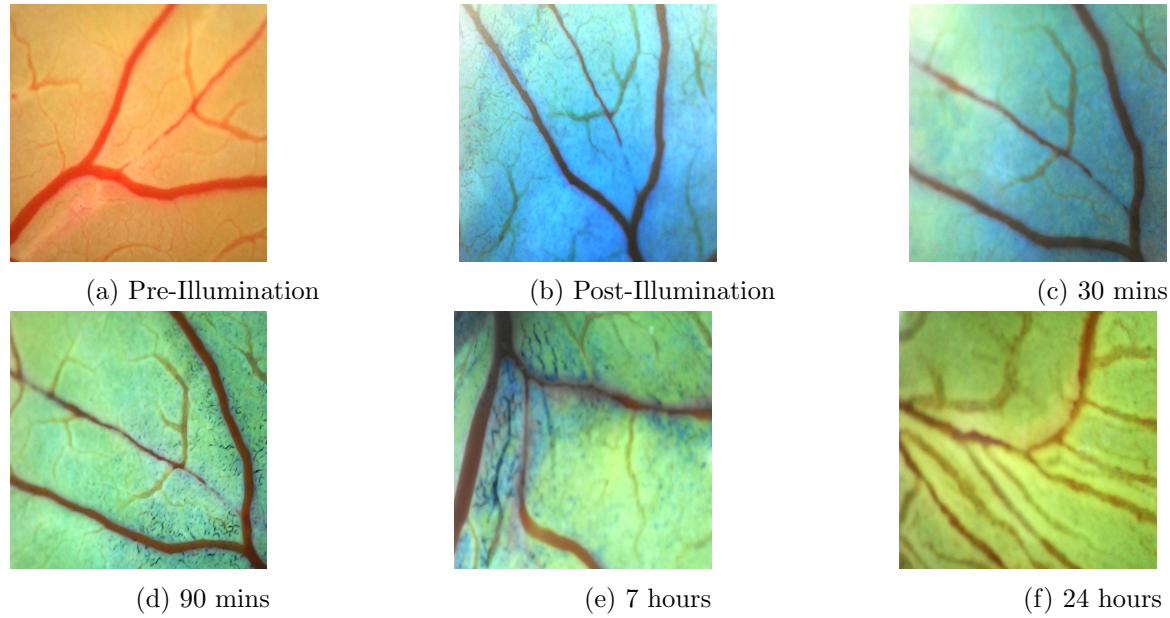


Figure 45: Group 3 (EDD8): Only Methylene Blue

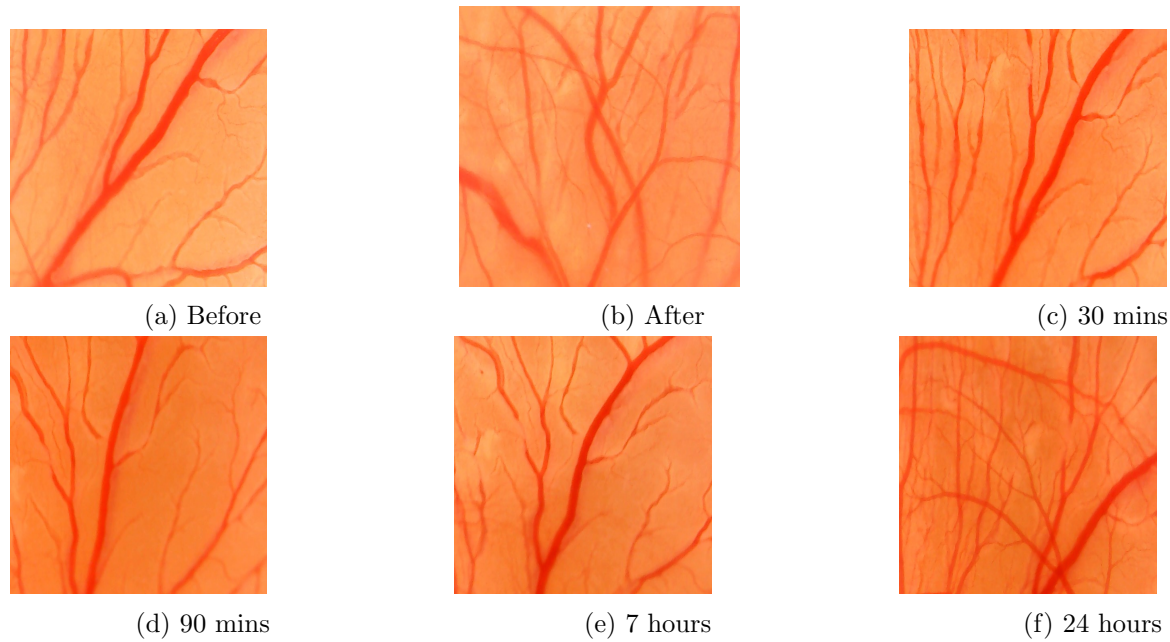


Figure 46: Group 4 (EDD8): Control

After 24 hours, for the groups without a destructive effect, it is possible to observe a slight increase in blood vessels in this qualitative analysis. This is expected, since the embryo has an accelerated metabolism and a high rate of angiogenesis [Nowak-Sliwinska et.al, 2014].

Now the same procedure is shown for eggs in EDD10. In Figure 47 what can be appreciated is the effect of the topical application for the PDT group (MB + light) and its chronological effect, were after 24 hours the blood vessels seemed heavily compromised. In Figure 48, the effect of only light does not affect the blood vessel network. Same is the case with only MB in Figure 49, where only the topical application of this chemical does not cause qualitatively significant changes. It is possible to follow the MB absorption for the vessels in the first hours. However, after 24 hours, it is clear the integrity of the blood vessels compared to the image pre illumination. Finally, in Figure 50 the control group were nothing substantial happened is shown.

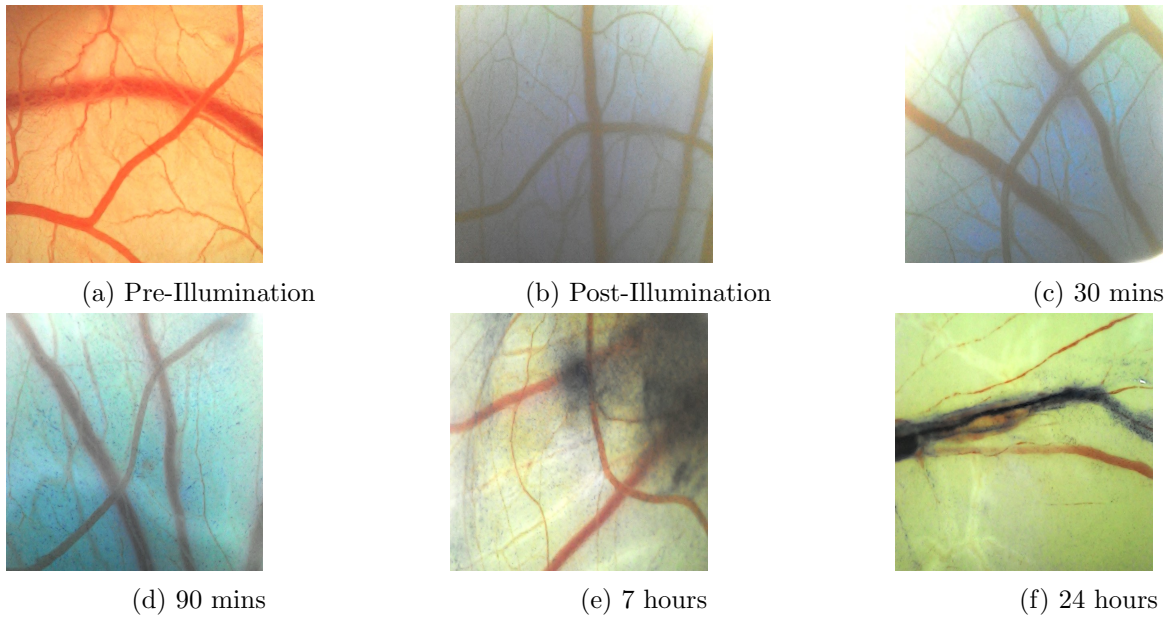


Figure 47: Group 5 (EDD10): Methylene Blue + Light

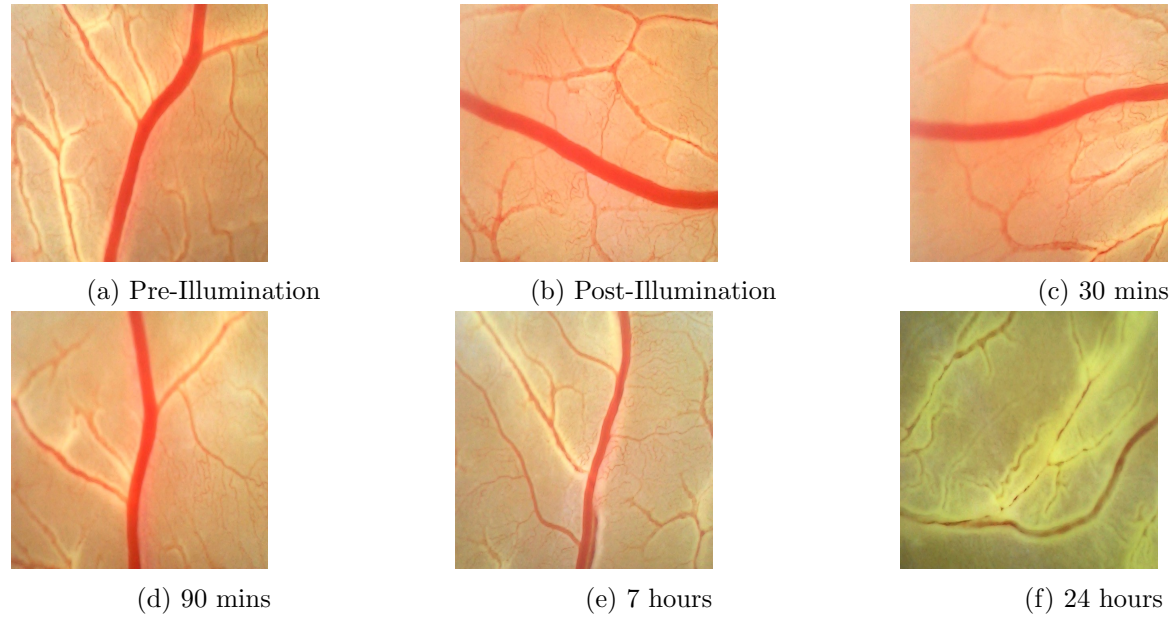


Figure 48: Group 6 (EDD10): Only Light

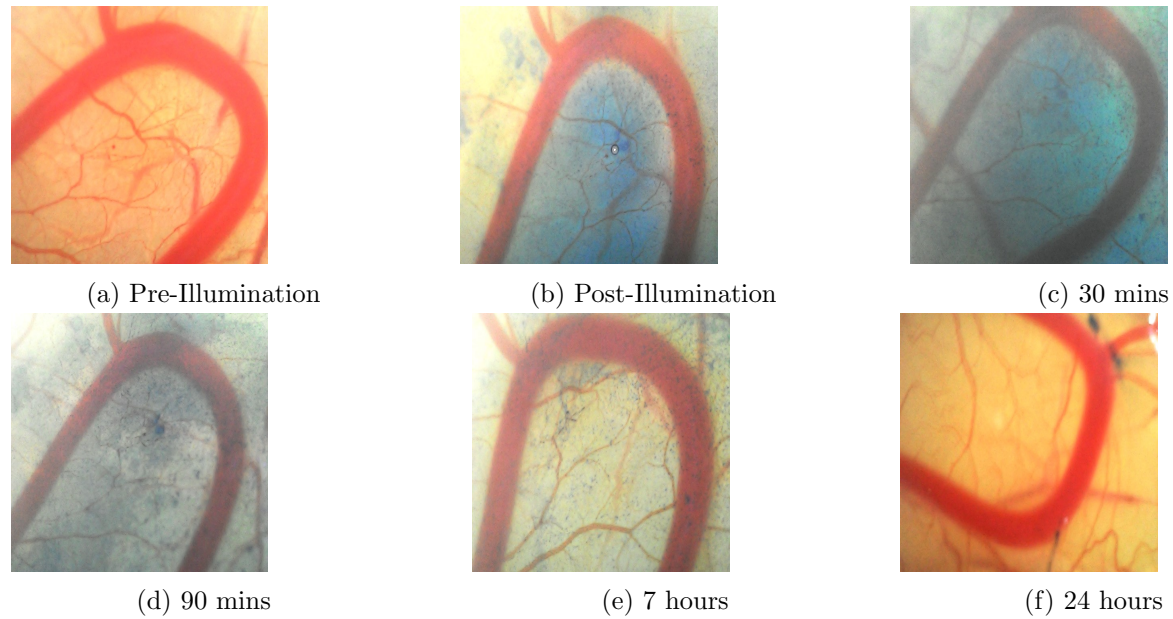


Figure 49: Group 7 (EDD10): Only Methylene Blue

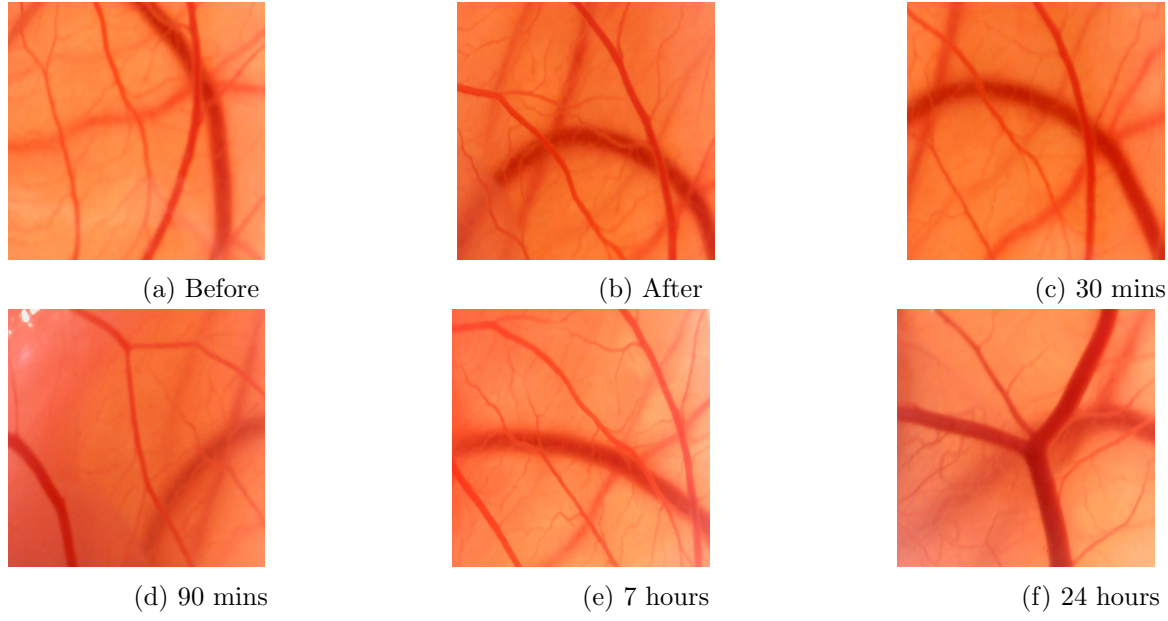


Figure 50: Group 8 (EDD10): Control

The previous set of images are the most representative for each group showing the chronological development of blood vessel ramifications for the different parameters. Using the image analysis software ImageJ, all the images of the groups to determine the number of ramifications can be analyzed. In the bar charts below what is shown is the change in the vascularization as a function of time for the 4 different groups. All the values were normalized to the number of ramifications taken before the therapy or light/PS in case of the other groups. Specifically, in Figure 51 it can be appreciated that the PDT groups at EDD8 decreased the ramifications by about 40 percent after 24 hours of the therapy while the other 3 groups remained close to each other at around 100%.

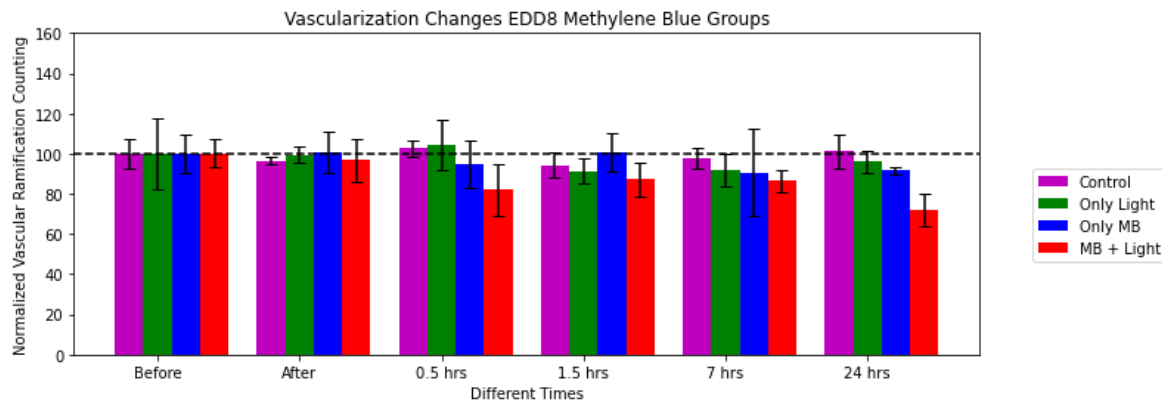


Figure 51: Bar charts EDD8 MB Groups

The reason that the selected days for the experimentation were always above 8 days of development was that after that time the CAM was vascularized enough. Before that, there are not enough blood vessels to attempt to do any kind of measurement of the effectiveness of a therapy. For a more detailed depiction of early-stage embryonic development refer to the Appendix in section 6.5.

In Figure 52, the same four groups are presented but for EDD10 instead of day EDD8. The main difference that can be appreciated is the stronger decline in the number of ramifications for the PDT group. The decline starts right after the application of the therapy and decreases by 60 percent of its original value after 24 hours. It is worth mentioning that the survival rate after 24 hours for both the PDT groups in these two bar charts was between 20 and 40 percent. Due to this reason, attempts to fill out the groups were made as to compensate for these deaths.

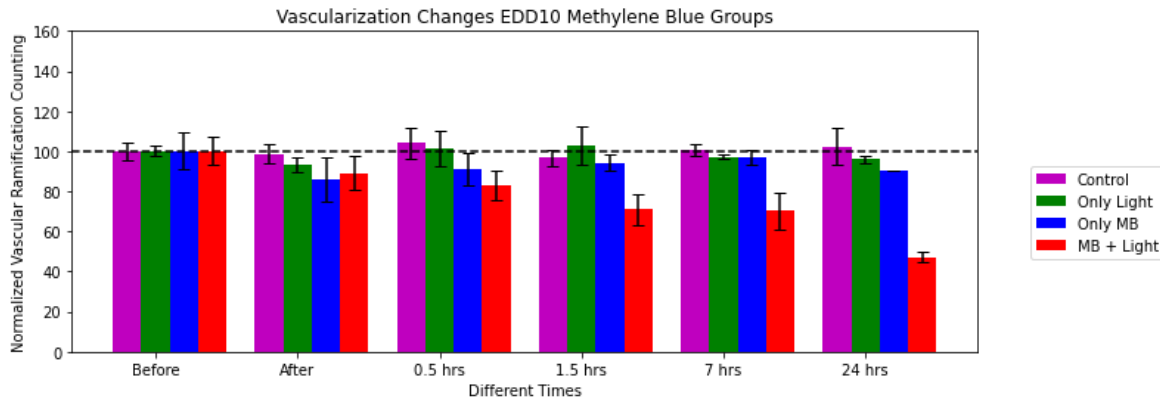


Figure 52: Bar charts EDD10 MB Groups

In the literature there is a vast amount of research focused on the CAM and the use of photosensitizers to achieve blood vessel reduction. For instance, porphyrin and chlorin were used in CAM assays to study how the average vessel area changed when external illumination was introduced and PDT induced. Naturally, it was found that for both cases there was a considerable effect in the diminishing of blood vessels with some variation if the PS was applied topically or intravenously [Buzzá et.al, 2014]. Furthermore, and even more relevant to this thesis work is the application of MB on CAM models to study its effect on angiogenesis. In a publication, it was found that MB alone was able to induce the reduction of blood vessels in the chicken embryo's CAM. For a specific concentration of MB, they found that the inhibition of angiogenesis reached up to 60 percent with respect to the control case [Zacharakis et.al, 2006]. In another scientific paper, the specific case of PDT using MB within a CAM model was studied for malignant ovarian tumors. It was found that after two days of applying PDT the engrafted tumors significantly reduced in size. After five days of performing the PDT it was found that all the treated tumors showed clear remission [Ismail et.al, 1999]. The results obtained in this thesis are consistent with the literature as it can be observed in Figures 51 and 52 where for EDD8 and EDD10 the application of PDT showed a consistent decrease in the

number of blood vessel ramifications in the CAM. The implication of this, at least at first order, is that the methodology that was used throughout the experiment is consistent and could be used to evaluate the interaction of other parameters in a CAM model such as microalgae.

3.2.3 Microalgae and Light

For this subsection we defined two groups for the same days of development (EDD8 and EDD10). In the first case, for EDD8, group 9 was defined as microalgae + light and group 11 as only microalgae which was used to analyze if the presence of algae affected the vascular network. In addition, for EDD10, group 13 was defined as microalgae + light and group 15 as only microalgae. In Figure 53 (EDD8) what is shown is the most representative egg where the effect of new vascular ramifications (represented by the small and thin vessels) is measured given the combination of algae and light. In Figure 54 (EDD8), only the algae by itself is presented and no significant changes happen in the network as no molecular oxygen is produced given the absence of light. In Figure 55 (EDD10) the number of blood vessel ramifications increase given the local production of oxygen. Compared to the effect of the same parameters at EDD8, at EDD10 the increase in the number of vessels occurred with larger diameters. After 7 hours, points of new vessels can already be observed, showing a faster effect. Finally, for Figure 56 (EDD10) only the algae was applied topically at no significant changes happen. These different combinations can be appreciated in Figures 53-56.

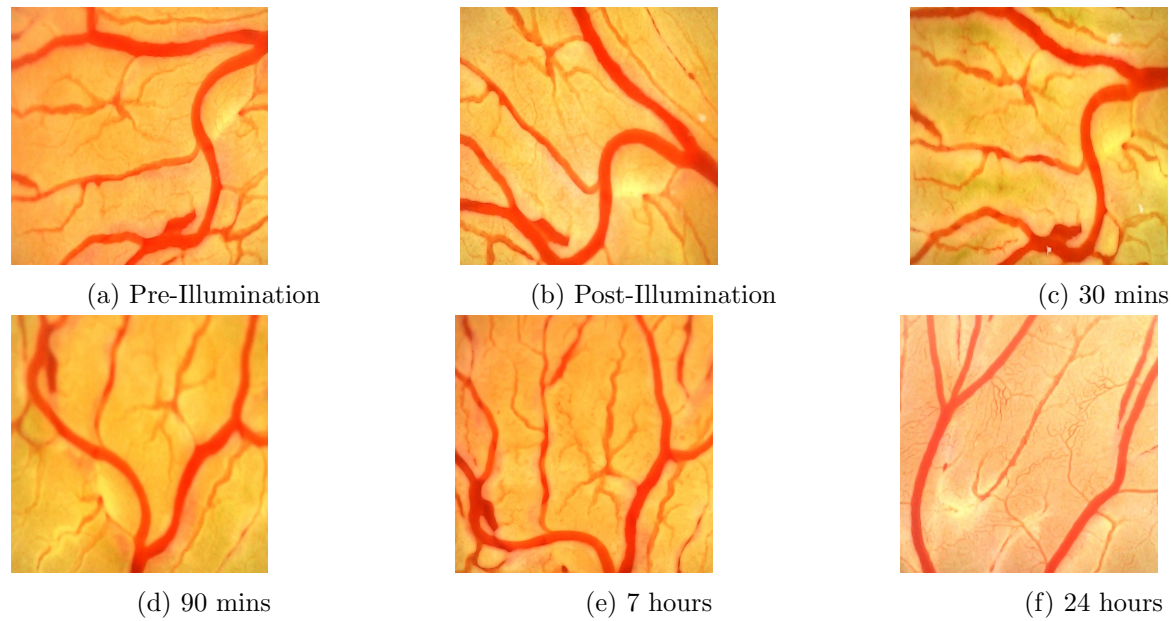


Figure 53: Group 9 (EDD8): Algae + Light

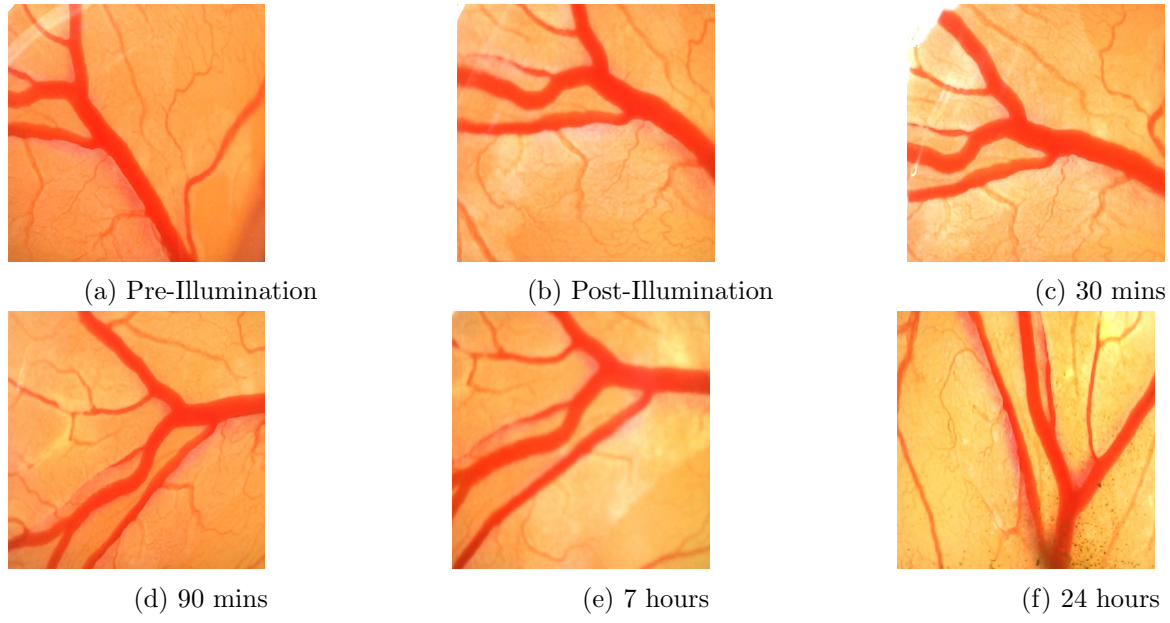


Figure 54: Group 11 (EDD8): Only Algae

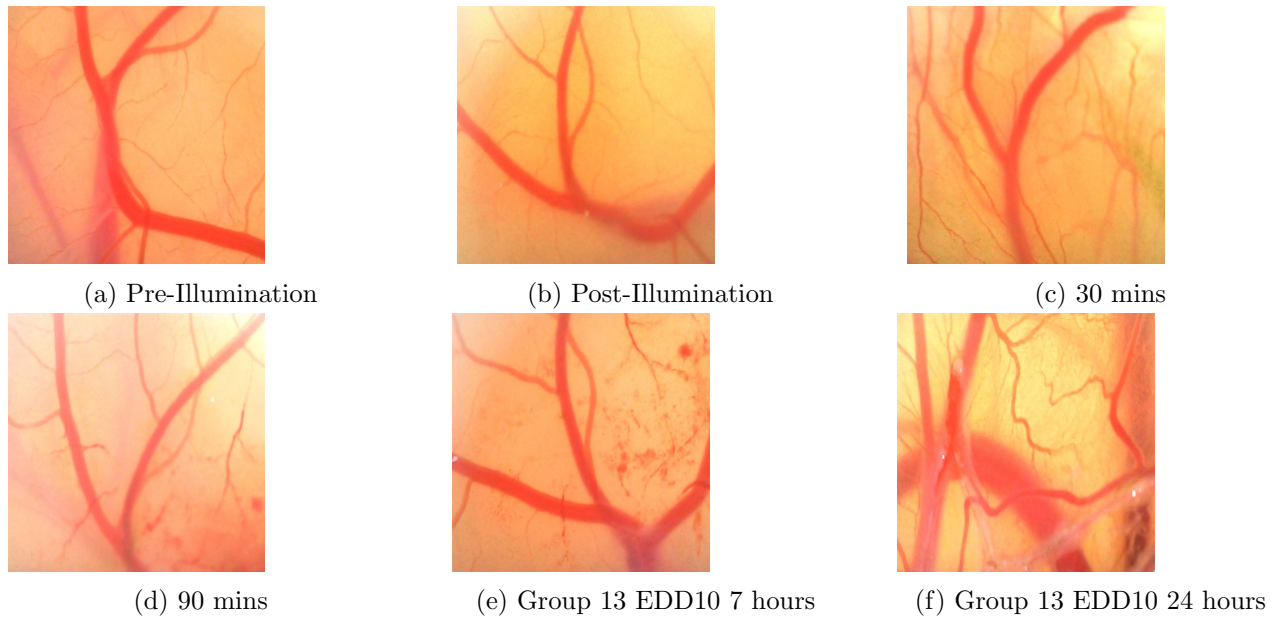


Figure 55: Group 13 (EDD10): Algae + Light

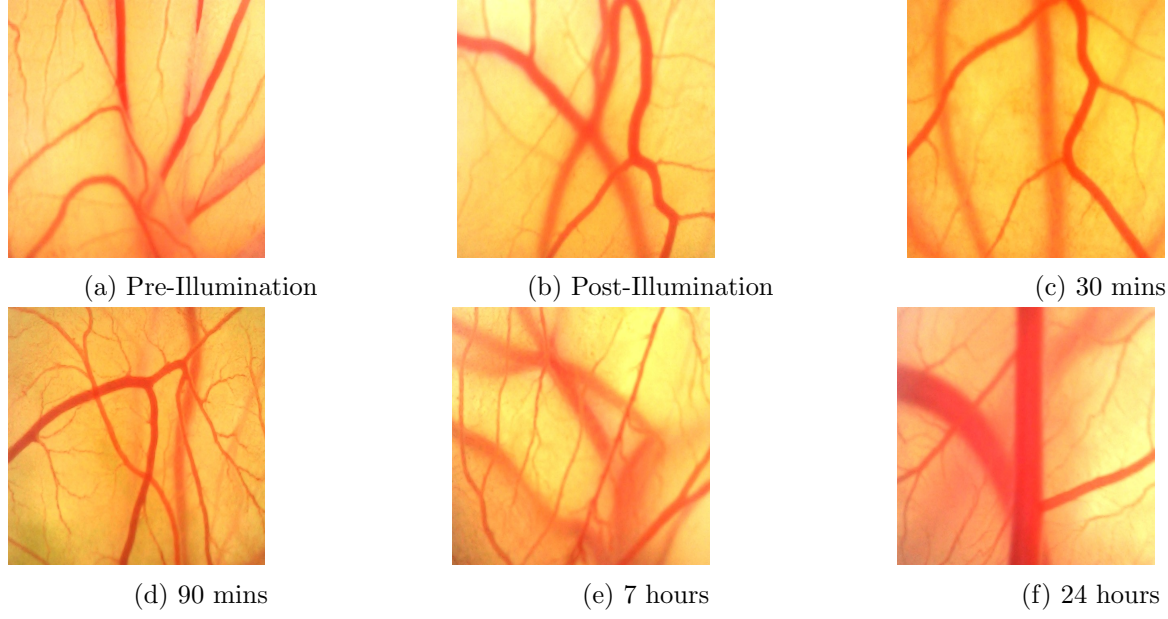


Figure 56: Group 15 (EDD10): Only Algae

As with the previous section, the most representative egg for each group for the microalgae and light case was chosen. At least qualitatively, it can be appreciated that the number of ramifications increase as a function of time. For a quantitative analysis the different combinations of microalage and light were performed. In the bar chart shown in Figure 57 the change in the vascularization on the CAM can be observed when the microalgae was tested. As with the previous section, the control group and the groups with only light or only microalgae remained with very similar ramification values throughout the experimentation. Meanwhile, the group that combined the microalge and light had a significant increase of about 30 percent after 24 hours with respect to the baseline value.

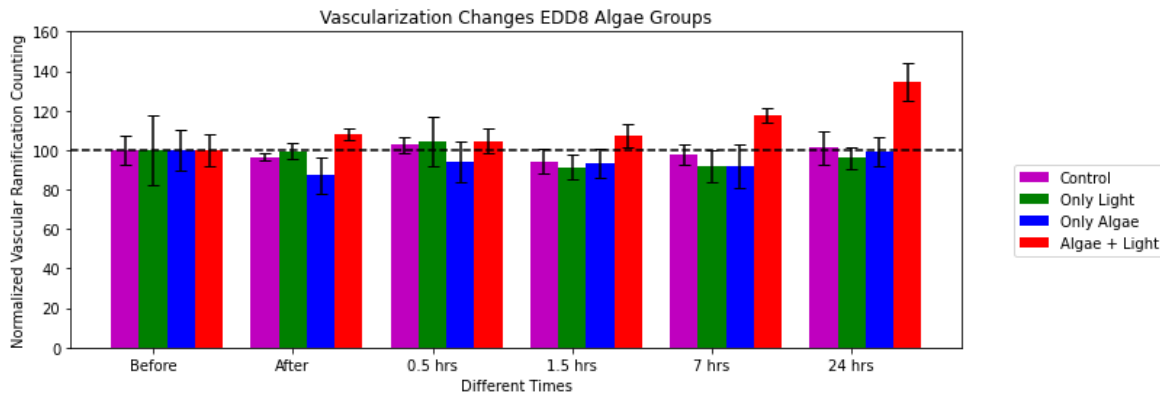


Figure 57: Bar charts EDD8 Microalgae Groups

In Figure 58, a similar pattern can be appreciated. For the group with the light and the photosynthetic microalge producing molecular oxygen the relative growth of ramifications increased by 20 percent after 24 hours of the initial therapy. Both of these two plots suggests that oxygen produced by the microalge induces vascular growth in the CAM.

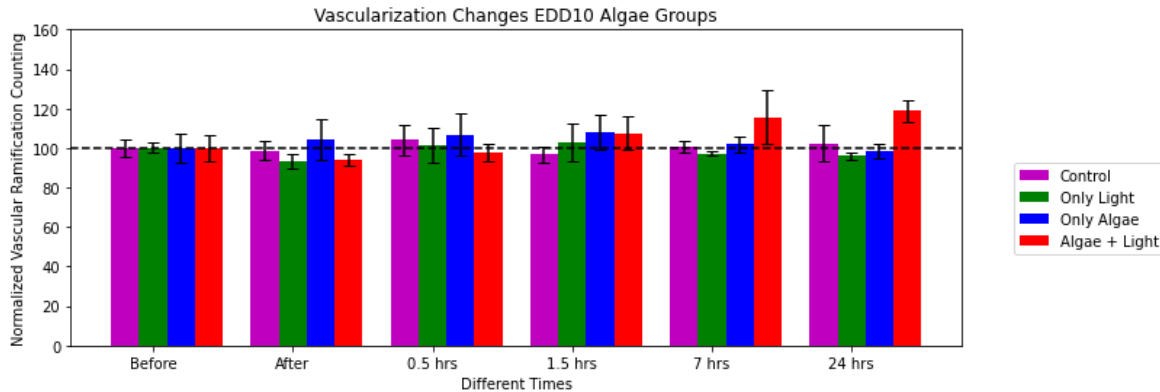


Figure 58: Bar charts EDD10 Microalgae Groups

This quantitative analysis showed the effect observed in the big number of small vessels of the EDD8 experiments. However, despite the smaller effective increase in the EDD10 group, the formed vessels showed larger diameters. The presence of oxygen increasing the vascular network was already described in the literature [Schenck et.al, 2015]. The use of *C. reinhardtii* and light in a CAM model has never been reported before, to our knowledge. Given the effects of individual PS and alga with and without light, it was possible to plan the combined use of the two compounds. The novel aspect of this thesis work is the inclusion of a photosynthetic microalgae topically applied over the CAM. There is no literature on this type of experiment done previously therefore the results presented here can potentially contribute to the knowledge of the field. In summary, when microalage and light are added to to the CAM 20 % - 30 % increase in blood vessel ramifications develop after a 24 hour period.

3.2.4 Microalgae, Methylene Blue and Light: High Concentration

For this subsection, we defined three groups for two different days of development (EDD8 and EDD10) as described in 2.4.4. This was performed to analyze if the stage of development when oxygen was produced could influence the PDT response. In Figure 59, what can be seen is the deterioration of the blood vessels for combination a) at different times, leading to the dead of all the embryos after 24 hours. In the groups with the combination b (Figure 60) and c (Figure 61) the same phenomena was observed where great damage is done to the chicken embryos at EDD8.

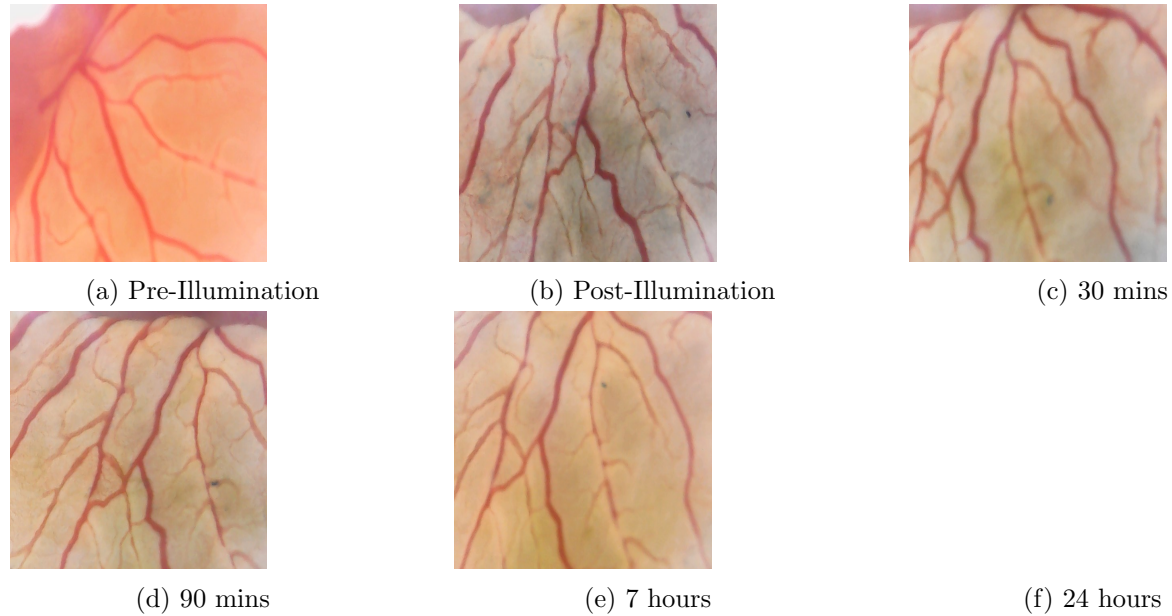


Figure 59: Group 17 (EDD8): Combination a) Algae + Light \rightarrow PS \rightarrow DLI \rightarrow + Light

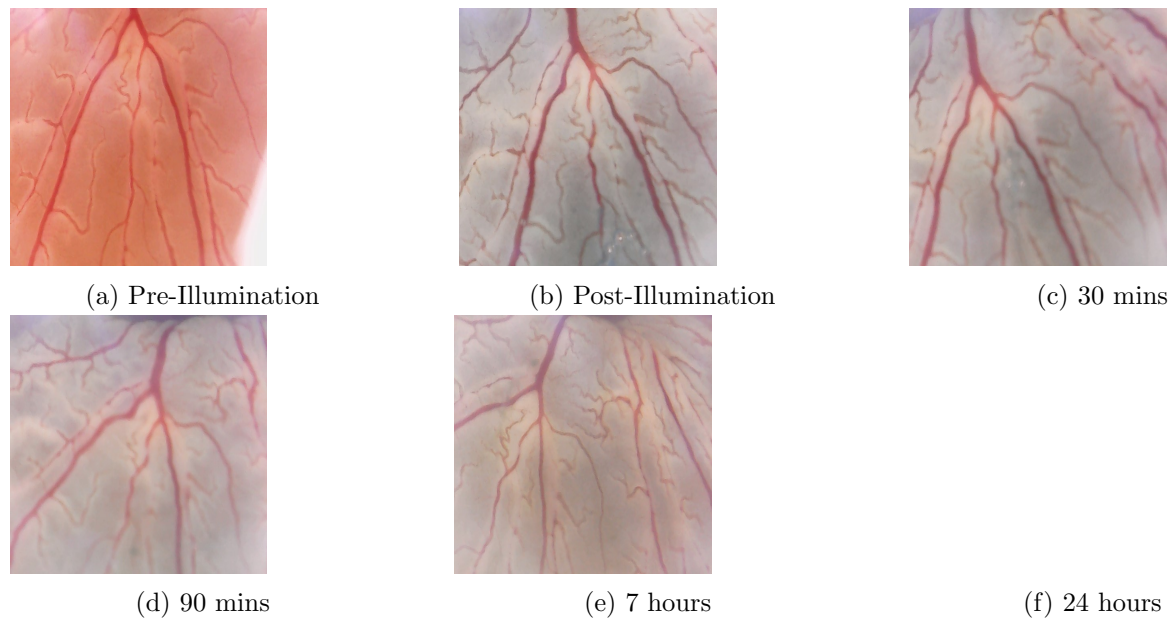


Figure 60: Group 18 (EDD8): Combination b) Algae + PS \rightarrow DLI \rightarrow + Light

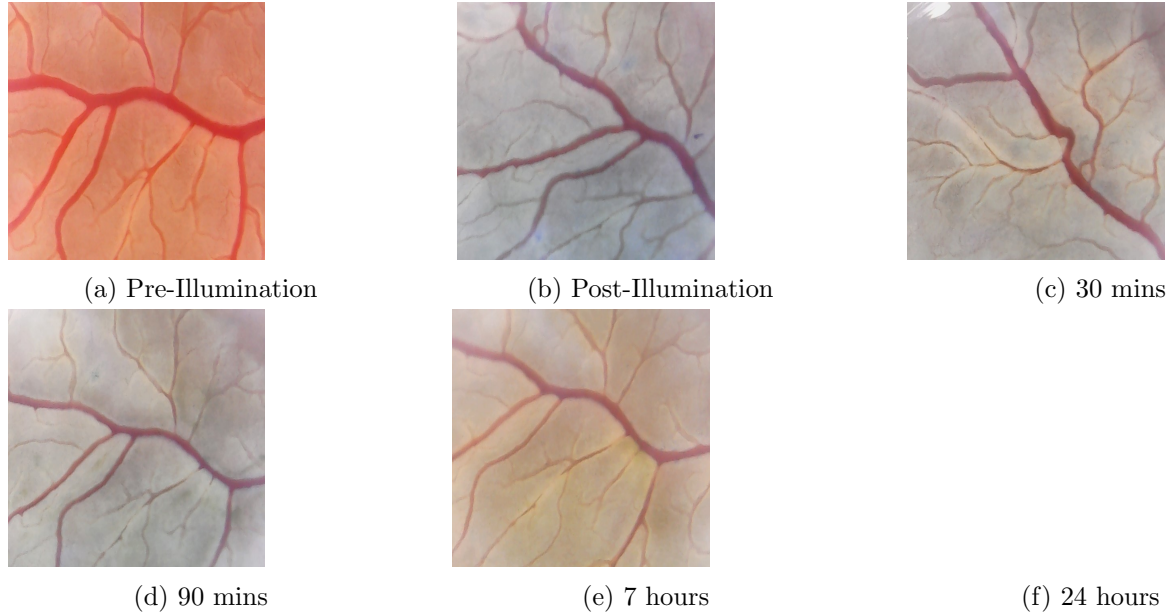


Figure 61: Group 19 (EDD8): Combination c) PS → DLI → Algae + Light

On the other hand, the same effect was observed for Figures 62, 63 and 64 where the different combinations were tried but instead at EDD10. In all of the cases there was a strong effect after 7 hours and a lethal effect after 24 hours.

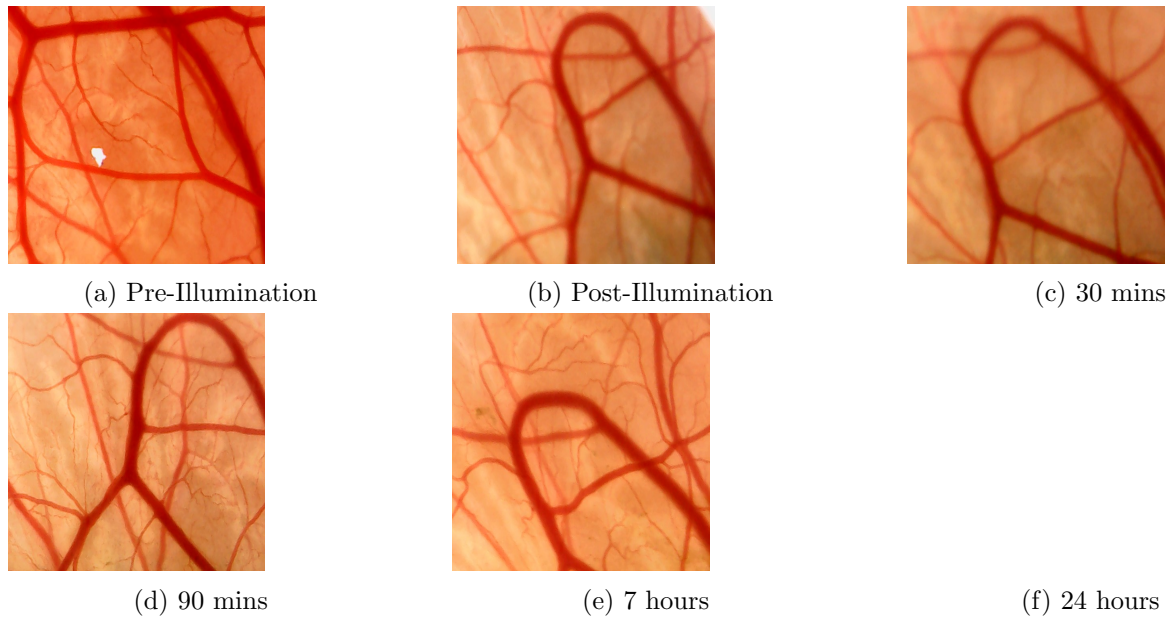


Figure 62: Group 20 (EDD10): Combination a) Algae + Light → PS → DLI → + Light

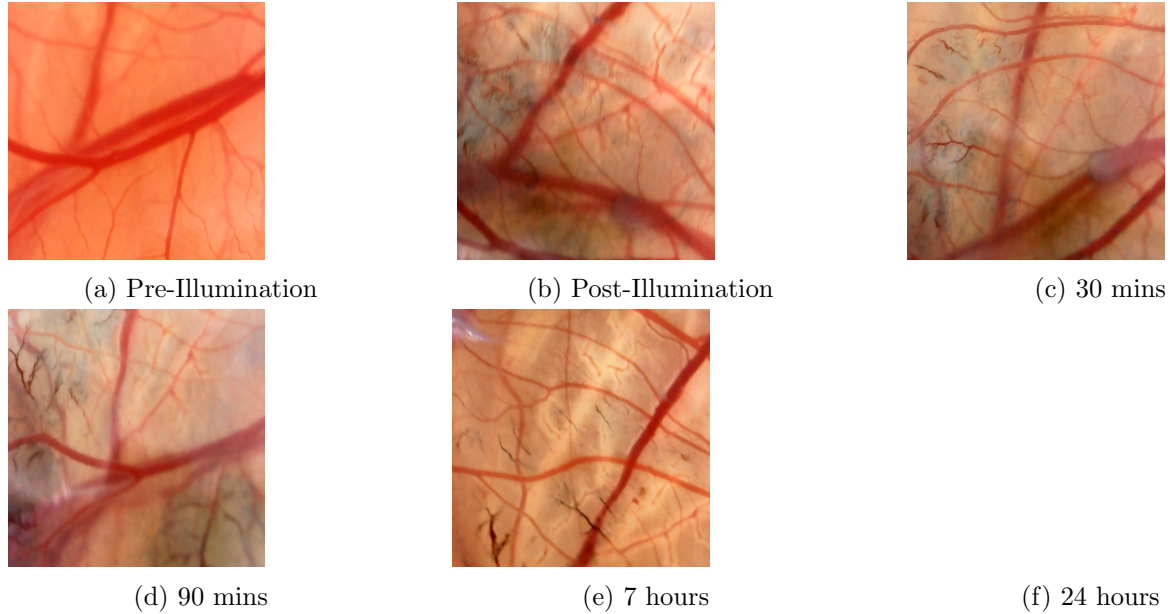


Figure 63: Group 21 (EDD10): Combination b) Algae + PS → DLI → + Light

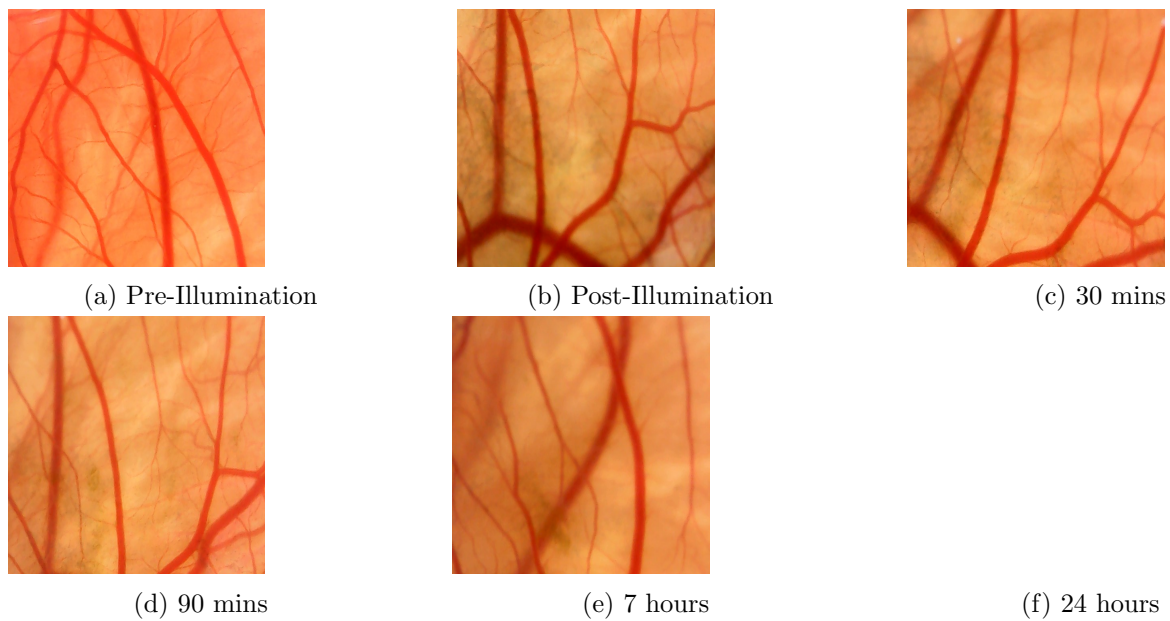


Figure 64: Group 22 (EDD10): Combination c) PS → DLI → Algae + Light

The images shown above depict the representative egg of the group. As with the previous subsections the times at which pictures were taken were: before, after, 30 minutes, 90 minutes, 7 hours and 24 hours, indicating the increase of the PDT effect compared with the use of the same PDT parameters without algae. For all the six groups of the combination of PDT and

microalgae none of the eggs survived after a period of 24 hours. For this reason, an image at this time was not shown. Figure 65 shows the quantitative effect of all combination (PDT and algae) and only the PDT group with the same MB and light parameters, at EDD8. What can be appreciated is that at first, there is not a very strong decrease in the number of ramifications but after 7 hours this begins to change with respect to the baseline values. After 24 hours the bar is non-existent due to the fact that all the eggs had died by then.

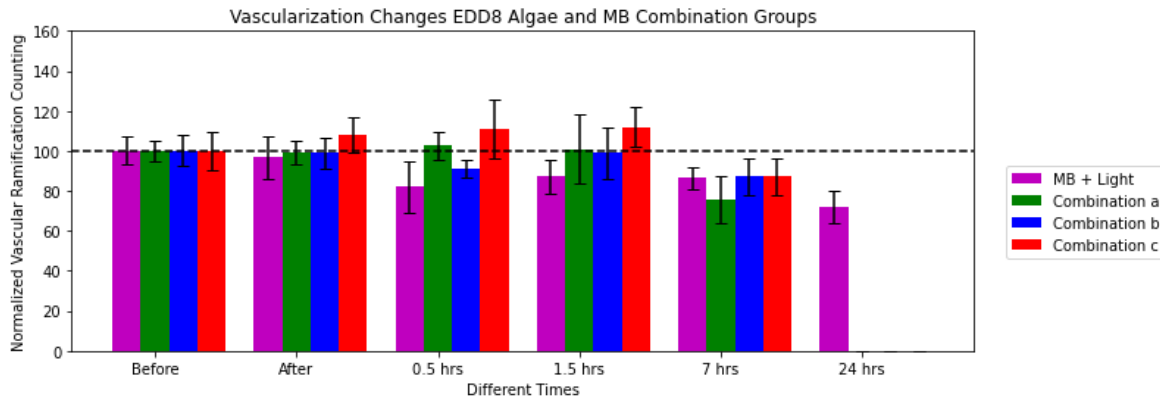


Figure 65: Bar charts EDD8 Combination Groups

In Figure 66, the quantitative analysis is showed for the combination and for PDT group at EDD10. What can be seen is that the effect of the oxygen-enriched PDT is stronger than for the EDD8 case given that all other variables are controlled for.

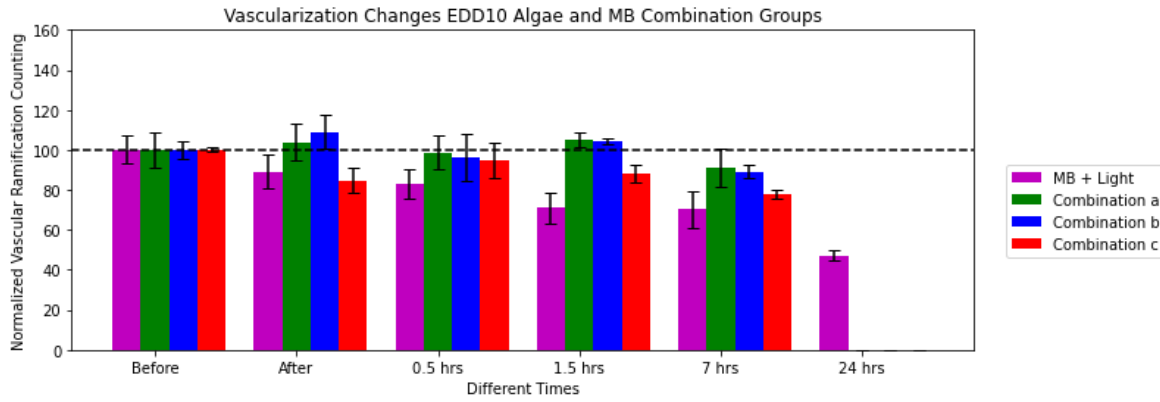


Figure 66: Bar charts EDD10 Combination Groups

Although these experiments showed that the vascular destruction effect of PDT was increased with the presence of algae, quantification was not possible due to the death of the embryos. Thus, for a more specific quantitative analysis, it was necessary to reduce the concentration of MB to obtain a sub-dose parameters.

3.2.5 Microalgae, Methylene Blue and Light: Sub-Dose

Using the MB stock concentration (0.3 mg/mL) when applying the PDT + microalgae caused a very strong effect on all the eggs resulting in their death after 24 hours. For this reason a dilution of x10 for the MB stock was done. Then 200 μ L was added to the CAM with half of them corresponding to the MB solution and the other half to the microalgae solution. The microalgae solution was not diluted to produce the same oxygen quantity. Using the previous groups, EDD10 was chosen as the best day for the experiment due to the higher probability of embryo survival. At the same time, as all combination of algae and PDT showed a great effect, we chose the sequence with more possibility of clinical application. This sequence was combination b) which added both the MB and the microalgae at the same time before waiting for the DLI of 20 minutes to initiate the illumination.

In figures 67 and 68, the most representative egg from each group is shown at different times. Figure 67 shows the observed effect for the PDT group at a sub-dose through a decrease in the number of ramifications. Figure 68 shows the PDT and algae combination at sub-doses and the interesting aspect that occurred was that, by decreasing the concentration of the MB dilution, after 24 hours the eggs did not die but instead showed a measurable decrease in their vascular network.

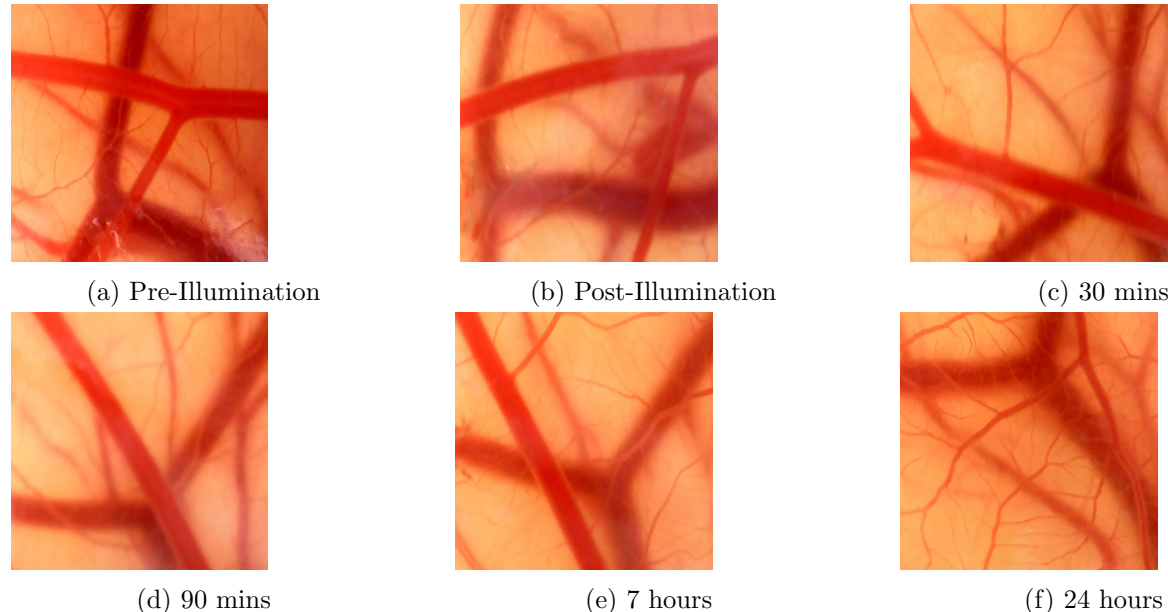


Figure 67: Group 23 (EDD10): Methylene Blue + Light Low Concentration

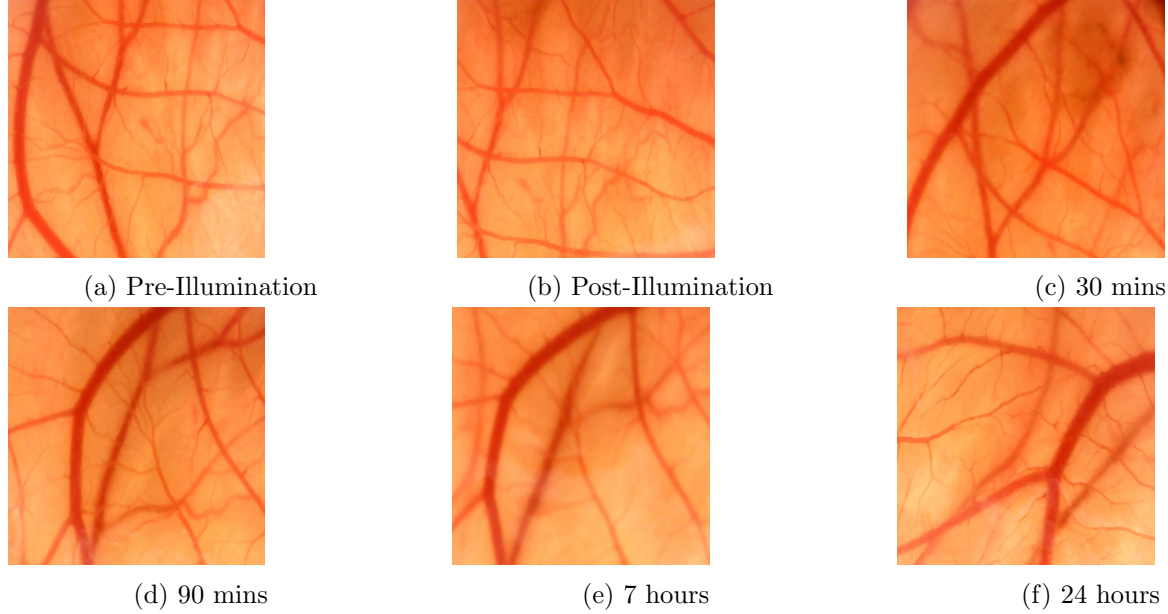


Figure 68: Group 24 (EDD10): Combination b) Low Concentration

What was found was that for the PDT the low concentration was less effective in destroying blood vessel ramifications than the higher concentration, something that was expected. On the other hand for the combination b), of the PDT + microalgae, it was found that at first the low concentration was more effective in causing damage but after 24 hours it did not cause the death of most of the eggs as the high concentration case. The chronological progression of the quantitative effect of the PDT and the PDT + microalgae for low and high concentrations is shown in Figure 69.

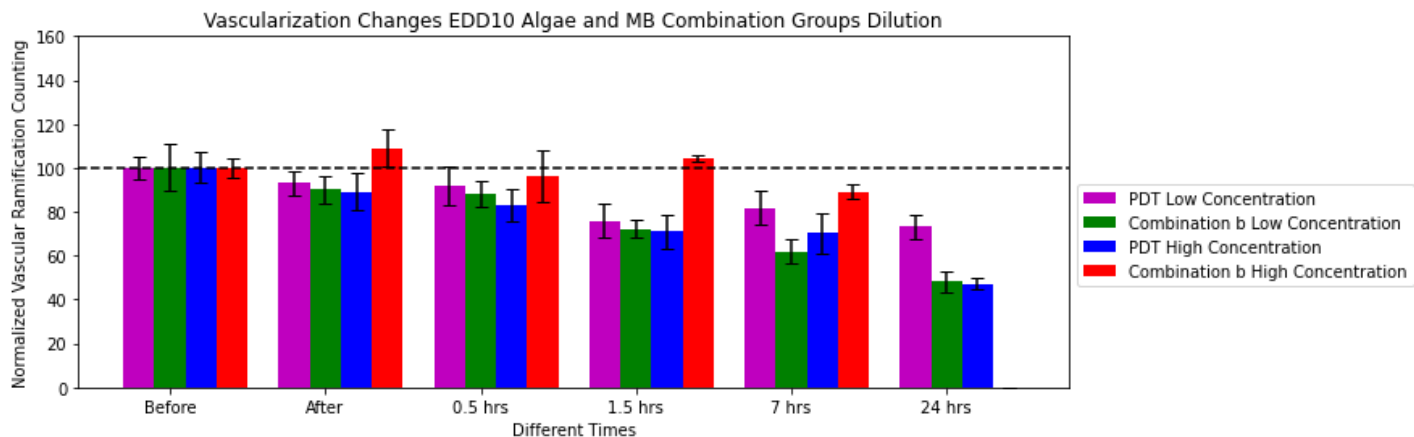


Figure 69: Bar charts EDD10 Diluted Combination Groups

When microalgae are added to the PDT for the high concentration case all of the eggs resulted

dead after a period of 24 for all the permutations. For a dilution of x10 to the MB it was found that the reduction for EDD10 in the number of ramifications was 30 % compared to 60 % using the high concentration solution. These results show an encouraging scenario for the application of photonic techniques in the treatment of diseases. Being able to locally increase the oxygen concentration and the number of vessels for the treatment of diseases that require tissue reconstruction and increased angiogenesis and, at the same time, being able to amplify the killing effect when adding a PS indicates a wide application of this combination. The results shown here somehow expand the knowledge of the general effects of the individual application of these microalgae and the combination with the well-known photodynamic effect and open doors to new lines of research that can lead to the treatment of cancer and other diseases. In addition, the treatment of infections and the more effective killing of microorganisms shows another possibility for the application of this combination. Regardless, of the positive results that were obtained in this part, there are still certain limitations that exist that might subtract credibility to these same results if they are not addressed properly.

4 Limitations of our work

There are several limitations of our work that are worth mentioning as to allow the reader to make an informed assessment of the validity of the results of this thesis. For the first part of this thesis, the photobleaching measurements were performed on different dilutions of methylene blue. The first thing that comes to mind is that the maximum peak of a MB is 664 nm whilst the administered LED light is 630 nm (red). This is clearly not optimal but the Bioblue instrument configuration could not be modified. A stronger photobleaching effect might have been stronger if the wavelength of the incident light were the same as the peak of the MB spectra and for this reason new possibilities of experimental analysis can be achieved by changing the wavelength. Another aspect related to the bleaching decaying curves of the microalgae is that, in contrast with the spectra of MB, there was no defined peak in the spectra. Based on the selection of a good estimated peak, the photobleaching curves were constructed. Finally, for the case of the combination of the microalgae and MB there was a lot of noise in the shorter wavelength regime of the spectra and it was clear that the MB component dominated at higher wavelengths. This means that photobleaching curves were constructed based on an MB-dominated spectra for this last case. The fitting of the degradation curves were based on a model by Nassar et.al, 2019 in which a sum of exponentials were used to describe them. Before writing down the final form of this fitting equation some other options were explored. It was naturally found that some of them were better than others, but we attempted to minimize the over-parametrization of the equation as much as possible.

For the second part of the thesis the analysis of the images of the CAM model were obtained to understand different effects of light, MB, microalgae and their combinations. A general limitation of our experimental work when dealing with the chicken embryos was their constant manipulation. On the one hand, an aperture to their shell was made allowing contaminants and light to enter into the egg. This naturally created stress to the organism and made it more likely for it to die. It is for this reason that the survival rate for after 24 hours of the experimentation for the control group was not one hundred percent. Furthermore, there was also the constant change of temperature and humidity conditions from the egg incubator at 37 Celsius and 65 % humidity to the room conditions inside the bio-security cabinet. This fact also induced stress to the organism and made it less likely to survive.

The other natural limitation of our experiment is that the experimental trials are performed in a CAM model and not in a mature mammalian animal such as a mice. The immunological and other environmental circumstances of a mice cannot be fully replicated in a developing chicken embryos. It is for this reason, that it is very important to take the results in this and any other CAM model trials with a healthy amount of skepticism with respect to its application in clinical trials. This implies that the results of this thesis might shed some light on how MB, microalgae and their combination might be used in mammalian animal trials.

5 Summary and Conclusions

This thesis was comprised of two parts: 1) photobleaching degradation curves and 2) CAM vascularization changes. Firstly, the spectra obtained for MB showed a peak value of 664 nm, which was selected as the reference value from which the decay curves were based upon. In parallel of performing the degradation measurements it was important to carefully characterize the irradiance of the illumination instrument. This was done in order to characterize the photobleaching curves as a function of the fluence. It was found that the photobleaching curves of the MB for low and high concentrations at the moment of irradiation behaved differently. For the low concentration of MB, a dilution of x100 (0.003 mg/ mL) was illuminated and then measured. For the high concentrations, a dilution of x40 (0.0075 mg/ mL) was illuminated and then a further dilution of x2.5 was done to adjust the spectra for the absorbance values to be between 0 and 1. It was found that the relative photodegradation curves had different decaying slopes. The higher concentration curve had a smaller negative slope as compared with the low concentration curve which had a more pronounced relative decay. The working hypothesis explaining this difference is that for a constant photon flux it would be natural that a higher concentration solution would have a relative smaller negative decay just because the total number of MB molecules is higher. For the case of the microalgae, we observed the inverse effect in which the higher concentration solution had a bigger decay whilst the lower concentration had a smaller one. When MB and microalgae were combined it resulted in a bigger decay of the degradation curves indicating, at least indirectly, that the production of singlet oxygen was enhanced in the presence of the molecular oxygen produced by the photosynthetic microalgae.

After the tests of the photodegradation of the solution the first thing that was studied, at least qualitatively, was the effect of light over the CAM for different doses. Three different groups with the different irradiance (30 mW/cm^2 , 30 mW/cm^2 and 10 mW/cm^2) and different exposure times (5 mins, 10 mins, 30 mins) respectively were selected and it was found that there were no significant changes in the vasculature. For the case of MB and light, it was found that if applied topically over the CAM, generated a progressive decrease of the vasculature as a function of time. For the case of EDD8, the relative decrease in vessel ramifications after 24 hours was about 40 percent whilst for the case of EDD10 the decrease was more pronounced and it amounted to almost 60 percent. These results are in accordance to the general tendency of a decreased vasculature when exposed to the toxic effects of PDT. On the other hand, the changes in the vascularization of the CAM when the microalgae was applied went the other way. For the same amount of topically applied microalgae there was a progressive relative increase in the ramifications of the CAM. For the EDD8 case, the increase was about 30 percent higher than the baseline after 24 hours while, for the EDD10 case, the increase for the same time frame was around 20 percent, indicating that oxygen produced by the illumination of algae can generate this vascular increase.

The novel aspect of this thesis lies on the combination of the microalgae and PDT and its vascular effect using the CAM model. It was found that for these combinations the toxic effect

after 24 hours on the vascular network was more pronounced. All the eggs in the combination groups for MB with concentration of 0.3 mg MB/ mL were dead after a day, strongly suggesting that the oxygen produced locally by the illuminated microalgae enhanced the PDT effect. To reduce the vascular effect to achieve a weaker but measurable effect a dilution of x10 for the MB stock solution was done and it was found that indeed the effect for the oxygen-enhanced therapy resulted in a 60% reduction in the vascular ramifications.

In conclusion, it was found that illuminated photosynthetic microalgae raises the effectiveness of PDT in CAM. The working hypothesis is that the locally produced oxygen elevates the toxicity of the therapy through the production of more singlet oxygen. These results open a new possibility of experiments to analyze in depth the interaction of oxygen produced by photosynthesis and its transformation into a reactive species by the photodynamic effect. In terms of the translational clinical opportunities that might result from this research there are two main ones. The first, the oxygen-enhanced PDT could be used to treat tumors through the destruction of its vascularization. Second, in the case of deep wounds the addition of microalgae by itself might help with the cicatrization process given that it stimulates the production of new blood vessels. More research needs to be done to explore other variations of these combinations. Also, experiments in small mammals with more complex immune, lymphatic and vascular systems would be necessary prerequisites before attempting to use these techniques in human patients.

6 Appendix

6.1 Methylene Blue Calculations

For the first trial were we found that the concentrations of MB were low as to not produce a differentiated set of degradation curves the following was done:

Given that we knew *a priori* the specific concentration needed to achieve an absorbance value of less than one based on previous empirical work we proceeded to reverse engineer the process. Knowing that the Beer-Lambert Law had a desired value of 0.6 for the absorbance for a concentration of about 3×10^{-6} mg/ μL of MB.

$$A = \epsilon c_1 \sim 0.6 \quad (4)$$

We proceed to use an initial MB concentration of:

$$c_1 = \frac{1.5 \text{ mg}}{5 \text{ mL}} = \frac{0.0003 \text{ mg}}{\mu L} \quad (5)$$

With this known fact and the law for mass conservation the corresponding calculation for the required quantity of this concentrated MB solution to perform the dilution was calculated.

$$c_1 v_1 = c_2 v_2 \quad (6)$$

$$v_1 = (c_2 v_2) / (c_1) \quad (7)$$

Where:

- $c_2 = 3 \times 10^{-6}$ mg/ μL
- $v_2 = 5000 \mu L$
- $c_1 = 0.0003$ mg/ μL

$$v_1 = \frac{3 * 10^{-6} \text{ mg}/\mu L * 5000 \mu L}{0.0003 \text{ mg}/\mu L} = 50 \mu L \quad (8)$$

The implication of this is that for the final irradiated solution, 50 μL of the MB concentrate was diluted in 4950 μL of water.

For the second attempt, we kept the same concentration of 1.5 mg of MB per 5 mL of water/TAP. The only difference was that instead of doing the dilution of x100 at first and then

irradiating the solution what was done was to do a dilution of x40 first, irradiate it and then perform an additional dilution x2.5 to do the measurement in the spectrometer.

Doing a simple cross multiplication we get that the amount of MB concentrated to be used is:

$$\frac{1}{40} = \frac{x}{3000} \quad (9)$$

$$x = 75 \mu L \quad (10)$$

We make sure to multiply this value for the corresponding number of wells needed to perform the trial. In this case, the multiplication factor is of 5 which gives a total amount of:

$$x = 375 \mu L MB \quad (11)$$

$$x = 14,625 \mu L H_2O \quad (12)$$

We proceed to do the irradiation and then do a dilution of x2.5 which means that for a 3,000 μL UV quartz cuvette the amount of the irradiated solution corresponds to 1,200 μL while the remaining 1,800 μL of the quartz is filled with either TAP or H₂O.

6.2 Microalgae Calculations

For the case of the microalgae (*Chlamydomonas reinhardtii*) solution it was necessary to determine the optimal dilution factor in order for us to get a value between 0-1 AU in the spectrometer. After trying out different dilution factors, it was found that the best one was a x5 dilution.

In order to make this a two step process an initial dilution value of 2 was performed. This meant that the amount of microalgae stock to be used is:

$$\frac{1}{2} = \frac{x}{3000} \quad (13)$$

$$x = 1,500 \mu L \quad (14)$$

We make sure to multiply this value for the corresponding number of wells needed to perform the trial. In this case, the multiplication factor is of 5 which gives a total amount of:

$$x = 7,500 \mu L microalgae \quad (15)$$

$$x = 7,500 \mu L TAP \quad (16)$$

We proceed to do the irradiation and then do a dilution of x2.5 which means that for a 3,000 μL UV quartz cuvette the amount of the irradiated solution corresponds to 1,200 μL while the remaining 1,800 μL of the quartz is filled with TAP.

6.3 Approval Document from Ethics Committee

 <p>PONTIFICIA UNIVERSIDAD CATÓLICA DE CHILE</p>	
Santiago, 21 de marzo de 2022	
<p>De acuerdo a lo declarado por el investigador Luis Lauro Aizpuru Vargas, en la plataforma de evaluación ética UC, la Unidad de Ética en Investigación, deja constancia que el proyecto titulado: "A study of the vascular effect with oxygen variation on chicken chorioallantoic membrane (CAM) vascularization networks", (ID 220107006), es declarado exento de evaluación ética pues no investigará con personas, datos personales y/o sensibles, ni participarán en él seres vivos o se utilizará materiales, tangibles o intangibles, especialmente protegidos en la investigación científica. Si bien, la investigación está exenta de evaluación ética no lo está en materia de seguridad de investigación debiendo ser aprobado por el comité institucional de seguridad.</p>	
<p>Le saluda atentamente,</p>	
 <p>Alejandra Santana López Coordinadora Unidad de Ética y Seguridad en Investigación Vicerrectoría de Investigación Pontificia Universidad Católica de Chile</p>	
<p>Casa Central. Av. Libertador Bernardo O'Higgins 340, 4to piso WWW.UC.CL</p> 	

Figure 70: Approval Document for Animal Use

6.4 Approval Documents from Lab Safety Committee

 <p>PONTIFICIA UNIVERSIDAD CATÓLICA DE CHILE</p> <p>COMITÉ INSTITUCIONAL DE SEGURIDAD EN INVESTIGACIÓN ACTA DE APROBACIÓN</p> <p>Miembros del Comité</p> <p>Sra. Ana María Guzmán Durán, Presidente, Facultad de Medicina. Sr. Rafael Medina Silva, Vicepresidente, Facultad de Medicina. Sra. Macarena Otto Medina, Secretaria Ejecutiva y Ministro de Fe del Comité (S) Sr. Alejandro Cabrera Oyarzún, Miembro externo. Sr. Andrés Zurita Silva, Miembro externo. Sr. Carlos Miranda Molina, Departamento de Prevención de Riesgos. Sr. Carlos Troncoso Troncoso, Dirección de Infraestructura. Sr. César Saldías Barros, Facultad de Química. Sra. Clara Quiroga Lagos, Facultad de Medicina. Sr. Felipe Ibáñez Reyes, Facultad de Química. Sr. Francisco Vera Gutiérrez, Facultad de Medicina. Sr. Gonzalo Recabarren, Facultad de Química. Sr. Hannetz Roschttardtz Choucroun, Facultad de Ciencias Biológicas. Sr. Jonathan Vargas Sepúlveda, Departamento de Prevención de Riesgos. Sr. Luis Carvacho Bart, Facultad de Historia, Geografía y Ciencia Política. Sr. Manuel Latud Rojas, Facultad de Ciencias Biológicas. Sr. Pablo Pastén González, Facultad de Ingeniería. Sra. Paola Caprile Etchart, Facultad de Física. Sra. Verónica Arenas Morales, Encargada Programa Laboratorio Seguro UC</p> <p>Participaron en la aprobación de este protocolo los miembros del Comité que asistieron a la sesión del día 09 de marzo de 2022.</p> <p>Título del proyecto: A study of the vascular effect with oxygen variation on chicken chorioallantoic membrane (CAM) vascularization networks</p> <p>Investigador responsable: Luis Lauro Aizpuru Vargas Institución: Facultad de Física, Pontificia Universidad Católica de Chile</p> <p>Académico responsable: Hilde Buzzá Harb Institución: Facultad de Física, Pontificia Universidad Católica de Chile</p> <p>Financiamiento: Fondos interdepartamentales (indicar) Fondos del Instituto de Física UC ID Protocolo: 220107006</p>  <p>PONTIFICIA UNIVERSIDAD CATÓLICA DE CHILE</p>

Figure 71: Approval Document for Lab Safety Pt.1



PONTIFICIA
UNIVERSIDAD
CATÓLICA
DE CHILE

**COMITÉ INSTITUCIONAL DE SEGURIDAD EN INVESTIGACIÓN
ACTA DE APROBACIÓN**

Fundamentación de la aprobación:

1. En el protocolo evaluado se utilizarán agentes de riesgo tales como:
 - Radiaciones
 - Reactivos químicos
 - Muestras biológicas de origen animal
 - Microorganismos pertenecientes al grupo de riesgo 1
2. El Comité ha determinado que el nivel de biocontención necesario para manipular los agentes biológicos es nivel 1.
3. Todos los agentes de riesgo serán manipulados según lo descrito en el protocolo de evaluación del Comité Institucional de Seguridad en Investigación adjunto en este documento.
4. El protocolo evaluado contempla las medidas de seguridad, contención, custodia e instalaciones necesarias para trabajar con los agentes de riesgo que se utilizarán en el proyecto.
5. El trabajo de experimentación se ajusta a las especificaciones contenidas en el "Manual de normas de bioseguridad y riesgos asociados" editado por CONICYT, versión 2018.
6. El protocolo evaluado implica la realización de salidas a terreno.
7. Las medidas de seguridad que se utilizarán en la salida a terreno son las indicadas en el protocolo de evaluación del Comité Institucional de Seguridad en Investigación adjunto en este documento.
8. El protocolo evaluado contempla las medidas de seguridad necesarias para asegurar la protección de los integrantes del equipo en la(s) salida(s) a terreno.

Resolución del Comité:

En la sesión del día 09 de marzo de 2022, el Comité Institucional de Seguridad ha determinado la **Aprobación** de este protocolo.



PONTIFICIA UNIVERSIDAD CATÓLICA DE CHILE

Figure 72: Approval Document for Lab Safety Pt.2



**COMITÉ INSTITUCIONAL DE SEGURIDAD EN INVESTIGACIÓN
ACTA DE APROBACIÓN**

Esta aprobación tiene vigencia por el período de duración del proyecto.

En la eventualidad de incorporar modificaciones a los procedimientos especificados en el protocolo aprobado, el investigador deberá notificarlo al comité para la emisión de una nueva acta de aprobación.

Los Responsables UC se comprometen a dar fiel cumplimiento al protocolo aprobado.

Los siguientes documentos han sido aprobados y están disponibles para ser descargados:

- Compromiso Seguridad en Laboratorios_Completado.pdf
- 005.5.1 COMPROMISO DE LOS RESPONSABLES SALIDA A TERRENO OK_Completado.pdf
- Protocolo Seguridad Investigación, V2020_Completado.docx
- Protocolo_seguridad_salidas_a_terreno_V2021.2_Completado.docx

Les saludan atentamente,

Macarena Otto Medina
Secretaria Ejecutiva y Ministro de Fe (S)

ANA MARÍA GUZMÁN D.
Presidenta

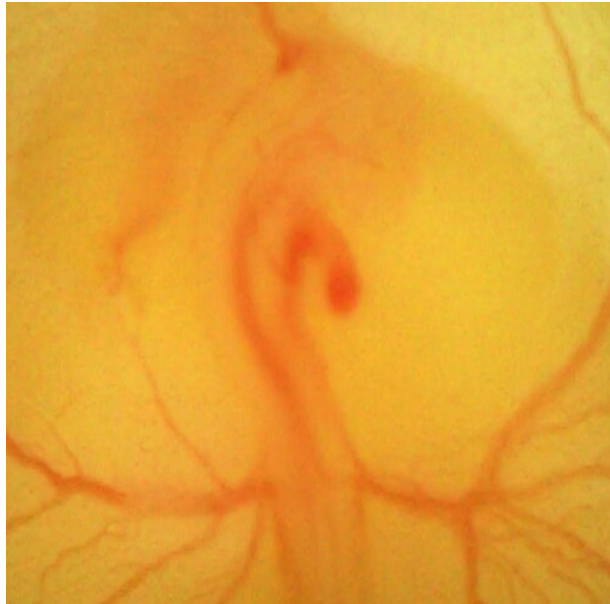
Santiago, 13 de abril de 2022



PONTIFICIA UNIVERSIDAD CATÓLICA DE CHILE

Figure 73: Approval Document for Lab Safety Pt.3

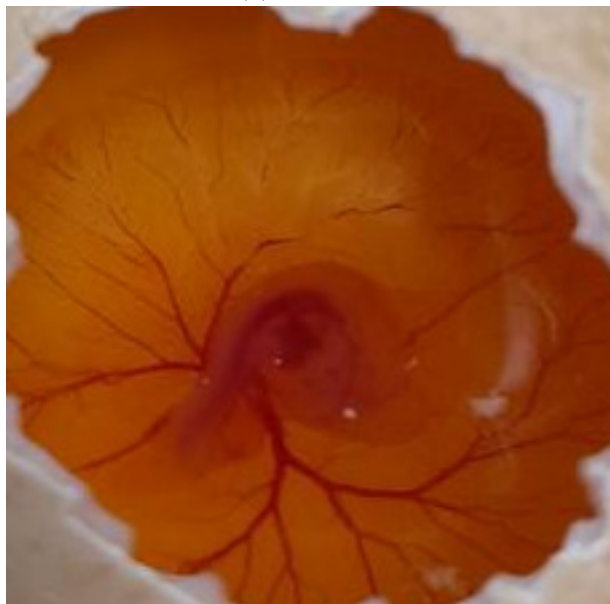
6.5 Chicken Development Stages



(a) EDD4



(b) EDD5



(c) EDD6



(d) EDD7

Figure 74: Chicken embryo development EDD4 - EDD7

7 Notes

- 1) The bibliographical references are shown in alphabetical order from A-Z using the last name of the first author to facilitate the reading of this thesis.

8 Bibliography

References

- [1] Arany, P.R. *Craniofacial Wound Healing with Photobiomodulation Therapy: New Insights and Current Challenges*. Journal of Dental Research 2016, Vol. 95(9) 977–984.
- [2] Barsanti, L; Coltelli, P; Evangelista, V; Frassanito, AM; Passarelli, V; Vesentini, N; Gualtieri, A; Evangelista, V; Barsanti, L; Frassanito, AM; Passarelli, V; Gualtieri, P. *Algal toxins: nature, occurrence, effect and detection*. Dordrecht: Springer; 2008. p. 353–91.
- [3] Beltukova, D.M.; Semenova, I.V.; Smolin, A.G.; Vasyutinskii, O.S. *Kinetics of photobleaching of Radachlorin photosensitizer in aqueous solutions*. Chemical Physics Letters 662 (2016) 127–131.
- [4] Brennan, L & Owende, P. *Biofuels from microalgae- a review of technologies for production, processing, and extractions of biofuels and co-products*. Renew Sustain Energy Rev. 2010;14:557–77.
- [5] Buzzá, H.H. ; Silva, L.V. ; Moriyama, L.T. ; Bagnato, V.S. ; Kurachi, C. *Evaluation of vascular effect of Photodynamic Therapy in chorioallantoic membrane using different photosensitizers*. Journal of photochemistry and photobiology. B, Biology, 2014, Vol.138, p.1-7.
- [6] Case Western Reserve University. *Policy for Use of Avian Embryos Institutional Animal Care and Use Committee Case Western Reserve University*. 2008.
- [7] Chen, Huanhuan; Cheng, Yuhao; Tian, Jingrun; Yang, Peizheng; Zhang, Xuerao; Chen, Yunhao; Hu, Yiqiao; Wu, Jinhui. *Dissolved oxygen from microalgae-gel patch promotes chronic wound healing in diabetes*. Science advances, 2020-05, Vol.6 (20)
- [8] Chilakamarthi, Ushasri & Giribabu, Lingamallu . *Photodynamic Therapy: Past, Present and Future*. Chemical Record, 2017-08, Vol.17 (8), p.775-802.
- [9] Cieplik, Fabian; Deng, Dongmei; Crielaard, Wim; Buchalla, Wolfgang; Hellwig, Elmar; Al-Ahmad,Ali; Maisch, Tim. *Antimicrobial photodynamic therapy – what we know and what we don't*. Critical Reviews in Microbiology 2018, VOL. 44, NO. 5, 571–589.
- [10] Clayton, TH & Harrison, PV. *Photodynamic therapy for infected leg ulcers*. Br J Dermatol 156(2):384–385 (2007).
- [11] Crespi-Abril, Augusto C & Rubilar, Tamara. *Moving forward in the ethical consideration of invertebrates in experimentation: Beyond the Three R's Principle*. Vol 69 No Suppl.1 (2021): Research on Echinoderms in Latin America V.

- [12] Cruz, P.M.R.; Mo, H.; McConathy, W.J.; Sabnis, N.; Lacko, A.G. *The role of cholesterol metabolism and cholesterol transport in carcinogenesis: a review of scientific findings, relevant to future cancer therapeutics*, Front. Pharmacol. 4 (2013) 119.
- [13] Delavary, Babak Mahdavian; van der Veer, Willem M; van Egmond, Marjolein; Niessen, Frank B; Beelen, Robert H.J. *Macrophages in Skin Injury and Repair*. Immunobiology (1979), 2011, Vol.216 (7), p.753-762.
- [14] DiPietro, Luisa A. *Angiogenesis and wound repair: when enough is enough*. Journal of leukocyte biology, 2016-11, Vol.100 (5), p.979-984.
- [15] Druyan, S.; Ruzal, M.; Shinder, D.; Haron, A. *Effects of low oxygen during chorioallantoic membrane development on post-hatch growing performance of broiler chickens*. Poultry science, 2018-06-01, Vol.97 (6), p.1961-1967.
- [16] Franco, Nuno Henrique. *Animal Experiments in Biomedical Research: A Historical Analysis* Animals (Basel), 2013-03-19, Vol.3 (1), p.238-273.
- [17] Gianelli, Marco & Bani, Daniele. *Appropriate laser wavelengths for photodynamic therapy with methylene blue*. Lasers in Medical Science (2018) 33:1837–1838.
- [18] Harb-Buzzá, Hilde; Zangirolami, Amanda C.; Davis, Arthur; Gómez-García, Pablo A.; Kurachi, Cristina. *Fluorescence analysis of a tumor model in the chorioallantoic membrane used for the evaluation of different photosensitizers for photodynamic therapy*. Photodiagnosis and photodynamic therapy, 2017, Vol.19, p.78-83.
- [19] Hemschemeier, Anja *Photo-bleaching of Chlamydomonas reinhardtii after dark-anoxic incubation*. Plant Signal Behav 2013 Nov;8(11):e27263. doi: 10.4161/psb.27263. Epub 2013 Dec 3.
- [20] Hooper, Ian *Molecular Aggregate*. URL: <https://www.exeter.ac.uk/research/metamaterials/team-a/ps/molecularaggregate/>
- [21] Huang, Z.; Xu, H.; Meyers, A.D.; Musani, A.I.; Wang, L.; Tagg, R; Barqawi, A.B.; Chen, Y.K. *Photodynamic therapy for treatment of solid tumors—potential and technical challenges* Technol. Cancer Res. Treat. 7 (2008) 309–320.
- [22] Ilev, Ilko; Boppart, Stephen; Andersson-Engelers, Stefan; Kim, Beop-Min; Perelman, Lev; Tucking, Valery . *Introduction to the Issue on Biophotonics*. IEEE Journal of Selected Topics in Quantum Electronics, VOL. 20, NO. 2, March/April 2014.
- [23] M.S Ismail, U. Torsten, C. Dressler, J.E Diederichs, S Hüske, H. Weitzel, H.P Berlien *Photodynamic Therapy of Malignant Ovarian Tumours Cultivated on CAM* . Lasers Med Sci 1999 Jun;14(2):91-6.
- [24] Joiner, Michael & van der Kogel, Albert. *Basic Clinical Radiobiology: Fourth Edition*. Great Britain 2009; Hodder Arnold.

- [25] Khan, Muhammad Imran; Shin, Jin Hyuk; Kim, Jong Deog. *The promising future of microalgae: current status, challenges, and optimization of a sustainable and renewable industry for biofuels, feed, and other products*. Microb Cell Fact (2018) 17:36.
- [26] Kunz, Pierre; Schenker, Astrid; Sähr, Heiner; Lehner, Burkhard; Fellenberg, Jörg . *Optimization of the chicken chorioallantoic membrane assay as reliable in vivo model for the analysis of osteosarcoma*. PloS one, 2019, Vol.14 (4).
- [27] Kwiatkowski, Stanisław; Knap, Bartosz; Przystupski, Dawid; Saczko, Jolanta; Knap-Czop, Ewa Kedzierska Karolina; Kotlińska, Jolanta; Michel, Olga; Kotowski, Krzysztof; Kulbacka, Julita. *Photodynamic therapy – mechanisms, photosensitizers and combinations*. Biomedicine & Pharmacotherapy 106 (2018) 1098–1107.
- [28] McFadden, Christopher. *Photodynamic Therapy Dose Planning for Peripheral Lung Cancer* . University of Toronto Dissertation Publishing 2020.
- [29] Maehle, A.H. & Tröhler, U. *Animal experimentation from antiquity to the end of the eighteenth century: Attitudes and arguments*. In *Vivisection in Historical Perspective*; Rupke, N.A., Ed.; Croom Helm: London, UK, 1987.
- [30] Maiya, Bhaskar G. *Photodynamic Therapy (PDT): Basic Principles*. Resonance, 2000-04, Vol.5 (4), p.6-18.
- [31] Meroli, Stefano. *The interaction of photons with the matter*. Life of an Engineer at CERN. URL: https://meroli.web.cern.ch/Lecture_photon_interaction.html
- [32] Merckx, Greet; Tay, Hanna; Lo Monaco, Melissa; van Zandvoort, Marc A.M.J; De Spiegeleire, Ward; Lambrechts, Ivo; Bronckaers, Annelies. *Chorioallantoic Membrane Assay as Model for Angiogenesis in Tissue Engineering: Focus on Stem Cells*. Tissue engineering. Part B, Reviews, 2020-12-15, Vol.26 (ja), p.519-539.
- [33] Mississippi State University. *Stages in chick embryo development*. 2022. URL: <http://extension.msstate.edu/content/stages-chick-embryo-development>
- [34] Miller, Walter J ; Kayton, Mark L ; Patton, Angela ; O'Connor, Sarah ; He, Mei ; Vu, Huan ; Baibakov, Galina ; Lorang, Dominique ; Knezevic, Vladimir ; Kohn, Elise ; Alexander, H Richard ; Stirling, David ; Payvandi, Faribourz ; Muller, George W ; Libutti, Steven K *A novel technique for quantifying changes in vascular density, endothelial cell proliferation and protein expression in response to modulators of angiogenesis using the chick chorioallantoic membrane (CAM) assay*. Journal of translational medicine, 2004, Vol.2 (1), p.4-4
- [35] Morais, José Athayde Vasconcelos ; Almeida, Letícia R ; Rodrigues, Mosar C ; Azevedo, Ricardo B ; Muehlmann, Luis A *The induction of immunogenic cell death by photodynamic therapy in B16F10 cells in vitro is effected by the concentration of the photosensitizer*. Photodiagnosis and photodynamic therapy, 2021, Vol.35, p.102392-102392.

- [36] Morton, David B. *Humane endpoints in animal experimentation for biomedical research: ethical, legal and practical aspects* London: Royal Society of Medicine Press, 1999, p.5-12.
- [37] Nassar, Sulafa Jamal M. ; Wills, Corinne ; Harriman, Anthony. *Inhibition of the Photo-bleaching of Methylene Blue by Association with Urea* . ChemPhotoChem, 2019, Vol.3 (10), p.1042-1049
- [38] Nowak-Sliwinska, Patrycja; Segura, Tatiana; Iruela-Arispe, M. Luisa. *The chicken chorioallantoic membrane model in biology, medicine and bioengineering*. Angiogenesis (London), 2014-08-20, Vol.17 (4), p.779-804.
- [39] Nowak-Stepniowska, A.; Pergoł, P.; Padzik-Graczyk, A. *Photodynamic method of cancer diagnosis and therapy—mechanisms and applications*. Postepy Biochem. 59 (2013) 53–63.
- [40] O'Malley, C.D. *Andreas Vesalius of Brussels*; University of California Press: Berkeley, CA, USA, 1964.
- [41] Obaíd, Miguel Luis; Camacho, Juan Pablo; Brenet, Marianne; Corrales-Orovio, Rocío; Carvajal, Felipe; Martorell, Ximena; Werner, Consuelo; Simón, Valeska; Varas, Juan; Calderón, Wilfredo; Guzmán, Christian Dani; Bono, María Rosa; San Martín, Sebastián; Eblen-Zajjur, Antonio; Egaña, José Tomás. *A First in Human Trial Implanting Microalgae Shows Safety of Photosynthetic Therapy for the Effective Treatment of Full Thickness Skin Wounds*. Front. Med., 30 November 2021.
- [42] Papoutsi, M; Tomarev, SI; Eichmann, A; Prols, F; Christ, B; Wilting, J. *Endogenous origin of the lymphatics in the avian chorioallantoic membrane*. Dev Dynam. 2001; 222(2):238–251.
- [43] Qi, Fenggang; Ji, Penghao; Chen, Zhixin; Wang, Liping; Yao, Heliang; Huo, Minfeng; Shi, Jianlin. *Photosynthetic Cyanobacteria-Hybridized Black Phosphorus Nanosheets for Enhanced Tumor Photodynamic Therapy*. Small (Weinheim an der Bergstrasse, Germany), 2021-10-21, Vol.17 (42).
- [44] Qiao, Yue; Yang, Fei; Xie, Tingting; Du, Zhen; Zhong, Danni; Qi, Yuchen; Li, Yangyang; Li, Wanlin; Lu, Zhimin; Rao, Jianghong; Sun, Yi; Zhou, Min . *Engineered algae: A novel oxygen-generating system for effective treatment of hypoxic cancer*. Science advances, 2020-05-20, Vol.6 (21).
- [45] Rahman, SU; Mosca, RC; Govindool Reddy, S; Nunez, SC; Andreana, S; Mang, TS; Arany, PR. *Learning from clinical phenotypes: Low-dose biophotonics therapies in oral diseases*. Oral diseases, 2018, Vol.24 (1-2), p.261-276.
- [46] Renwick, MJ; Simpkin, V; Mossialos, E. *Targeting innovation in antibiotic drug discovery and development: the need for a One Health – One Europe – One World Framework*. Copenhagen (Denmark): European Observatory on Health Systems and Policies. Health Policy Series, No. 45 (2016). ISBN-13: 9789289050401.

- [47] Ribatti, Domenico. *The chick embryo chorioallantoic membrane (CAM): A multifaceted experimental model*. Mechanisms of development, 2016-08, Vol.141, p.70-77.
- [48] Scales, BS & Huffnagle, GB. *The microbiome in wound repair and tissue fibrosis*, J Pathol, 2013, 229(2):323–331.
- [49] Schenck, Thilo Ludwig; Hopfner, Ursula; Chávez, Myra Noemi; Machens, Hans-Günther; Somlai-Schweiger, Ian; Giunta, Riccardo Enzo; Bohne, Alexandra Viola; Nickelsen, Jörg; Allende, Miguel L; Egaña, José Tomás *Photosynthetic biomaterials: A pathway towards autotrophic tissue engineering*. Acta biomaterialia, 2015, Vol.15, p.39-47
- [50] Sen, CK; Gordillo, GM; Roy, S; Kirsner, R; Lambert, L; Hunt, TK; Gottrup, F; Gurtner, GC; Longaker, MT. *Human skin wounds: a major and snowballing threat to public health and the economy*, Wound Repair Regen, 2009, 17(6):763–771.
- [51] Spinoza, B.T. *The Ethics*; Echo Library: Teddington, Middlesex, UK, 2006.
- [52] Steffens, GC; Yao C; Prevel, P; Markowicz, M; Schenck, P; Noah, EM; Pallua, N. *Modulation of angiogenic potential of collagen matrices by covalent incorporation of heparin and loading with vascular endothelial growth factor*. *Tissue Eng.* 2004; 10(9–10):1502–1509. [PubMed:15588409].
- [53] Tiburcio, M.A; Rocha, A.R; Romano, R.A; Inada, N.M; Bagnato, V.S; Carlos, R.M; Buzzá, H.H *In vitro evaluation of the cis-[Ru(phen)2(pPDIp)]2+** complex for antimicrobial photodynamic therapy against *Sporothrix brasiliensis* and *Candida albicans**. Journal of photochemistry and photobiology. B, Biology, 2022, Vol.229, p.112414-112414 .
- [54] Tu, Ping-hua; Huang, Wen-jun; Wu, Zhan-ling; Peng, Qing-zhen; Xie, Zhi-bin; Bao, Ji; Zhong, Ming-hua. *Induction of cell death by pyropheophorbide- α methyl ester-mediated photodynamic therapy in lung cancer A549 cells*. Cancer medicine (Malden, MA), 2017, Vol.6 (3), p.631-639.
- [55] University of Michigan Health. *Diabetic Foot Ulcers*. 2022 URL: <https://www.uofmhealth.org/conditions-treatments/podiatry-foot-care/frequently-asked-questions-diabetic-foot-ulcers>.
- [56] Vargas, A; Zeisser-Labouebe, M; Lange, N; Gurny, R; Delie F. *The chick embryo and its chorioallantoic membrane (CAM) for the in vivo evaluation of drug delivery systems*. *Adv Drug Deliver Rev.* 2007; 59(11):1162–1176.
- [57] Veloso-Giménez, Valentina; Escamilla, Rosalba; Necuñi, David; Corrales-Orovio, Rocío; Riveros, Sergio; Marino, Carlo; Ehrenfeld, Carolina; Guzmán, Christian Dani; Boric, Mauricio P.; Rebollo, Rolando ; Egaña, José Tomás . *Development of a Novel Perfusionable Solution for ex vivo Preservation: Towards Photosynthetic Oxygenation for Organ Transplantation*. *Front. Bioeng. Biotechnol.*, 15 December 2021.

- [58] von Staden, H. *Herophilus: The Art of Medicine in Early Alexandria*; Cambridge University Press: Cambridge, UK, 1989.
- [59] Voss, Logan J; Plouviez, Maxence; Whittle, Nicola *Microalgae-based photosynthetic strategy for oxygenating avascularised mouse brain tissue – An in vitro proof of concept study*. Brain research, 2021, Vol.1768, p.147585.
- [60] Wang, Haoran; Guo, Yunfei; Wang, Chao; Jiang, Xing; Liu, Honghui; Yuan, Ahu; Yan, Jing; Hu, Yiqiao; Wu, Jinhui. *Light-controlled oxygen production and collection for sustainable photodynamic therapy in tumor hypoxia*. Biomaterials, 2021-02, Vol.269, p.120621-120621.
- [61] Wenzl, Tatiana & Wilkens, Jan J . *Modelling of the oxygen enhancement ratio for ion beam radiation therapy*. Physics in medicine & biology, 2011-06-07, Vol.56 (11), p.3251-3268.
- [62] Willemen, Niels G.A; Hassan, Shabir; Gurian, Melvin; Li, Jinghang; Allijn, Iris E; Shin, Su Ryon; Leijten, Jeroen. *Oxygen-Releasing Biomaterials: Current Challenges and Future Applications*. Trends in biotechnology (Regular ed.), 2021-11, Vol.39 (11), p.1144-1159.
- [63] Xia, Lei; Bo, Liu; Huang, Zheng; Wu, Jinjin. *A Clinical study of photodynamic therapy fro chronic skin ulcers in lower limbs infected with Pseudomonas aeruginosa*, Arch Dermatol Res (2015) 307:49–55.
- [64] Yalcin, M; Bharali, DJ; Lansing, L; Dyskin, E; Mousa, SS; Hercbergs, A; Davis, FB; Davis, PJ; Mousa, SA. *Tetraiodothyroacetic acid (tetrac) and tetrac nanoparticles inhibit growth of human renal cell carcinoma xenografts*. Anticancer Res. 2009; 29(10):3825–3831.
- [65] N. Zacharakis, P. Tone, C.S. Flordellis, M.E. Maragoudakis, N.E. Tsopanoglou. *Methylene blue inhibits angiogenesis in chick chorioallontoic membrane through a nitric oxide-independent mechanism*. J Cell Mol Med. 2006 Apr-Jun;10(2):493-8.
- [66] Zheng, Pengli; Fan, Miao; Liu, Huifang; Zhang, Yinghua; Dai, Xinyue; Li, Hang; Zhou, Xiaohan; Hu, Shiqi; Yang, Xinjian; Jin, Yi; Yu, Na; Guo, Shutao; Zhang, Jinchao; Liang, Xing-Jie; Cheng, Ke; Li, Zhenhua. *Self-Propelled and Near-Infrared-Phototoxic Photosynthetic Bacteria as Photothermal Agents for Hypoxia-Targeted Cancer Therapy*. ACS nano, 2021-01-26, Vol.15 (1), p.1100-1110.